CHALMERS
UNIVERSITY OF TECHNOLOGY

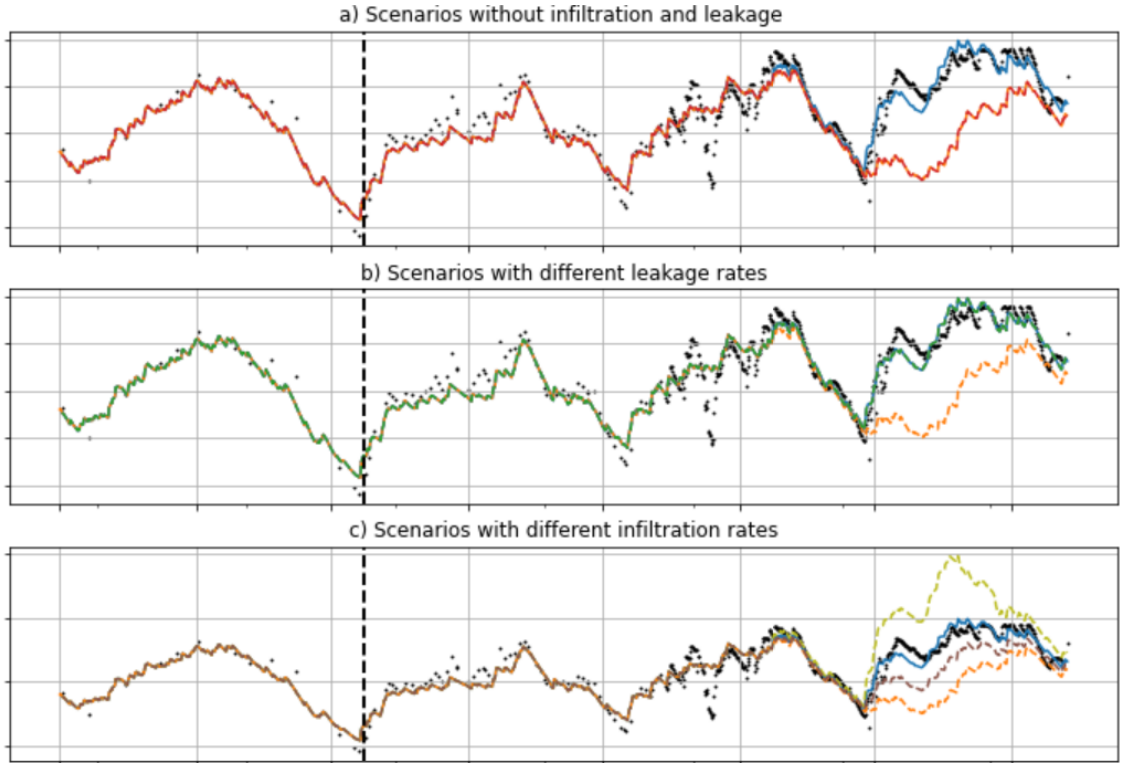

Evaluating transfer-function models to understand groundwater level impacts

A study of head changes due to drainage and infiltration in an underground infrastructure project

Master's thesis in Infrastructure and Environmental Engineering

LOVISA BOSTRÖM
ANNA LINDBLOM

DEPARTMENT OF ARCHITECTURE AND CIVIL ENGINEERING
CHALMERS UNIVERSITY OF TECHNOLOGY
Gothenburg, Sweden 2021
www.chalmers.se

Master's thesis 2021

Evaluating transfer-function models to understand groundwater level impacts.

A study of head changes due to drainage and infiltration in an underground infrastructure project.

LOVISA BOSTRÖM
ANNA LINDBLOM

CHALMERS
UNIVERSITY OF TECHNOLOGY

Department of Architecture and Civil Engineering
Division of Geology and Geotechnics
Engineering geology
Chalmers University of Technology
Gothenburg, Sweden 2021

Evaluating transfer-function models to understand groundwater level impacts
A study of head changes due to drainage and infiltration in an underground infrastructure project
LOVISA BOSTRÖM
ANNA LINDBLOM

© LOVISA BOSTRÖM, ANNA LINDBLOM, 2021.

Supervisor: Ezra Haaf, Division of Geology and Geotechnics
Jonas Sundell, Trafikverket

Examiner: Lars Rosén, professor in the Division of Geology and Geotechnics

Master's Thesis 2021
Department of Architecture and Civil Engineering
Division of Geology and Geotechnics
Engineering geology
Chalmers University of Technology
SE-412 96 Gothenburg
Telephone +46 31 772 1000

Cover: Simulated groundwater heads for a well based on different stress scenarios.

Typeset in LaTeX
Printed by Chalmers Reproservice
Gothenburg, Sweden 2021

Evaluating transfer-function models to understand groundwater level impacts
A study of head changes due to drainage and infiltration in an underground infrastructure project

LOVISA BOSTRÖM
ANNA LINDBLOM
Department of Architecture and Civil Engineering
Chalmers University of Technology

Abstract

When analysing the effect of underground construction on groundwater levels, process based models are often applied. They generally require a detailed conceptualisation of the study area supported by a large amount of information and a thorough description of the flow system. The use of time-series driven transfer function-noise models is a less time consuming approach to assess the effect from groundwater drawdown. They require fewer types of input data and are easier to apply and could therefore show potential in groundwater modeling to complement or replace process based models. This study aims to evaluate how transfer function-noise models can be used to evaluate groundwater head changes, as a result of infiltration and drainage from an underground infrastructure project. The study uses an area surrounding the Haga service tunnel, part of the Västlänken project in Gothenburg, as a site study. The transfer function-noise models are created with the use of groundwater head observations, estimated recharge, leakage measurements and infiltration measurements. After a completed calibration process, the model outcome is used to perform stress simulation scenarios, cluster analysis of residuals and parameters as well as an analysis of parameter correlations. The stress simulations are performed in order to quantify the impact from infiltration and drainage on the groundwater heads. Furthermore, the cluster analysis is performed to establish the spatial impact in the area and to evaluate how the model is parameterised. Lastly the analysis of parameter correlations is performed to examine the possible relations of the model parameters against site physical characteristics. This study demonstrates that transfer function-noise models show potential to be used to identify and quantify the stress that has caused a disturbance, identify missing or inaccurate stress measurements and to simulate different stress scenarios. The study also show that the groundwater levels in the site study area have been impacted by the service tunnel and the spatial impact could be established with a cluster analysis.

Keywords: Transfer function-noise modeling, Pastas, time-series analysis, groundwater head changes, underground infrastructure project.

Acknowledgements

This study was performed during the spring of 2021. The idea behind this study was introduced to us by our supervisor Ezra Haaf at Chalmers, whom we would like to thank for providing us with an interesting topic and for providing guidance when needed. We would also like to recognize the support from our supervisor Jonas Sundell at Trafikverket for the shared knowledge about the study site and the project as well as for important insights during the study. Due to the special circumstances of the Covid-19 pandemic the work and all meetings were conducted digitally from home. We would therefore also like to thank our supervisors for quick answers and rewarding digital meetings.

Lovisa Boström & Anna Lindblom, Gothenburg, June 2021

Contents

List of Figures

List of Tables

1

Introduction

Groundwater drawdown is a common consequence of excavations in underground infrastructure projects (Yoo et al., 2012). This often originates from underground infrastructure projects, such as tunnels, being constructed in highly permeable materials. To reduce and control the groundwater inflow during tunneling the pre-grouting technique, where a watertight shell is constructed around the tunnel, is commonly used. However, even when adopting this technique it is inevitable that a certain amount of water inflow will occur during the tunneling, especially if the quality of the pre-grouting is not properly controlled. The subsequent groundwater drawdowns can lead to settlements damaging already existing structures as well as posing a risk to sensitive nature resources, energy- and water-wells. To avoid these types of damages, in addition to reducing unwanted costs for society, robust methods for analysis of groundwater impacts are crucial.

Among such methods, is groundwater modeling which is commonly applied in underground infrastructure projects as both a decision making- and predictive tool. Groundwater modeling requires a mathematical representation of the hydrogeologic processes which can be solved either by numerical or analytical methods (Anderson et al., 2015). Numerical models are the most commonly used models where a detailed conceptualisation of the study area in the form of a large amount of information and a thorough description of the flow system is required (Kumar, 2013). The numerical groundwater model can thus provide information regarding the water balance as well as other hydrogeological properties in the modelled area, however, it is a highly data demanding and time intensive task (Mohanty et al., 2013). Analytical models require less conceptualisation and simpler governing equations compared to numerical models. More complex analytical models are preferably solved using computer based code (Anderson et al., 2015).

Time series analysis is a data analytical method that can be used to assess if a groundwater drawdown has occurred and what the source might be. Time series analysis is less time consuming, requires fewer types of input data and is easier to apply and could therefore give another perspective to groundwater modeling by complementing or replacing numerical models (Bakker & Schaars, 2019). Examples of time series models used for groundwater modeling are regression models (Chen et al., 2002), auto-regressive models (Mirzavand & Ghazavi, 2015) and similarity-based models (Haaf et al., 2020). A model that can provide insight to how and why the groundwater head varies as well as quantify the contribution stresses such as evaporation, rainfall, pumping and surface water has on the aquifer has potential in

the analysis of groundwater impact. Transfer function-noise (TFN) modeling based on predefined impulse response functions is a type of times series analysis that show potential to be applied for this purpose (Bakker & Schaars, 2019). The concept of TFN modeling is to translate one or several input series to an output series with the use of a statistical model (Collenteur et al., 2019). For the purpose of performing TFN modeling with predefined impulse response functions the open source Python package Pastas can be used (Bakker & Schaars, 2019).

This study will evaluate the use of TFN models, in a tunneling project, using the Pastas package. The TFN models will be evaluated to establish if this method can be used as a groundwater modeling tool to quantify groundwater level impacts and to clearly identify the cause of the impact. More specifically it will be evaluated if it is possible to use the method to asses to what extent, both spatial and regarding time, an infrastructure project with infiltration and drainage has affected the groundwater levels in an area.

The study will use an area surrounding the Haga service tunnel, part of the Västlänken project in Gothenbrurg, as a site study. Data used for the modeling will be data that is usually available in infrastructure projects such as groundwater head-, tunnel leakage- and infiltration measurements. Available climate data such as precipitation and evaporation will also be used to set up the models. After a completed calibration process the models are used to perform stress simulation scenarios, cluster analysis of residuals and parameters as well as an analysis of parameter correlations. The stress simulations are performed in order to quantify the impact from infiltration and drainage on the groundwater heads. Furthermore, the cluster analysis is performed to establish the spatial impact in the area and to evaluate how the model is parameterised. Lastly the analysis of parameter correlations is performed to examine the possible relations of the model parameters against site physical characteristics.

1.1 Aim

The aim of this study is to assess if transfer function-noise models can be used to evaluate to what extent a change in groundwater heads, as a result of infiltration and drainage from an underground infrastructure project, has occurred and where. The potential for using the model to asses a change in groundwater heads will be evaluated in terms of area of use, uncertainty, model fit, spatial aspects, data requirements and model limitations. For the modeling, data will be used from the Haga service tunnel for the Västlänken project in Gothenburg. Consequently the eventual impact on the groundwater heads in the area from the service tunnel will be evaluated.

1.2 Research questions

- What are the potentials and limitations of using TFN models and how can they be applied in underground infrastructure projects to evaluate groundwater head changes due to drainage and infiltration based on aspects such as conceptualisation, data, areas of use, spatial applicability, uncertainty, model fit and time?
- What impact does the service tunnel have on the groundwater heads at the study site?

1.3 Limitations

The report will be limited to studying the groundwater impact in Guldhedsdalen and Annedal as a result of one segment of the Västlänken project, the Haga service tunnel.

1.4 Disposition

The study will after this introductory chapter, first present the study site to give an overview of relevant information concerning the area that will be used for the model set up and evaluation of model outcome. Next a chapter on the general strategy of this study followed by information about data retrieval and manipulation as well as methods applied in the modeling process will be presented. The results will be presented in two parts, the evaluation of the TFN model and results from the model outcome. The discussion will focus on answering the research questions based on the results obtained in this study. To summarize the report conclusions will be drawn based of the findings made in the project.

2
Study site

2.1 Study site selection

An area surrounding the Haga service tunnel was chosen as a site study since the tunnel is connected to the Västlänken project and the tunneling process had been completed prior to commencement of this study. Available data from groundwater wells, infiltration- and leakage measurements in the area was decisive when choosing the site study. Seeing that the Västlänken project is an extensive infrastructure project, a sufficient amount of data could be provided by the Swedish transportation administration, Trafikverket, for this study.

Project Västlänken entails the construction of an 8 km long double-track railway in the city centre of Gothenburg. 6 km of the railway will be constructed as a tunnel passing through both rock and clay formations. In addition to this, three underground stations will be constructed at Gothenburg central station, Haga and Korsvägen (Trafikverket, 2018). The construction started in 2018 with an estimated finalization in 2026 (Göteborgs stad, 2020).

2.2 Haga service tunnel

The Haga service tunnel (Sundkvist, 2016) is a 910 m long tunnel driven in rock from Linnéplatsen connecting with the main tunnel at Södra Viktorigatan, see Figure 2.1.

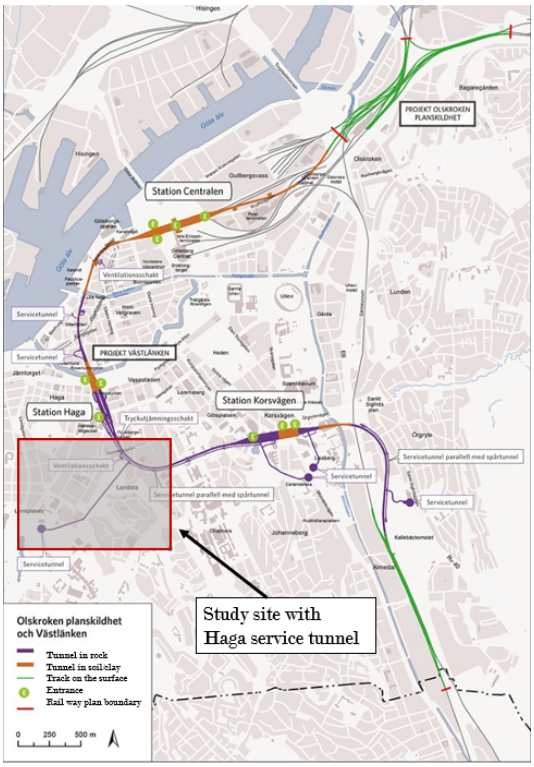

Figure 2.1: The extension of the Västlänken project with the study site marked in red enclosing the Haga service tunnel (Sundkvist, 2016). Adapted with permission.

2.3 Geology

The site study area surrounding the Haga service tunnel is a high lying area with numerous exposed rock surfaces of rock type Breccia but the bedrock in the area consists of gneiss, Figure 2.2 displays a contour map for the bedrock in the area. There are several smaller weakness zones in the area and a larger weakness zone near Konstepidemien with dominating fractures in the NNW-SSE direction, however the rock is generally highly crushed. There are also a few weakness zones along the service tunnel with a NW-NNW strike and dip in western direction (Lithén & Wadsten, 2016).

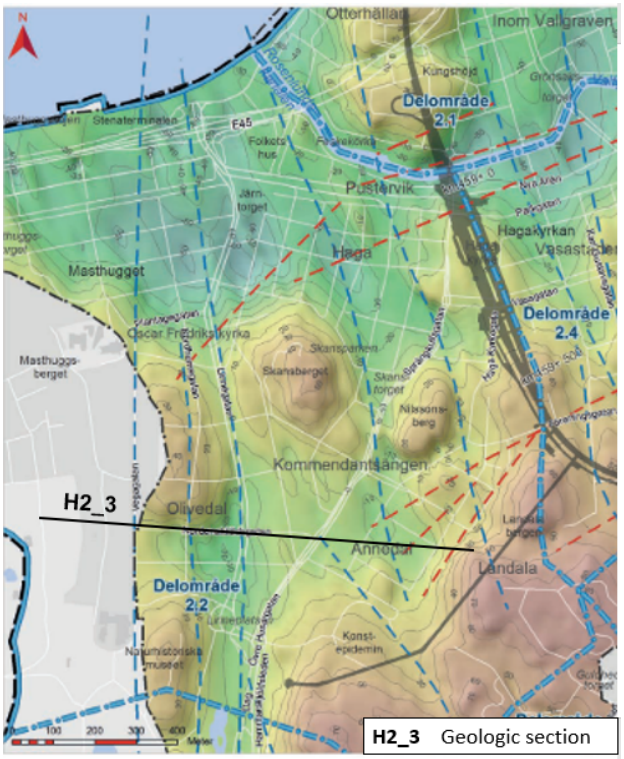

Figure 2.2: Contour map of modelled bedrock levels in the site study area. Blue lines visualize presumed weakness zones with a western dip and red lines visualize presumed steep weakness zones (Sundkvist & Wallroth, 2016). Adapted with permission.

In the study area the soil layers mainly consist of frictional soil with a clay layer covering the frictional soil in low lying valleys. The frictional soil mostly consists of glacial till which covers the underlying rock surface. There also exists a few areas where the till is covered either by glaciofluvial sand or gravel. The top layer in the area is generally made up of filling material. The filling material is a result of construction in the area as it has been deposited to even out the ground surface. Material for road construction makes up the top part of the filling material whereas the deeper sections consist of clay, sand, organic soil and silt (Sundkvist & Wallroth, 2016). In Figure 2.3 the geologic section H2_3 in the area can be seen, with corresponding location according to Figure 2.2.

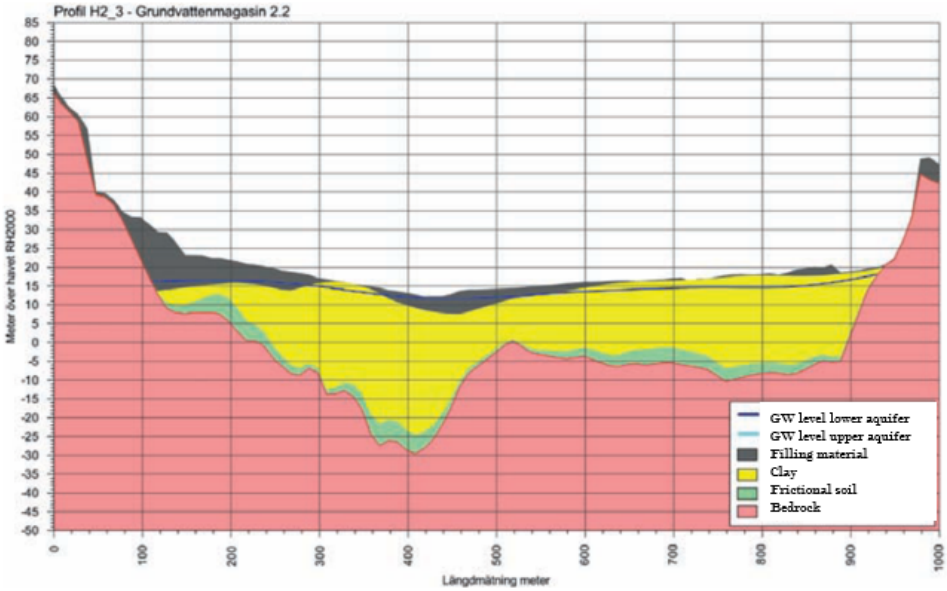

Figure 2.3: Geologic section H2_3 along Nordenskiöldsgatan in the direction toward Guldhedsberget, in the Olivedal-Annedal aquifer. (Sundkvist & Wallroth, 2016). Adapted with permission.

2.4 Hydrogeology

The soil layers in the study area are in general uniform and therefore it can be said that two soil aquifers exist in the area, a lower and upper soil aquifer. The lower aquifer is located in the frictional soil on top of the bedrock whereas the upper aquifer exist in the filling material. Figure 2.4 displays the lower soil aquifer with predominant groundwater flow directions in the area. The lower soil aquifer can be divided into a north and south aquifer where the south one, the Olivedal-Annedal aquifer, is located south of Skansberget in proximity to the Haga service tunnel. The Olivedal-Annedal aquifer consist of a relatively uniform frictional soil layer with high rock levels acting as hydraulic boundaries in both east and west direction. Narrow valleys filled with soil act as hydraulic boundaries in the south and north direction. The groundwater mainly flows in a north direction from high lying areas in the south to lower lying areas bordering the north aquifer. Ultimately the Olivedal-Annedal aquifer discharges into the north aquifer trough the valleys along Linnégatan and Övre Husargatan (Sundkvist & Wallroth, 2016).

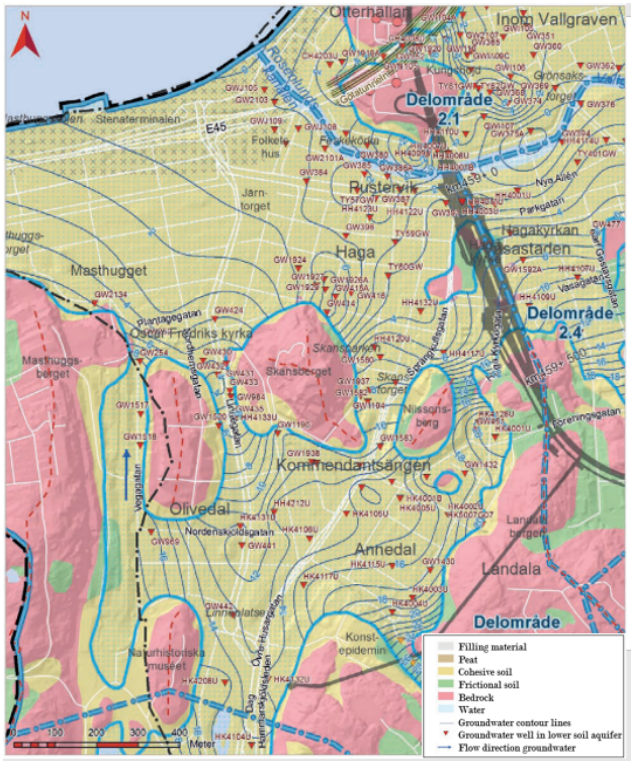

Figure 2.4: Observation wells and groundwater flow directions in the lower soil aquifer. (Sundkvist & Wallroth, 2016)

Rock aquifers also exist in the area and these are affected by draining underground structures which has lowered the groundwater levels in the area. There are only a few wells located in rock, see Figure 3.2, and these are generally located in the eastern part near the Haga service tunnel. The aquifer in whole is considered to be affected by drainage from existing underground structures (Sundkvist & Wallroth, 2016).

3
Data and methods

In this chapter the data used for the groundwater modeling is presented together with the methods applied in the modeling and process of the study.

3.1 General strategy

The research method used for this study was a mixed method combining both quantitative and qualitative data analysis. It was used to evaluate the TFN model, as a tool to assess groundwater head changes due to a tunnel project, and was implemented in the entire process from setting up the model to finally evaluating the results. The TFN modeling was performed in the open source Python package Pastas. The reason as to why the modeling was performed in the Python package Pastas was due to it being a well documented open source software tool where transfer function modeling, based on impulse response functions, can be performed (Collenteur et al., 2019). A similar working process for the groundwater modeling as presented in Figure 3.1, which has been suggested by (Anderson et al., 2015), has been implemented in the process for this study. The difference being that instead of translating the conceptual model into a numerical model (step 4) it was translated into the TFN model. Also this workflow has the objective of forecasting but it can be altered for other type of groundwater modeling, as in this study where predictive scenarios have been made based on a calibrated model.

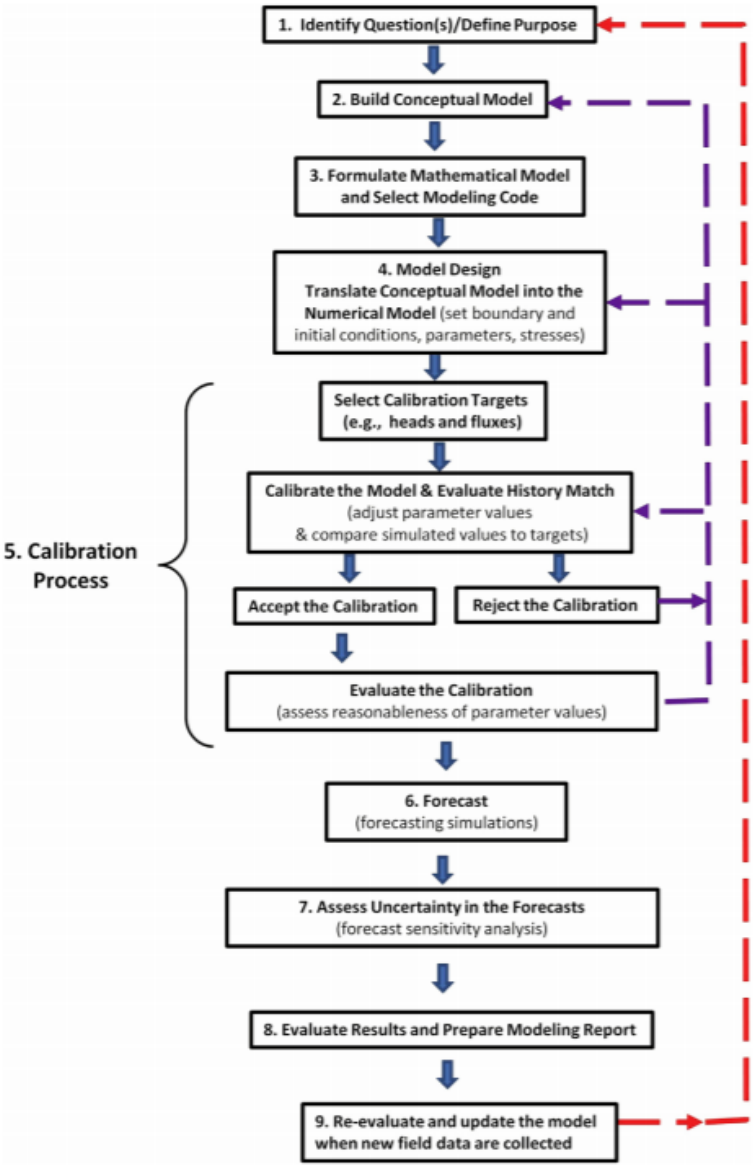

Figure 3.1: Suggested workflow for groundwater modeling developed by (Anderson et al., 2015).

Regarding the evaluation of quantitative aspects, factors such as time, amount of data and the areas of use were considered. Also an evaluation of the achieved model fit for the groundwater model simulations was performed. In addition to this, a cluster analysis based on the model outcome was performed to evaluate the spatial impact in the area as well as the parameterisation of the model. Regarding the qualitative aspects a literature review was conducted to evaluate the use of a TFN model, this is presented in the result section 4.1. In Table 3.1 the type of quantitative and qualitative aspects considered are summarised.

Table 3.1: Table of questions for evaluation of the TFN modeling.

Evaluation criteria	Questions to be considered
Conceptualisation	What type of conceptualisation is needed for the model? How extensive is the conceptualisation process?
Data	What type of data is required? Is there a need for data processing?
Area of use	What type of scenarios can the model be applied to? What can be evaluated with the model?
Spatial apsects	How well does the model perform in evaluating spatial aspects?
Uncertainty and model fit	What type of uncertainty is associated with the model? What aspects impact the model fit and how can it be improved?
Time aspect	How time consuming is the modeling process?

3.2 Data used in the modeling process

In this section the data used in the TFN model is presented.

3.2.1 Head observations

The well data was retrieved from Trafikverkets database TMO, the data was made available for this study and can not be accessed by the public. From a list of all wells in the area, the wells with a sufficient amount of data was selected. The groundwater data used for the modeling was not modified in any way to maintain authentic results and to evaluate the model fit based of the observed data acquired. Also since the head observations is the dependent time series, meaning the time series that is to be explained based on the added stresses, it does not according to Collenteur et al. (2020) require regular time steps.

The location of the observation wells that have been used as the basis for this case study can be seen in Figure 3.2 which also displays the location of the measuring mounds for the tunnel leakage and the two infiltration wells.

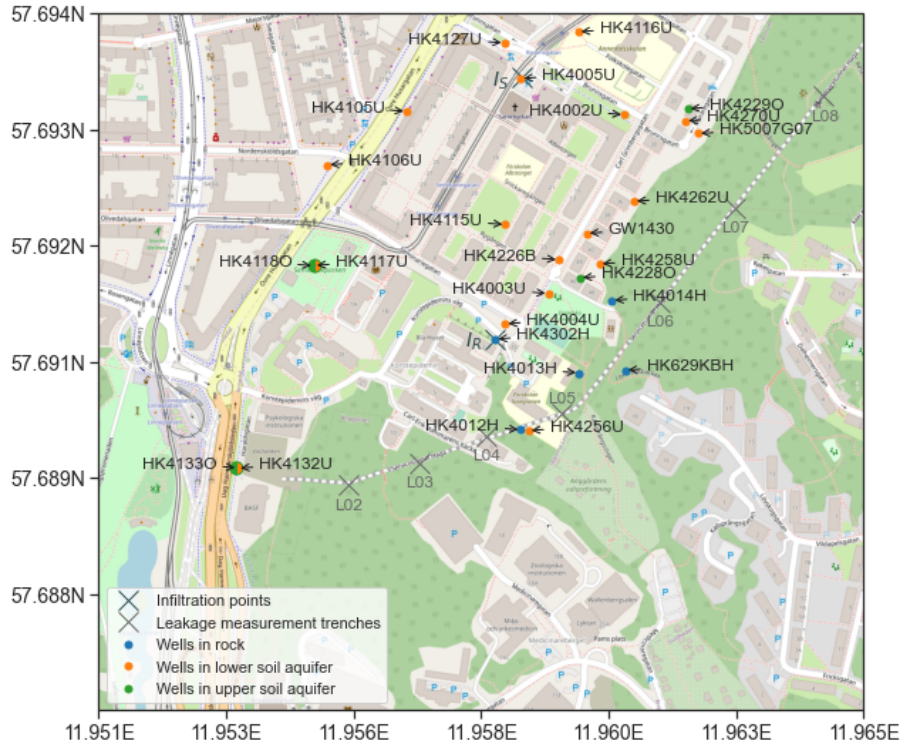

Figure 3.2: Geological placement of the wells in the area.

3.2.2 Evapotranspiration

Five parameters were used to calculate the evapotranspiration. The temperature, sun hours, wind velocity, relative humidity and shortwave radiation. These parameters were used with a daily data frequency, further for the calculations the height above sea level and latitude of the weather station was used.

The environmental data used for the calculation of the evapotranspiration was retrieved from the meteorological observation database provided by SMHI (SMHI, n.d.). Most environmental data came from the weather station "Göteborg A". However for the relative humidity the weather station "Landvetter Flygplats" was used instead as it had more recent measurements. This was assumed to be acceptable, since relative humidity during concurrent periods at both stations had a high correlation ($r>.8$).

The evapotranspiration was calculated with the Penman-Monteith equation using the open source Python package ETo version 1.1.0 created by Kittridge (2019). The package is based of the UN-FAO 56 report by Allen, Pereira, Raes, and Smith (1998) that gives a detailed description on how to calculate evapotranspiration using the Penman-Monteith equation and also a function to estimate missing parameters that are necessary for the equation. See Appendix A.1 for full calculations.

Most of the data needed for the Eto package was imported to Python in the same unit

that was given when the data was downloaded. However, the shortwave radiation data was retrieved expressed in W/m^2 but the unit expected in the evapotranspiration function was MJ/m^2. A column was therefore added to the csv-file containing the shortwave radiation, to preserve the original data, and the data was converted into the new unit in the added column. The unit of the sun hour data was also changed as it was retrieved in sec/h but it was expected in h/day. This change was made after the data had been imported to Python, by dividing the column containing the sun hour data by 3600.

It should be noted that the estimated evapotranspiration is the same for the entire case study area and the calculations do not account for different type of land use. As the environmental parameters were collected from two different weather stations in the Gothenburg area the evapotranspiration should be considered as a general estimation for the Gothenburg area. The evapotranspiration is affected by the type of land use (Fetter, 2014) and the fact that the land use varies greatly at the study site, see Figure 3.2, is a contributing factor of uncertainty.

3.2.3 Precipitation

The precipitation data was retrieved from the weather station Göteborg A, the data was provided by SMHI:s meteorological observation database (SMHI, n.d.).The precipitation data was obtained in mm/day and was not altered before or during use.

3.2.4 Leakage data

In the site study area the leakage data has been measured in seven measuring mounds along the service tunnel called E04-ST210-02 - E04-ST210-08 but in this study they are referred to as L02-L08. This data was received from Trafikverket in one file. It was therefore processed so that the data for each measuring mound could be handled separately. Coordinates for each measuring mound were also received from Trafikverket. The leakage is an independent time series and according to Collenteur et al.(2020) it needs to be assigned regular time steps when handled in Pastas. The leakage data was therefore assigned a daily frequency by interpolating the obtained measurements.

It should be noted that the leakage measurements during a tunnel construction is unavoidably subjected to uncertainty. Aspects that inject uncertainty include the placement of the measuring mounds, the scope for measuring, the time period for the measurements, how often the measurements are conducted, type of measuring equipment, maintenance of equipment and calibration of equipment (Hansson et al., 2010). The blasting for Haga servicetunnel was initiated in august 2018 (Göteborgs Stad, 2018) and leakage measurements are available from July 2019, see subplot *b)* Figure 3.3, with the measuring mounds being installed step-wise as the tunnel progressed. This one year delay in available leakage measurements and the fact that the measurements were sparse in the obtained data should be considered as

contributing factors of uncertainty.

3.2.5 Infiltration data

Infiltration data acquired from Trafikverket was for both infiltration in rock and infiltration into the lower soil aquifer. The data was for the two infiltration wells HK4001BINF, which infiltrates water into the lower soil aquifer and HK4302HINF, which infiltrates water into the rock aquifer. In this study they are referred to as I_S and I_R respectively. The data was converted from L/min to m^3/day with a conversion factor of 1.44. The corresponding coordinates for the infiltration wells were also received from Trafikverket. Likewise as for the leakage, the infiltration is an independent time series and requires regular time steps. The data was therefore assigned a daily frequency by interpolating the obtained measurements. Infiltration data were available from February 2020 for the infiltration into soil and from July 2020 for infiltration in rock, see subplot *c)* Figure 3.3.

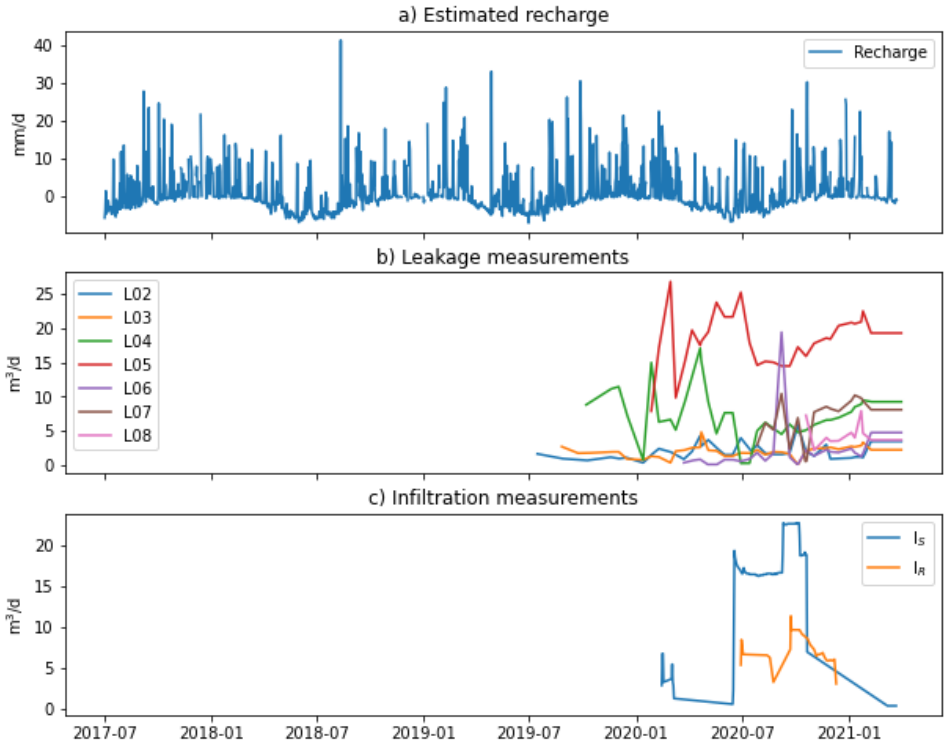

Figure 3.3: Data for recharge, leakage and infiltration which have been used as the three stresses for the groundwater modeling

3.3 Transfer function-noise modeling

Transfer Function-Noise (TFN) modeling, is transient modeling that converts one or several time series inputs through a statistical model to a single output series, a simulation (Collenteur et al., 2019). For simulations of groundwater heads a simple TFN model is:

$$h(t) = \sum_{m=1}^{M} h_m(t) + d + r(t) \tag{3.1}$$

h(t): Observed head
$h_m(t)$: Contribution of a stress m to head
d: base elevation of model
r(t): residuals
t: time

For equation 3.1 there could be several number of stresses M that affects the head. A stress m impacts the groundwater head and is obtained through convolution of the stress time series and a response function:

$$h_m(t) = \int_{-\infty}^{t} s_m(\tau)\theta_m(t-\tau)d\tau \tag{3.2}$$

S_m: The time series of the stress m
θ_m: The response function of the stress m

A stress and a response function is converted into a head contributor, $h_m(t)$, through a *StressModel* like equation 3.2. Each stress can be supplied a different *StressModel*, allowing unique response functions for the stresses. Two or more stresses can be combined into one, as for recharge where $recharge = precipitation - evaporation$ in some cases, then S_m is replaced with the combined stresses as with an appropriate response function (Collenteur et al., 2019).

The response function connects variations in the stress, that is applied to the head, to the fluctuations in the head. Some response functions corresponds better with a certain type of stresses (Bakker & Schaars, 2019). The Gamma distribution is a regularly used response function, that works well for areal recharge according to Collenteur et al. (2019). The impulse response of the gamma response function writes as:

$$\theta(t) = At^{(n-1)}e^{(\frac{-t}{a})} \tag{3.3}$$

A: scaling factor
a and n: shape parameters

The Hantush response function instead better represents the stress caused by a pumping or extraction according to Collenteur et al. (2019). The Hantush response

function is calculated with:

$$\theta(t) = \frac{A}{t} e^{(\frac{-t}{a} - \frac{-ab}{-t})} \tag{3.4}$$

A: scaling factor
a,b: shape parameters

There are a number of response functions that can be used with the *StressModels*, depending on which type of stress is modeled and its expected behavior.

When solving a TFN model, the fit with corresponding goodness of fit metrics and optimal parameter values of the model can be retrieved (Collenteur et al., 2020).

The TFN modeling was performed using the open source Python package Pastas v.0.17.0 (Collenteur et al., 2020). Because of an issue in the objective function $LmfitSolve$ which occurred after updating to this version, the development branch was used instead since the issue had been solved by the creators there and it will be fixed in the next version.

Pastas is dependent on the open source Python package pandas (The pandas development team, 2020) to read, store and manipulate data in so called pandas data frames. From this data Pastas uses transfer function-noise modeling to create a simulated groundwater head time series from groundwater stresses, while also trying to fit the simulation to observed groundwater levels.

The Pastas documentation (Collenteur et al., 2020) provides examples, with the corresponding code, on how TFN models can be used to analyse groundwater levels. For the creation of the model used in this report code from the examples on the website was implemented, with slight alterations to fit the case study of the report. A basic model was constructed and infiltration and leakage were added as additional stresses.

3.3.1 Model parameters

Model parameters are derived with the response function selected for the *StressModel*, when the stresses affecting the groundwater head is modeled as the simulation. The parameters shape the simulation. The parameters will be named after the stress, but denoted with the type of parameter it is based on which depends on what parameters the response functions contains. A ground water model can contain several stresses, all stresses added to the model will generate separate parameters. Some parameters are not connected to the response function, a constant d is generally existing for all models and there is an additional parameter f if modeling a stress with the linear recharge-model.

In the modeling for this study the Gamma response function, see equation 3.3, was used in combination with the linear class of the *RechargeModel* stress-model to simulate the effect of the recharge. For the leakage data and infiltration data a

WellModel stress-model was used that takes the radial distance between the observation well and measuring point of the leakage or infiltration into account. For this stress-model only the *Hantushwellmodel* response function can be used due to the distance factor.

A part of this study is to evaluate in what ways a TFN model can be utilized in infrastructure projects. If the parameters show relation to a physical factor, this could be used to simulate head values where no data exists. Therefore the model parameters that are relevant to evaluate are from the simulation that only has the stress of the recharge. The other stresses used for the calibration were to confirm the impact from leakage and infiltration. Thus, the parameters that will be analysed are Gamma parameters for the *RechargeModel*. Parameters for the other stresses are described and can be found in the Pastas documentation (Collenteur et al., 2020).

All models contain a parameter named constant_d, it is an estimation of the mean of all observed groundwater levels in the model and can be viewed as the base level for the simulation (Collenteur et al., 2020). This parameter, however present in all models, will not be evaluated in the results.

The parameters present in the Gamma response function are the scaling factor A and the shape parameters a and n. More detailed information about the parameters can be found in the Pastas documentation (Collenteur et al., 2020).

When modeling with the linear class of the *RechargeModel*, where precipitation and evapotranspiration is combined, there is an additional parameter f referred to as the evaporation factor. The equation used for the linear *RechargeModel* is (Collenteur et al., 2020):

$$R = P - f * E \tag{3.5}$$

R: Recharge
P: Precipitation
f: Evaporation factor
E: Evaporation

The evaporation factor is calculated based on the response magnitudes of the precipitation and evaporation, on the estimation that they share the same shape parameters since they are modeled in one stress-model with the same response function. The factor f as expressed by (Obergfell, Bakker, & Maas, 2019) is:

$$f = \frac{M_e}{M_p} \tag{3.6}$$

M_e and M_p : Response magnitudes

The factor f is calibrated when solving the TFN model. The parameter f has an upper limit of 0 and lower limit of -2, that regulates the actual evaporation between zero and twice the reference evaporation (Collenteur et al., 2019).

3.3.2 Goodness of fit metrics

After solving a TFN model in Pastas a fit report on the simulation fit can be retrieved showing settings from the solve of the model, a range of goodness of fit metrics and optimal values of some parameters obtained from the fitting procedure. The goodness of fit metric presented in the fit report are the Explained Variance Percentage (EVP), coefficient of determination (R^2), Root Mean Squared Error (RMSE), Bayesian Information Criterium (BIC) and Akaike Information Criterium (AIC).

R^2 was used for evaluating the model fit in this study. The R^2 value is a measure of how much of the model input that can be tied to the variation in the simulation, it has a maximum value of 1 that implies a perfect fit of the simulation to the observed values (Collenteur et al., 2020).

The use of R^2 as a goodness of fit metric has been widely discussed according to Hagquist and Stenbeck(1998). A few points brought up in the article by Hagquist and Stenbeck (1998) are that the range that is set between 0 and 1 leaves no interpretation of the variance that has to be explained to obtain a good fit, that the metric is sample-specific and the R^2 value therefore can differ between samples that have otherwise similar regression coefficients. Some debate, as described by Hagquist and Stenbeck (1998) that R^2 can be used as a goodness of fit metric but not a statistic test for the goodness of fit. Further in the article it is argued that R^2 can be used as long as the results between samples are not compared or that these limitations of the metrics are known when interpreting the results. The R^2 goodness of fit metric was therefore still used for evaluation of the fit of the model in this study, the cautions from the article were considered even tough only one data set was modeled at a time.

3.3.2.1 Checking model diagnostics

If a model is to be used for inference, a model diagnostic check should be preformed according to Colleteur et al. (2020). Pastas has a method for automatic diagnostic checking, producing a report containing the statistical tests performed and what they test for, which are further explained in the Pastas documentation (Collenteur et al., 2020) .

In Pastas the residuals of the TFN model is what is evaluated when conducting a diagnostic check (Collenteur et al., 2020). Residuals can be seen as the differentials between observed values and simulated values. Large residuals will mean a simulation less fitted to the observed values (Anscombe & Tukey, 1963). Auto correlations between residuals indicate that not all information from the time series, like trends or seasonal effects, was used for the simulation resulting in a simulation that is less fitted to the observed values (Hyndman & Athanasopoulos, 2018). If a noise model was incorporated in the modeling process in Pastas the residuals can also, or instead, be in the form of a noise series. Noise is the presence of errors in the data that does not reflect the reality, unexpected variances that disrupts simula-

tions based of the data (Djeddou, 2016). Noise is always present in a model, but for a model that can be considered sufficient the noise should preferably act as white noise. White noise is when the series errors are altogether random and is what is left when the model has extracted all information possible from the input time series (Brownlee, 2020). By default a noise model is used in the TFN model in Pastas, to convert the residual time series to a noise series that is more similar to white noise. Statistical tests in Pastas evaluates if the residuals act as white noise, based on if the residuals are independent,normally distributed or homoscedastic(Collenteur et al., 2020).

3.4 Modeling strategy

3.4.1 Model setup

Choices for the model such as the selection of stress-model, response function, objective function and usage of a noise model or not were based mostly of recommendations from the examples in the Pastas documentation (Collenteur et al., 2020). However a trial was also made where different settings were run and compared for a majority of the wells, this trial supported the choices motivated by the literature.

Two stress models were used for the groundwater modeling in this study, to simulate the behavior of two different kind of stresses. A linear *RechargeModel* was selected as recommended in several examples in the Pastas documentation (Collenteur et al., 2020) since it calculates the recharge using both precipitation and evapotranspiration to simulate the impact made on the groundwater head (Collenteur et al., 2019). The linear class of the *RechargeModel* was selected as it gave the best fit for the model. It uses the response function to consider the effect of the root zone to the recharge and therefore often requires a more complex response function. Some hydrogeological conditions are, however, hard to compensate for and can result in a less than adequate fit, like low soil moisture content (Collenteur et al., 2020). Using a linear *RechargeModel* class is likely to give decent results for wells that act linearly, which is often true for shallow wells located a few meters below the ground surface in temperate climates (Bakker & Schaars, 2019). It should be noted that for this case study several deep wells were used for the modeling and it can be questioned whether their response is in fact linear. As stated by Colleteur et al. (2020) the linear class can still be used when modeling groundwater levels although not optimal for all wells. For the leakage and infiltration a *WellModel* was used since this stress model can account for reduced or increased impact on the groundwater depending on the distance between the observation well and the place of the stress measurement (Collenteur et al., 2020).

For the recharge a Gamma response was used since it, as written by Collenteur et al. (2019) , is an adverse response function that can be used for many stresses on groundwater levels and simulates the effects of areal recharge well. When adding the leakage and infiltration the *Hantushwellmodel* response function which is an adapted version of the Hantush response function, which allows for an extra input

argument containing the radial distance between the well and place of measure for the stress, was used (Collenteur et al., 2020).

For the objective function in Pastas the *LmfitSolve* was used which is a non-linear least square minimization. This was selected over the otherwise default *LeastSquares* option, on recommendations from the documentations by Colleteur et al. (2020) as a bug can occur, in the Pastas version used when writing this study, that can make the result unreliable when using a *Wellmodel* with the *LeastSquares* objective function if the parameters estimated were much smaller than one.

The transfer functions noise models in Pastas can be run without a noisemodel. According to Collenteur et al. (2019) using a noise model when modeling with high frequency data , which was specified as days or shorter intervals, the default noise models can cause a more sensitive parameter estimation and thereby a less fitted simulation compared to when modeled without a noise model. For the modeling in this study a noise model was therefore not used as a daily frequency was used. A new noise model has been developed for the Pastas package, however, there was no time to properly test this on the model in this study. When modeling without a noise model, inference should not be conducted on the results according to Collenteur et al. (2020).

3.4.2 Calibrating the TFN model

A poor model fit could be the result of one or several missing stresses in a model as mentioned by Bakker and Schaars (2019). The fit of a basic model, were only recharge effects the groundwater level, should therefore be analysed to evaluate if a better fit could be acquired by adding additional stresses if available. As it was known that tunnel leakage and infiltration had occurred in the area modeled in this study, it was assumed that a higher model fit could be obtained by adding the missing stresses. Seeing that the aim of the study also was to evaluate if the model could be used to asses the change in groundwater heads, as a result of drainage and infiltration, the corresponding stress had to be added for this purpose as well.

Leakage was added as a *WellModel* as described by Collenteur et al. (2020) with the measuring mounds being represented as multiple groundwater pumping wells. If the model fit was improved, after the addition, this could be seen as an indication that the leakage had impacted the groundwater head for the well. The infiltration was also added to the model as a *WellModel*, the only difference being that the groundwater response was changed so that the groundwater levels would go up as a result of the infiltration compared to the impact from the leakage that lowers the levels. If the model fit was improved by the addition of the infiltration it could indicate that the well had been impacted by the infiltration in the area.

The model containing recharge, leakage and infiltration is from now on referred to as the calibrated model in this study, see Appendix A.2 for full model set up. The model fit of the calibrated model for all wells in the area with the corresponding

stress contribution to the simulated groundwater heads is presented in section 4.2.1. The stress contribution was extracted from one day, 2021-10-01, where the leakage and infiltration measurements displayed overall high rates. The stress contribution was divided for the the two infiltration wells and seven measuring mounds to enable for a quantification of their respective contribution. In addition to this, five wells which had been affected differently by the drainage and infiltration were selected to visualize the calibration process as well as to enable a more in depth analysis on the impact on the groundwater heads for the specific wells. The selected wells were HK4004U, HK4117U, HK4226B, HK4014H and HK4116U. They were chosen since they displayed one well that had been less affected by the tunnel construction, one that had been clearly affected by the leakage, one that had been clearly affected by the infiltration, one that was placed in the rock aquifer and one that displayed a lower model fit. This is presented in section 4.2.2 coupled with a stress contribution plot for the calibrated model in order to quantify the contribution on the groundwater heads for the respective stress. The contribution from the infiltration in the plot represents the combined contribution from the two infiltration wells and likewise the contribution from the leakage represents the combined contribution from the seven measuring mounds.

3.4.3 Simulating different leakage and infiltration scenarios

After a calibration process is finalised the produced calibrated model can be used as a basis for predictive analysis of different stress scenarios. Although it can be evident after the calibration process if the evaluated well has been impacted by drainage or infiltration, by looking at the change in model fit, this can be better quantified by making a predictive analysis based on the calibrated model. By removing the contribution of the drainage and infiltration from the calibrated model, but still keeping the obtained optimal parameters, a simulation of the groundwater heads could be made to evaluate which groundwater levels the wells would have had without the tunnel construction. In addition to this, the contribution from the drainage and infiltration was altered and a predictive analysis of different scenarios was conducted based on the calibrated model.

Three different stress scenarios were sub-plotted for comparison. The first plot visualises the calibrated model compared to a simulation without the contribution from infiltration and a simulation with both the contribution from infiltration and leakage removed, in other words a simulation that represents what the groundwater levels would have been without the tunnel construction. In the second plot the leakage contribution was altered but the infiltration contribution from the calibrated model was kept. In the third plot the infiltration contribution was altered but the leakage contribution from the calibrated model was kept. The full model set up for the stress simulations is presented in Appendix A.2.

3.5 Cluster analysis

To evaluate which wells had similar impact by the tunnel construction a cluster analysis was performed. Agglomerative hierarchical clustering was selected as the clustering method, it groups the input data based on how similar the data is starting from the conception that each input data is one cluster (Chaitanya Reddy Patlolla, 2018). The hierarchical clustering was carried out using the Ward algorithm together with Euclidean distance. This combination was selected as the ward algorithm has been demonstrated by Haaf and Barthel (2018) to result in clusters which are both consistent and homogeneous and the euclidean distance sufficiently distinguishes similarities in the time domain.

The agglomerative hierarchical clustering was performed on two data sets, residual series and model parameters. To group the modeled observation wells together according to the impact from the the tunnel, the residuals of the modeled scenario were only recharge affects the groundwater levels were used. This clustering was preformed to evaluate if the impact could be connected to the location of the wells or other physical factors. The residuals were calculated by subtracting the values from the simulation with the head values observed. The residual series were centralized for all wells in the cluster analysis. Some residual series have more data than others. To cluster the series, data was required with the same frequency (days in this case), the data missing was therefore interpolated. This method gave a more coherent result than filling the missing dates with zeros.

The parameters of the recharge stress model from the calibrated model were also evaluated using cluster analysis to examine how the model is parameterised. If a pattern of some sort is found among the parametrisation of the simulations for the wells, this could be used to model simulations of groundwater head values belonging to the same category even if no measured data is available. The parameters were normalised before conducting the cluster analysis, as parameters with larger values otherwise dominates the clustering. Some factors that the parameter clusters will be compared to are the geologic location, the filter depth, the groundwater levels and how effected they might be from the tunnel construction.

The clustering was preformed in Python with functions from the scipy.clustering.hierarchy package (Virtanen et al., 2020) and also through a library named Dendrogramts (Teo, 2021), which when called creates a dendrogram with the time series plotted besides the dendrogram. This package was still in development during this study. Therefore the graphs had to be manually altered to add the well ID labels and in some cases place the clustered series in correct order. A dendrogram is a branch diagram, see Figure 3.4, which is built on the principle where each series start in a separate cluster, a leaf. The series are grouped with the most similar series, a clade is placed at the distance separating them. Series are grouped until a suitable number of clusters are reached, a greater distance means series less related.

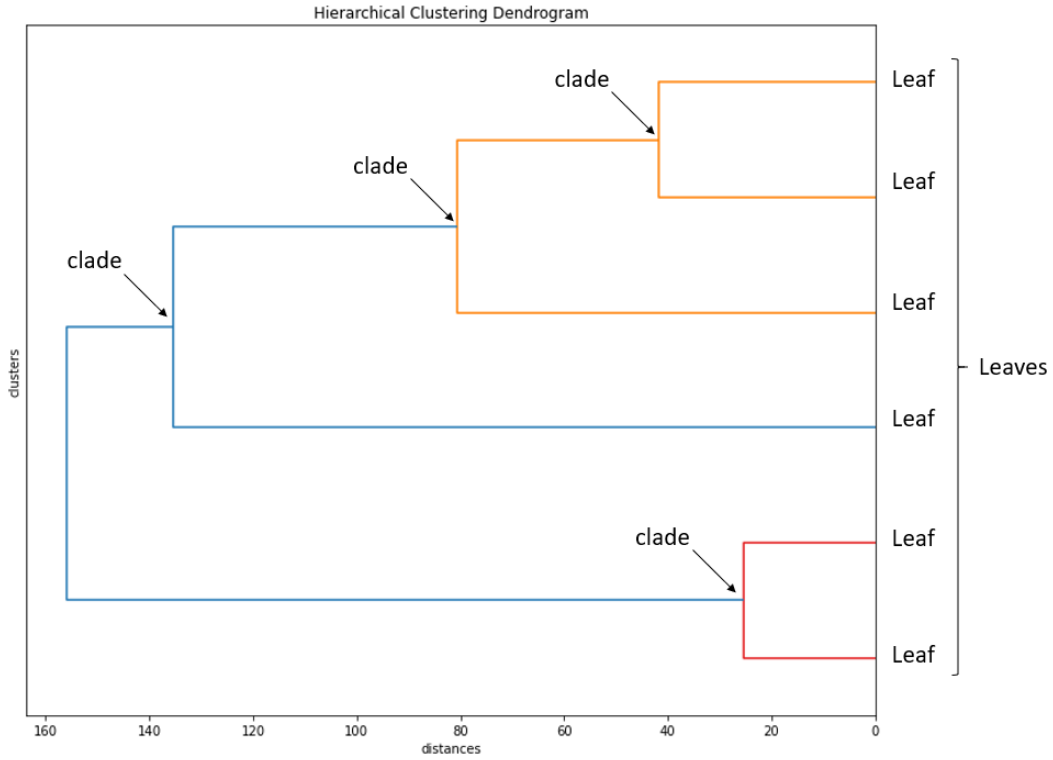

Figure 3.4: Structure of a hierarchical clustering dendrogram.

3.6 Relationship between model parameters and site physical characteristics

To examine the possible relations of the model parameters against site physical characteristics such as certain height variables, the correlations of the two were evaluated. Height variables as the mean, minimum and maximum ground water level were extracted from the observed groundwater head series. The correlation of the filter depth and ground level against the parameters are of interest to evaluate if the parametrisation, which regulates the fit of the simulation to the observed values, can be tied to variables which are not present in the data processed by the model. Parameters are estimated when solving the model. The calibrated model, from which the parameters were retrieved, was solved with non-linear least square minimisation.

The evaluation of the correlation was performed using Pearson and Spearman correlation coefficients. For the analysis coefficient values of 0-0.3 will be considered as no correlation, 0.3-0.5 as weak positive correlation, 0.5-0.8 moderate positive correlation and 0.8-1 as strong positive correlation. The same goes for negative correlations. To analyse the correlation between the parameters and the variables further the wells were also stratified according to their geological placement, rock or soil. The correlation matrices were calculated with the pandas (The pandas development team, 2020) correlation function *.corr*(). The visualisation was then performed with Matplotlib (Hunter, 2007) boxplots and scatter plots as well as Seaborn (Waskom, 2021) heatmaps.

3.7 Spatial plotting

For this study the spatial plotting was made using the Python package Cartopy (Met Office, 2010 - 2015). The code to plot a map over the site study area with the observation wells was retrieved from an example made by Hirsko (2020). The map is based of a shape-file retrieved from Trafikverket.

4
Results

4.1 Evaluation of TFN models as a groundwater modeling tool

This section aims to present information on how transfer function-noise models can be applied when evaluating groundwater head changes and the associated potential and limitations with the model. This is done by answering the stated questions in Table 3.1.

4.1.1 Conceptualisation

What type of conceptualisation is needed for the model and how extensive is the conceptualisation process?

Unlike a regular process based groundwater model, which often requires an extensive conceptualisation of the study area, TFN models only require a small number of parameters as input for the model (Bakker & Schaars, 2019). Although not vital to build TFN models a rough conceptualisation of the geologic and hydrogeologic conditions can contribute with important knowledge when evaluating the robustness of the results as well as enabling conclusions to be drawn of why the groundwater heads vary in the area. For the site study it was necessary to establish the stresses that could have an impact on the groundwater levels in the area, namely the recharge, the infiltration in the area and the tunnel leakage. Placement of the groundwater observation wells in relation to the infiltration wells and the tunnel also had to be established.

4.1.2 Data

What type of data is required and is there a need for data processing?

The type of data needed to build TFN models depends on the area of use. At a minimum one stress, preferably the recharge for the area, as well as head observations for the observed well are necessary. To calculate the recharge, climate data for precipitation and evapotranspiration are required which in Sweden is readily available from the Swedish Meteorological and Hydrological Institute, SMHI at a large number of locations within Sweden. Other examples of stresses could be leakage, infiltration, pumping or contributions from rivers.

The small amount of data processing that is required to construct TFN models in Pastas, could easily be handled in the Python package pandas and the use of a large amount of data is also easily handled in pandas. The type of data processing that is required is making sure that the independent time series have regular time steps with the same frequency (Collenteur et al., 2020). This can be achieved through interpolation if the obtained data does not have regular time steps.

Preferably long time series with high frequency data should be available to obtain the best possible model fit. In addition to this, the groundwater heads should be inspected before use, to evaluate if there are any deviating groundwater levels or big gaps in the time series data that should be accounted for. Assessing if the seasonal variations are reasonable is also important (Bakker & Schaars, 2019).

4.1.3 Area of use

What type of scenarios can the model be applied to and what can be evaluated with the model?

TFN models can according to Bakker and Schaars (2019) help in evaluating the effects caused by stresses on groundwater heads in observation wells, they can be used to discover groundwater diversions or to assess influences of seasonal fluctuations or developments caused by climate change. They could also be a valuable compliment to numerical modeling. According to Bakker and Schaars (2019) establishing a TFN model and analysing the time series before creating a numerical model can save time. From a time series analysis, outliers and other disturbances in the data set can be detected and cleared, if necessary, from the series. It can also be possible to evaluate what stresses and or processes that should be included in the process based numerical model. Also, as written by Bakker and Schaars (2019) the fit of a TFN model simulation can indicate what results to obtain from a numerical model. They further state that a bad fit on a TFN model based of certain stresses seldom generates a significantly better result when modeled with a numerical model. A head series which produces a model with a bad fit should therefore be cautiously used, as it is not an accurate representation of the aquifer.

4.1.4 Spatial representation

How well does the model perform in evaluating spatial aspects?

Pastas has no built in spatial plotting. If spatial relations are requested for the TFN model, this has to be carried out with an external method. There are several packages available for Python that can be used for this purpose. To get relevant spatial plots a cluster analysis, as presented in section 4.2.3, could be used to group observation wells with similar responses. Unlike numerical groundwater models, for example MODFLOW, which could be used to simulate groundwater head changes over the entire case study area (Kumar, 2013), the TFN model can only simulate

the groundwater head changes for the observed wells. If a more comprehensive visualisation of the groundwater heads in the area is required to evaluate the impact due to leakage or infiltration, an additional method must be applied.

4.1.5 Uncertainty and model fit

What type of uncertainty is associated with the model? What aspects impact the model fit and how can it be improved?

Like for all groundwater models a TFN model is inevitably subjected to uncertainty. Challenges in transient groundwater modeling include assessing the accuracy of the model fit as well as improving the model fit. There is a need to assess the accuracy of the model fit to evaluate if it is possible to make statistical conclusion based on the simulation. If a poor model fit is obtained it poses challenge to establish the reason behind it. Example of events that can cause a poor model fit, this is also true for regular groundwater models, are: inaccurate head measurements, inaccurate stress measurements, missing stresses, missing or inaccurate hydrogeological processes in the model or that there has been a substantial change in the system behaviour. As mentioned this is also true for regular groundwater models. However, during TFN modeling a constant comparison of modeled heads with measured heads is performed with the aim to achieve the best possible model fit, as a result the modeller is continuously made aware of these challenges (Bakker & Schaars, 2019).

There are several calibration options that can be performed to obtain a higher model fit of the TFN models in Pastas as described by Collenteur et.al (2020). These include removing observations, changing the calibration period, adapting the initial parameters, changing the response function, changing the solve method, changing units and normalising the time series. The methods for doing this is described in the Pastas documentation.

It should be noted that in order to reduce the uncertainty associated with calibrated models a diagnostic check should be performed, if a noise model has been used and inferences will be drawn from the results. The diagnostic checking is important if you want to evaluate if the calibrated model can be used to make any type of inferences, especially if standard errors for the obtained parameters are used for any assumptions. If the residuals and noise agree with a few assumptions it can be assumed that the standard errors are estimated accurately. A method for doing diagnostics checking on residuals or noise, if a noise model was used, is available in Pastas. The diagnostics checking include checking for auto correlation, homoscedasticity and normality (Collenteur et al., 2020).

4.1.6 Time aspect

How time consuming is the modeling process?

According to Bakker and Schaars (2019) time series analysis is a much quicker

method for the evaluation of groundwater heads compared to developing a regular groundwater model for the same purpose. This is largely due to the fact that a regular process based groundwater model requires a much more detailed conceptualisation process. The experience during this study was that the creation of a first basic model did not require much time. This was greatly facilitated by the fact that the code to set up a basic was readily available on Pastas website. The only time consuming aspect was the data processing but still this was also facilitated by the use of pandas. The entire calibration process was rather quickly performed. The process of making predictive analysis based on the calibrated model was however somewhat more time consuming. This was largely due to trying different approaches before deciding on the one presented in section 3.4.3. Thus it can be said that once a framework for using the TFN model to evaluate groundwater head changes due to drainage and leakage is produced, the modeling is a rather quickly performed task. By creating for loops in Python several wells in the site study area could be modeled simultaneously. It was however discovered during this study that running the model for some wells in the case study area was a more time consuming task, with run times ranging up to an hour. This was often true for the wells that had large gaps in the data, a small amount of data or clear outliers and the model fit was generally lower for these wells.

4.2 Model outcome

In Section 4.2.1 the obtained model fit, expressed as R^2, after calibration for all the selected wells in the area is presented coupled with the corresponding stress contribution to the simulated groundwater heads . In Section 4.2.2 the results from the calibration process for five of the wells in the site study area are presented. The stress simulation results based on the calibrated model for the same wells are also presented.

4.2.1 Obtained model fit and stress contribution for the observation wells

In Table 4.1 the R^2 for the calibrated model for the observation wells with the corresponding stress contribution to the simulated groundwater heads is presented. As HK4012H was cast closed in in September 2019 no stress contribution can be seen for this well.

Table 4.1: R^2 value and the stress contribution, for 2020-10-01, from the two infiltration wells and the seven leakage measuring mounds for each observation well.

Well ID	R^2	Stress contribution [m]								
	[%]	I_S	I_R	L02	L03	L04	L05	L06	L07	L08
GW1430	94	0.466	0.197	-0.002	-0.002	-0.019	-0.090	-0.021	-0.038	0
HK4002U	95	1.610	0.374	-0.012	-0.006	-0.031	-0.101	-0.019	-0.053	0
HK4003U	86	0	0.217	0	0	0	0	0	0	0
HK4004U	81	0.013	0.166	-0.002	-0.005	-0.038	-0.088	-0.001	0	0
HK4005U	94	7.08	0	-0.060	-0.006	-0.070	-0.228	-0.005	-0.083	0
HK4012H	74	-	-	-	-	-	-	-	-	-
HK4013H	47	0	0	-0.052	-0.063	-0.388	-2.242	-0.269	-0.164	0
HK4014H	84	0.129	0.273	-0.050	-0.050	-0.209	-0.771	-0.187	-0.182	0
HK4105U	78	2.121	0.002	-0.100	0	-1.070	-1.825	-0.063	-0.002	0
HK4106U	69	0.178	0.016	-0.019	-0.024	-0.068	-0.105	-0.055	-0.013	0
HK4115U	92	0.629	0.283	-0.002	-0.004	-0.020	-0.068	-0.041	-0.018	0
HK4116U	24	0	0	0	0	-0.002	-0.002	-0.001	0	0
HK4117U	95	0.055	0.054	-0.043	-0.034	-0.115	-0.260	-0.048	-0.034	0
HK4118O	74	0	0	-0.196	-0.171	-0.459	-0.992	-0.050	-0.018	0
HK4127U	97	0	0	0	0	0	0	0	0	0
HK4132U	89	0.124	0.175	-0.479	-0.024	-0.001	0	0	0	0
HK4133O	52	0	0	0	0	0	0	0	0	0
HK4226B	83	0.698	0.342	0	0	0	0	0	0	0
HK4228O	50	0	0	0	0	-0.007	-0.037	-0.012	0	0
HK4229O	60	0	0	0	0	0	-0.001	-0.001	-0.023	0
HK4256U	79	0	0.937	-0.178	-0.118	-0.653	-1.946	-0.215	-0.199	0
HK4258U	68	0	0	0	0	0	0	0	0	0
HK4262U	85	0.873	0.231	0	0	-0.001	-0.005	-0.020	-0.019	0
HK4270U	91	0.871	0.004	-0.001	-0.002	-0.025	-0.139	-0.128	-1.217	0
HK4302H	23	0	0	-0.009	-0.034	-0.338	-1.014	-0.019	0	0
HK5007G07	91	1.288	0.028	-0.004	-0.008	-0.068	-0.312	-0.247	-1.451	0
HK629KBH	93	0	0.025	-0.230	-0.186	-0.803	-2.724	-0.403	-0.450	0

When evaluating the the model fit results of the basic model for several wells in the area it was evident that for many the fit was poor. After the calibration of the model the fit had increased. The model fit of the calibrated model was plotted on a map, see Figure 4.1, where a high value of R^2 represent a good fit.

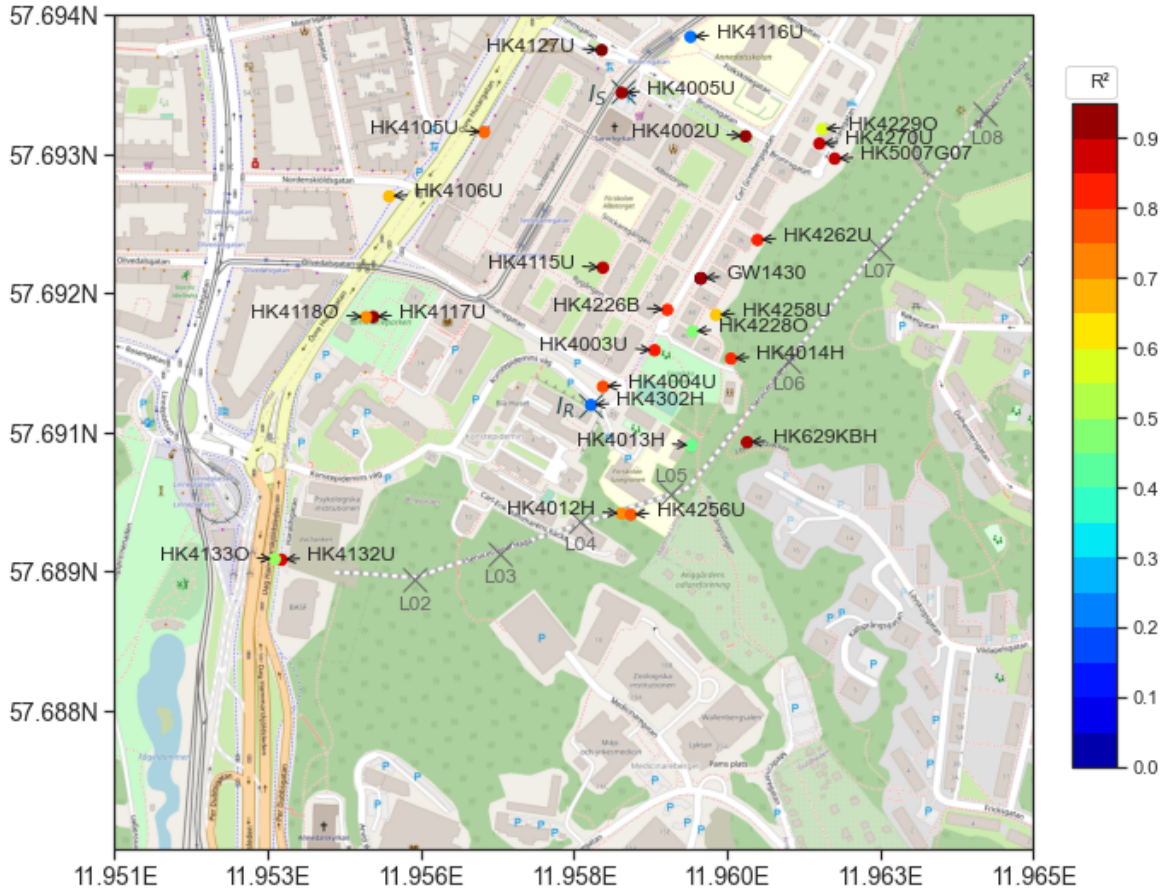

Figure 4.1: Map showing model fit in the area with the color representing the R^2 value for the simulation of that well.

Although the R^2 of the model fit is generally high in the area, for six of the observed wells the obtained model fit was slightly lower with an R^2 value below 60%, see Table 4.1. After evaluating the simulation results for these seven wells some contributing factors could be established. Three out of these six wells are wells located in the upper soil aquifer namely HK4229O, HK4133O and HK4228O. When looking at the head observations for these wells some outliers could be identified during the entire simulated time period and thus it can be said that these observations are likely not a result of the tunnel construction. However, there exists shallow drainage in the area which most likely affects wells in the upper aquifer. Seeing that this stress is not accounted for in the simulations this could be one contributing factor for wells in the upper aquifer achieving a lower model fit. Removing a clear outlier in the groundwater head observations for HK4133O improves the model fit slightly with 5 percentage points. Measures taken to improve the model fit for HK4229O and HK4228O included removing outliers and changing the calibration period. However, this did not result in an improved model fit and thus this should be further

investigated before doing any type of predictive analysis based on these simulations.

One well is also placed in the lower soil aquifer, HK4116U, and reviewing the simulation results for this well shows that the simulation is not able to account for significant drops in the groundwater levels that occur each summer. These drops occurred even before the start of the tunnel construction and almost no stress contribution from leakage can be seen for this well, so it is likely that there is something else causing these drops which can not merely be attributed to seasonal changes. There are several draining underground structures in the area and this might be what is causing the significant drop of groundwater levels each summer in combination with a lowered recharge rate. It can be said that shortening the calibration period significantly improved the model fit from 24% to 77%. This as there were more available head observations, leakage and infiltration measurements toward the end of the simulation. Consequently, an overall better fit is achieved.

Two of the wells are also placed in the rock aquifer HK4013H and HK4302H. When analysing the results for HK4013H it is clear that the reason for a low model fit for this well is due to the fact that the simulation is not able to account for a significant drop in the groundwater level at the beginning of 2020. This drop is likely due to leakage from the tunnel construction since the stress contribution plot indicates that this is when the impact from the leakage begins. It can be said that the well has been greatly impacted by the leakage and the stress contribution is significant, still the simulation is not able to account for the lowered groundwater levels. The drop at beginning of 2020 occurs rapidly and this is likely an immediate response on the groundwater levels due to the leakage. One reason for the simulation not being able to account for an immediate response might be due to limitations of the incorporated Hantush response function or simply due to incomplete or missing leakage measurements. When changing the calibration period for HK4013H to begin after the significant drop the model fit is significantly improved from 47% to 71%. Regarding HK4302H a significant drop in the groundwater level occurred shortly before October 2019. Again the fact that the simulation is not able to account for this drop is likely due to the fact that no leakage measurements were available at this point in time. Likewise as for HK4013H changing the calibration period for HK4302H to begin after the significant drop in groundwater level improves the model fit from 23% to 54%.

4.2.2 Calibration and stress simulation results

This section presents the calibration and stress simulation results for five selected wells in the site study area.

4.2.2.1 Well HK4004U

HK4004U is located in the lower soil aquifer with the groundwater flowing from south of the well toward the center of the aquifer, see Figure 2.4. The simulation results for HK4004U, in Figure 4.2, indicate that tunnel construction has had a low impact on the groundwater levels for this specific well. This since seeing that the

model fit only improves slightly with approximately 5 percentage points when adding additional stress from tunnel leakage and infiltration. However, it can be seen in the stress contribution plot, in Figure 4.2, that both the infiltration and leakage has had a small but counteracting effect on the groundwater levels. This is likely the cause for the small improvement of the model fit for the calibratd model. When looking at the stress contribution it is clear that the recharge is the stress that has the biggest impact on the groundwater level simulation and this is further supported by the clear seasonal variation demonstrated by the well. However, HK4004U is located right next to the rock infiltration well I_R thus it could be expected that the infiltration would have a larger impact on the well, even despite the fact that the leakage has counteracted the impact to some extent. Looking at Table 4.1 it can, as expected, be seen that it is the rock infiltration which has the most contributing impact on the groundwater levels and a smaller impact can be seen from the soil infiltration. One explanation for the rock infiltration not having a more significant impact might be the fact that the fractures in the rock carried the groundwater in a different direction from the well.

It can be noted that the simulation manages to account for the high peaks in the groundwater levels but does not account for the low levels to the same extent. This might be due to limitations with using a linear recharge model one a well that demonstrates non-linear behaviour. However, according to Colleteur et al. (2020) a linear recharge model is on the contrary more likely to overestimate low groundwater levels. Thus it is more likely that the low groundwater levels are due to draining underground structures or missing leakage measurements which are not accounted for in the simulation. HK4004U demonstrates similar behaviour to several other wells in the area, wells that are less impacted by the tunnel construction, and this is further discussed in section 4.2.3.2.

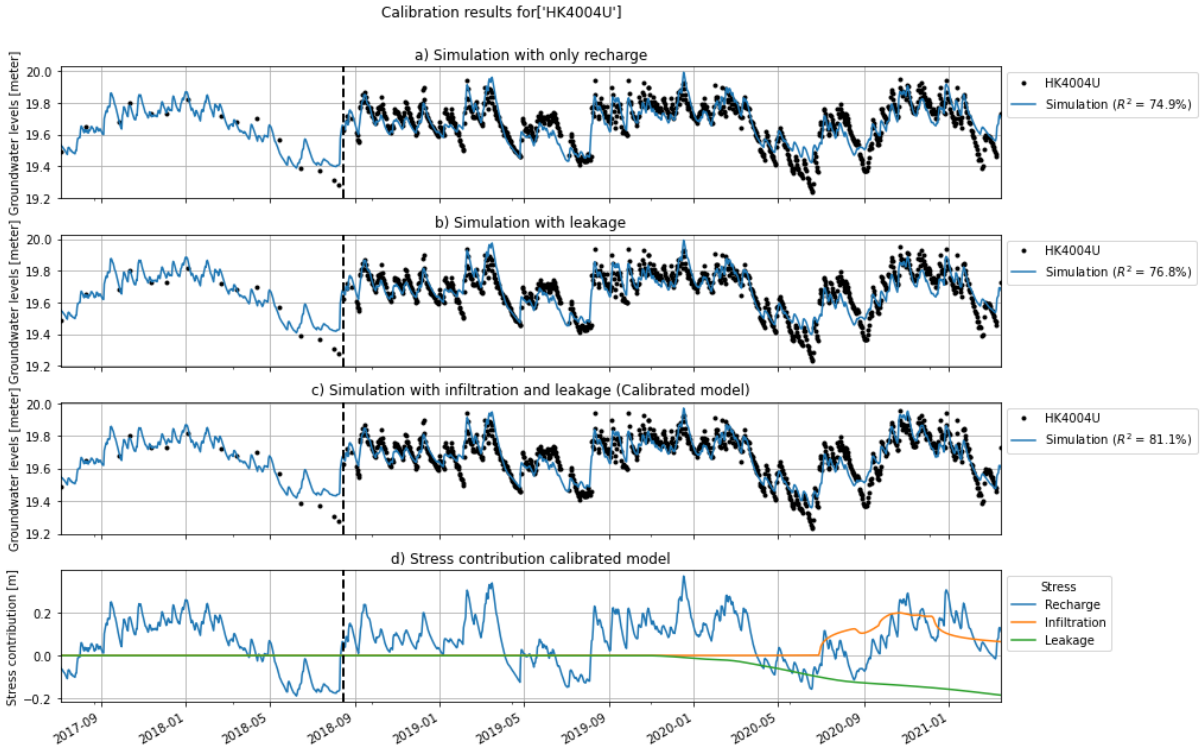

Figure 4.2: Calibration results for HK4004U. The black line visualizes the start of the construction of Haga service tunnel

In Figure 4.3, the simulation results for different stress scenarios for HK4004U are presented. When looking at Figure 4.3 it is clear that only a small difference can be seen between the different scenarios. This is of course directly linked to the fact that the stress contribution from both the leakage and infiltration for the calibrated model is small, even when making the contribution twice as large or twice as small. Simulation scenario 'Simulation w/o leakage or infiltration' in orange visualizes what the groundwater levels would have been without the tunnel construction. In Figure 4.4 the average difference in groundwater head between the calibrated model and the different stress scenarios can be seen. The fact that the mean difference in groundwater head between this simulation and the calibrated model is only 0.025 m further emphasizes that the tunnel construction has had a low impact on well HK4004U. It can also be seen in Figure 4.4 that without the counteracting effect from the infiltration the groundwater levels would have been on average approximately 0.075 m lower. Thus the reason for the well not being significantly impacted by the tunnel construction is due to the counteracting effect of leakage and infiltration.

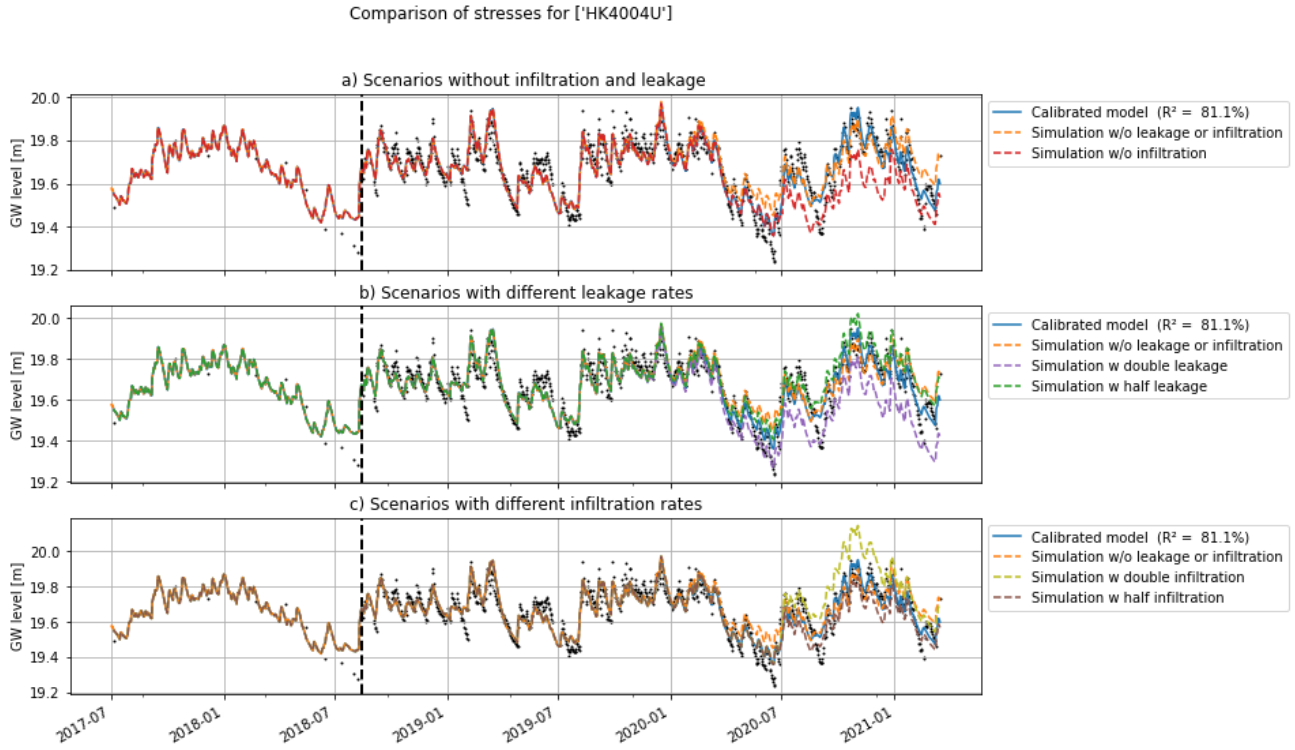

Figure 4.3: Stress simulation results for HK4004U. The black line visualizes the start of the construction of Haga service tunnel

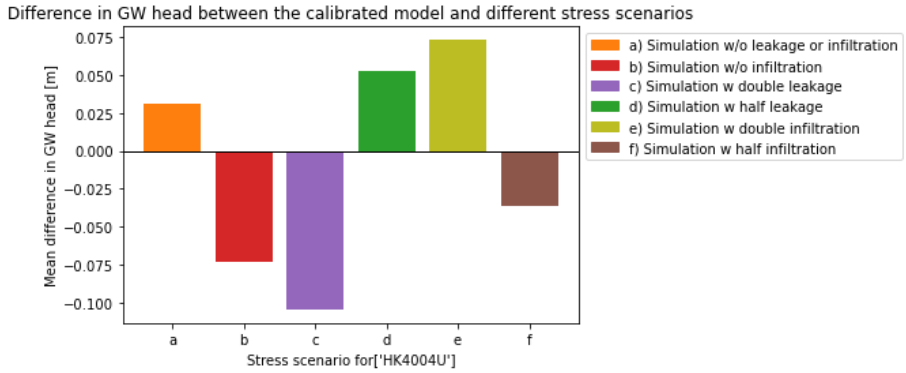

Figure 4.4: Mean difference in groundwater head, during 2020-01-01 to 2021-03-24, between the calibrated model and different stress scenarios for HK4004U

4.2.2.2 Well HK4117U

The simulation results for well HK4117U, in Figure 4.5, indicate that the the tunnel leakage has had an impact on the groundwater levels for the well. This is based on the fact that adding leakage significantly improves the model fit of the simulation. The model fit does not significantly improve when adding infiltration and therefore it can be argued that the infiltration in the area has not impacted the well. Hower, when looking at stress contribution plot in Figure 4.5 and Table 4.1 it is obvious that both infiltration wells has had a small and similar stress contribution, still the total stress contribution during the entire time period from the leakage is higher and thus the impact from the infiltration is less evident. The calibrated model achieve a very high model fit of 94.6% and is thus likely that the calibrated model include the relevant stresses. The simulations try to achieve the best possible fit to all observation points and this is why the lowered groundwater levels due to leakage results in the simulation underestimating the groundwater levels from the beginning of the simulation until around July 2019 for the simulation that only uses recharge as a stress. The drop from the middle of July 2020 can not only be attributed to natural driving forces and when adding leakage this also improves the model fit before the leakage has occurred, this since the model can better determine what the natural variation due to recharge is.

Likewise as for HK4004U, HK4117U is located in the lower soil aquifer but located further away from the tunnel at a lower altitude, see Figure 2.4. The groundwater can be said to flow from the location of the tunnel toward HK4117U in a north western direction. HK4117U is also located in proximity to the large weakness zone with dominating fractures in the NNW-SSE direction which stretches from the service tunnel to Övre Husargatan see Figure 2.2. The connection through the weakness zone to the service tunnel is a likely reason for the well being impacted by the tunnel leakage. HK4117U demonstrates similar behaviour to several other wells in the area, classified as wells that are less impacted by the tunnel construction. This is likely due to the contribution from the leakage being quite small in comparison to other wells and the fact that the infiltration has a counteracting effect, this is discussed further in section 4.2.3.2.

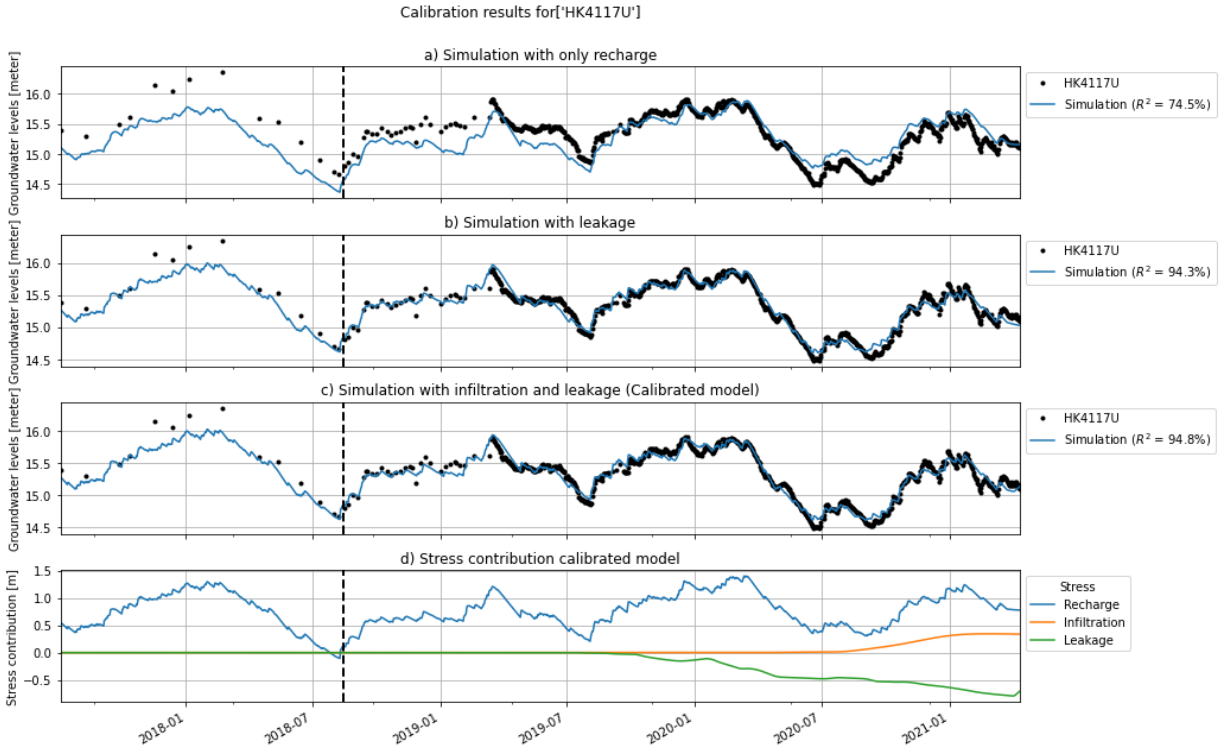

Figure 4.5: Calibration results for HK4117U. The black line visualizes the start of the construction of Haga service tunnel

In Figure 4.6, the simulation results for different stress scenarios for HK4117U based on the calibrated model are presented. Simulation scenario 'Simulation w/o leakage or infiltration' in orange visualizes what the groundwater levels would have been without the tunnel construction. In Figure 4.7 the average difference in groundwater head between the calibrated model and the different stress scenarios can be seen. The results illustrates that the tunnel construction has, on average, lowered the groundwater levels with approximately 0.4 m and that the impact started at the beginning of 2020. It can also be seen that double the leakage would have significantly lowered the groundwater levels whereas half the leakage illustrates groundwater levels closer to those that would have been without the tunnel construction.

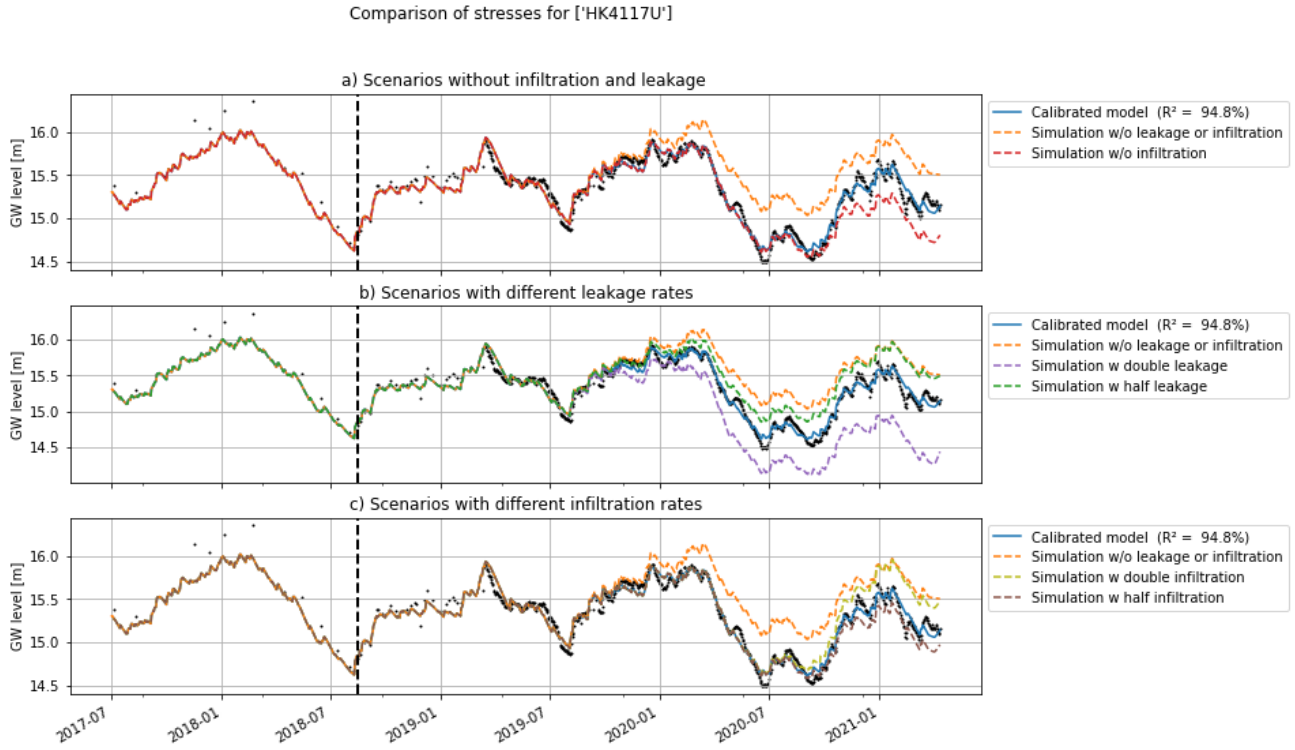

Figure 4.6: Stress simulation results for HK4117U. The black line visualizes the start of the construction of Haga service tunnel

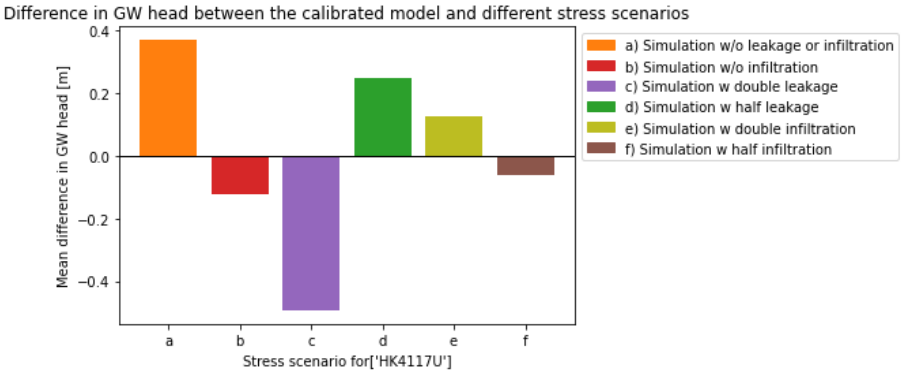

Figure 4.7: Mean difference in groundwater head, during 2020-01-01 to 2021-03-24, between the calibrated model and different stress scenarios for HK4117U

4.2.2.3 Well HK4226B

The simulation results for HK4226B, in Figure 4.8, indicate that the infiltration in the area has impacted the groundwater levels for the well. Adding leakage as a stress does not improve the model fit and this suggests that the well has not been impacted by the tunnel leakage. This is facilitated when looking at the stress contribution plot, in Figure 4.8, where only a contribution from infiltration can be seen. As can be seen in Table 4.1 both infiltration wells has had an impact although the stress contribution from the soil infiltration is twice as large. This despite the fact that

HK4226B is located closer to the rock infiltration well, see Figure 4.1. Again this might be due to the fracturing of the rock however, it can also be said that the infiltration rate for the soil infiltration was approximately twice as high during this specific day, see Figure 3.3, and this is most likely the cause. However, despite adding infiltration the simulation does not fully capture the low groundwater levels in September 2018 and the end of 2019. The low groundwater levels in September 2018 is likely due to the unusually hot summer of 2018 which the simulation is not able to account for. There are available leakage measurements at the end of 2019, see Figure 3.3, but the simulation is not able to fully account for this drop. Again this could be a result of missing or inaccurate leakage measurements from the tunnel construction. Likewise as for HK4117U, adding additional stresses also improves the simulation during the time period before infiltration and leakage occurred in the area as the simulation can better establish what the natural variations in the groundwater level are. HK4226B demonstrates similar behaviour to several other wells in the area, wells that display drawdowns each season and that are affected by infiltration toward the end of the simulation, this is discussed further in section 4.2.3.2.

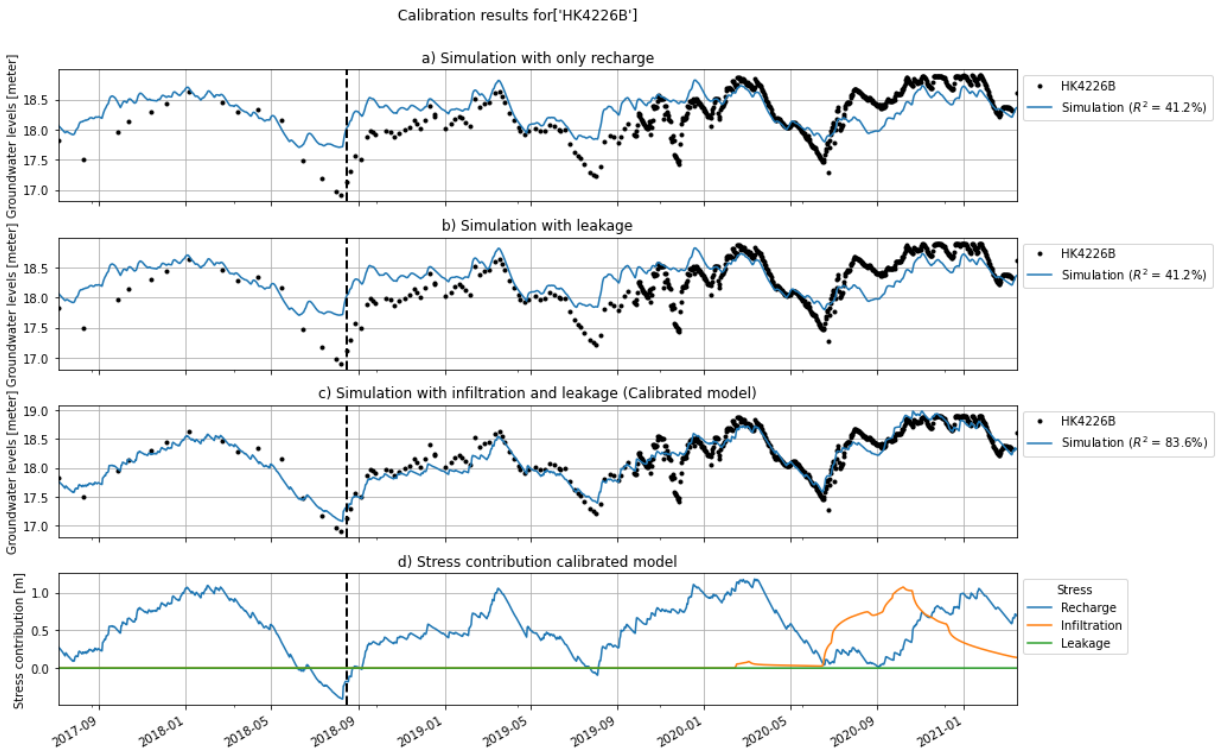

Figure 4.8: Calibration results for HK4226B. The black line visualizes the start of the construction of Haga service tunnel

In Figure 4.9, the simulation results for different stress scenarios for HK4226B based on the calibrated model are presented. Simulation scenario 'Simulation w/o leakage or infiltration' in orange visualizes what the groundwater levels would have been without the tunnel construction. In Figure 4.10 the average difference in groundwater head between the calibrated model and the different stress scenarios can be seen.

These results highlight that the infiltration in the area has one average increased the groundwater levels with approximately 0.3 m from the beginning of 2020 until the beginning of 2021. Even when adding twice or half the contribution from the leakage no change in groundwater level can be seen and this is of course directly linked to the stress contribution from leakage being non-existent. Also even adding half the infiltration would have increased the groundwater levels for the well. Ultimately, the simulation results for the different infiltration scenarios illustrates that for this specific well performing infiltration in the area was not necessary.

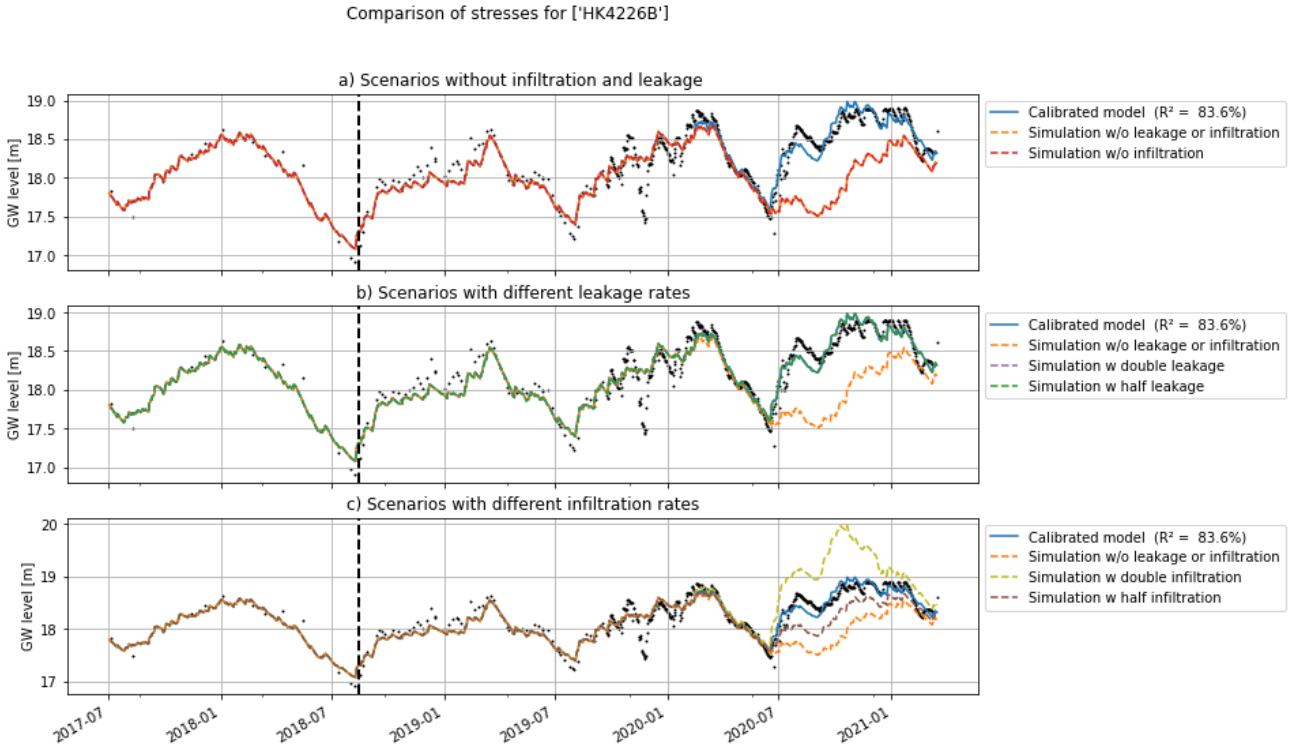

Figure 4.9: Stress simulation results for HK4226B. The black line visualizes the start of the construction of Haga service tunnel

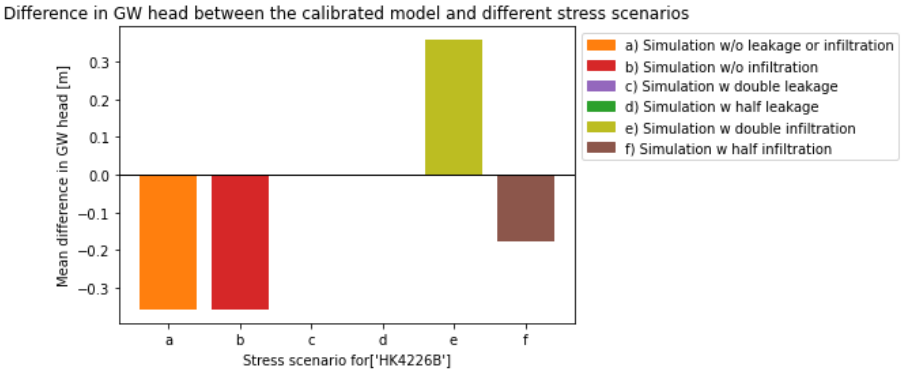

Figure 4.10: Mean difference in groundwater head, during 2020-01-01 to 2021-03-24, between the calibrated model and different stress scenarios for HK4226B

4.2.2.4 Well HK4014H

The simulation results for well HK4014H, in Figure 4.11, indicate that the tunnel leakage has impacted the groundwater levels for the well. This is demonstrated by the increased model fit when adding leakage. Looking at the stress contribution plot, in Figure 4.11, it is obvious that the leakage has had a larger contribution to the groundwater level simulation compared to the infiltration and this is why the model fit does not significantly improve when also adding infiltration. The fact that HK4014H is affected by the tunnel leakage is expected since it is located in the rock which the tunnel is driven through creating a direct connection, see Figure 4.1. As can be seen in Table 4.1 both infiltration wells has had an impact on the groundwater levels for the well although the rock infiltration displays twice the contribution, this might be expected since the well is placed in rock and located closer to this specific well. Still the combined contribution from the infiltration wells is not able to counteract the total contribution from the leakage. Likewise as for well HK4226B, the simulation for HK4014H is not able to account for a time period with low groundwater levels, in this case just before September 2019. Again this could be a result of missing or inaccurate leakage measurements from the tunnel construction. HK4014H demonstrates similar behaviour to several other wells that are located in rock in the area, this is further discussed in section 4.2.3.2.

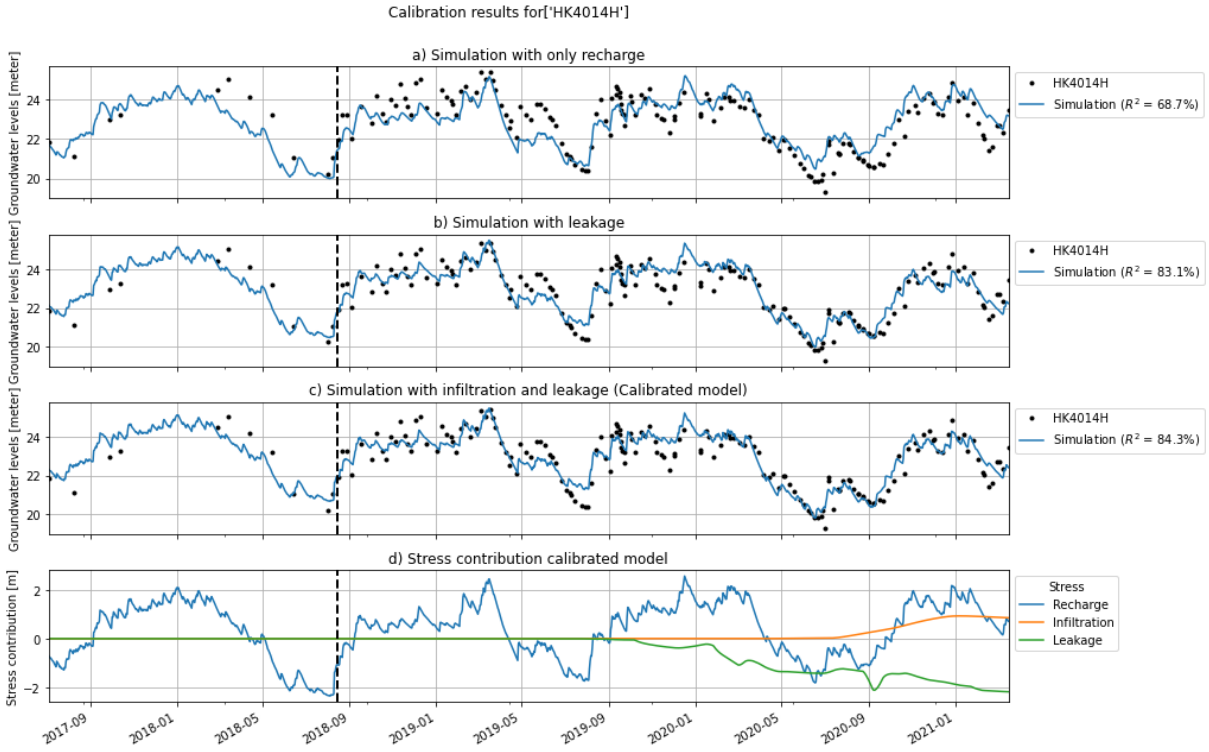

Figure 4.11: Calibration results for HK4014H. The black line visualizes the start of the construction of Haga service tunnel

In Figure 4.12, the simulation results for different stress scenarios for HK4014H based on the calibrated model are presented. Simulation scenario 'Simulation w/o leakage or infiltration' in orange visualizes what the groundwater levels would have been without the tunnel construction. In Figure 4.13 the average difference in groundwater head between the calibrated model and the different stress scenarios can be seen. The results illustrate that the tunnel construction has on average lowered the groundwater levels with 1 m for the well from the beginning of 2020 until the end of the simulation. The simulation with double the contribution for leakage show significantly lowered groundwater levels which is expected since the contribution in the calibrated model is relatively high. If instead the contribution from the leakage is half the size the impact is significantly lowered. This simulation show groundwater levels at the end of the simulation that are in line with those that would have been if there was no tunnel construction. This is of course due to the fact that the infiltration has a small contribution toward the end of the simulation.

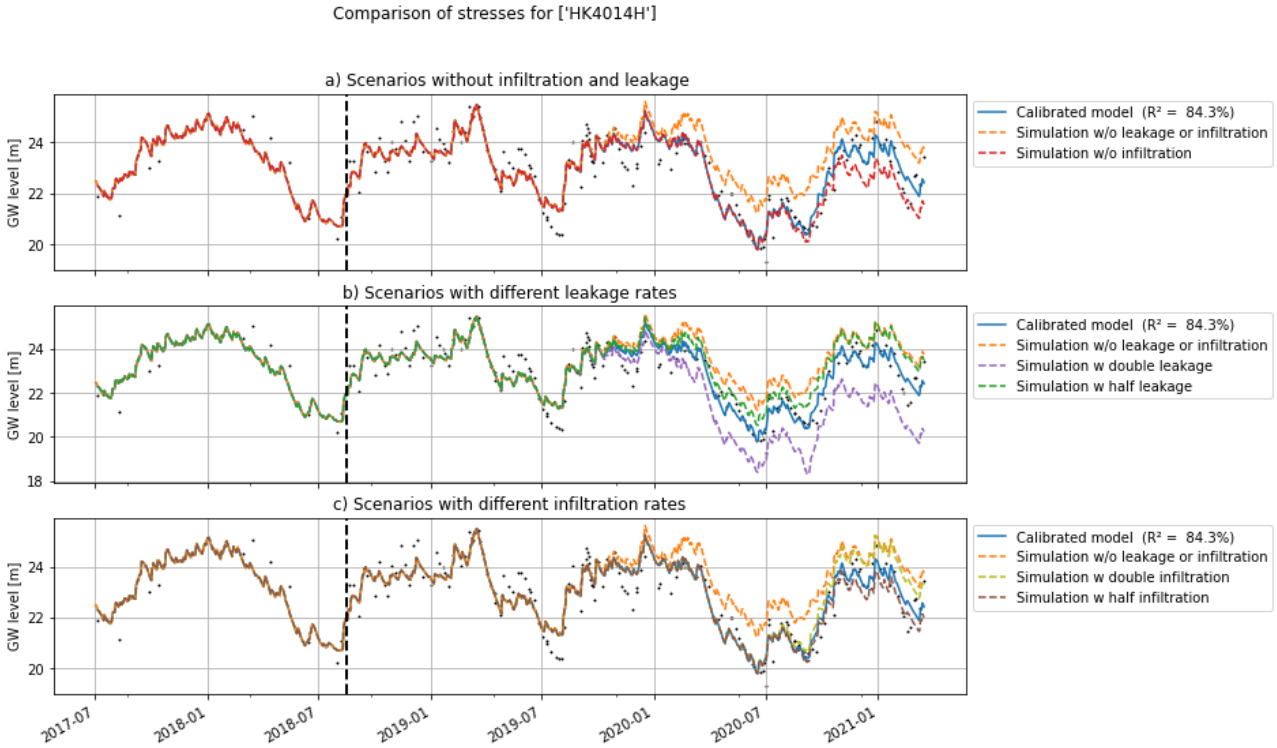

Figure 4.12: Stress simulation results for HK4014H. The black line visualizes the start of the construction of Haga service tunnel

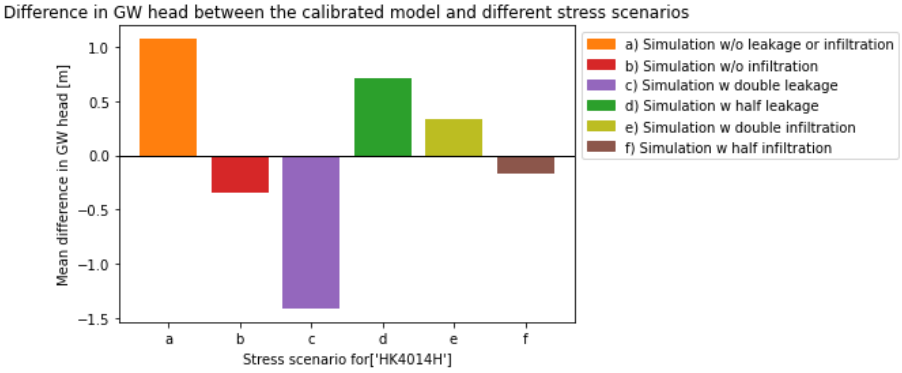

Figure 4.13: Mean difference in groundwater head, during 2020-01-01 to 2021-03-24, between the calibrated model and different stress scenarios for HK4014H

4.2.2.5 Well HK4116U

The simulation results for well HK4116U, in Figure 4.14, show a lower model fit compared to the previously evaluated wells. It is evident that adding the different stresses does not improve the model fit considerably. As discussed in section 4.2.1 the simulation is not able to account for the low groundwater levels each summer. Beyond limitations with the linear recharge model not being able to represent the seasonal changes this big drop is likely a cause of an additional stress, such as underground draining structures. Looking at the stress contribution plot almost no contribution from the leakage and infiltration can be seen. As the groundwater levels increase toward the end of the simulation it can be argued that perhaps a stress causing the levels to go up is missing. It is likely that this is in fact due to missing or inaccurate measurements of the infiltration in the area. As this simulation show a low model fit, measures should be taken to improve the simulation before using the calibrated model for any type of predictive analysis. Consequently the calibrated model for this well has not been used for different stress simulations scenarios in this study. It is suggested that the missing stress causing the low groundwater levels each summer is identified and applied to obtain a better model fit. This well shows similar behaviour as well HK4105U which is further discussed in section 4.2.3.2.

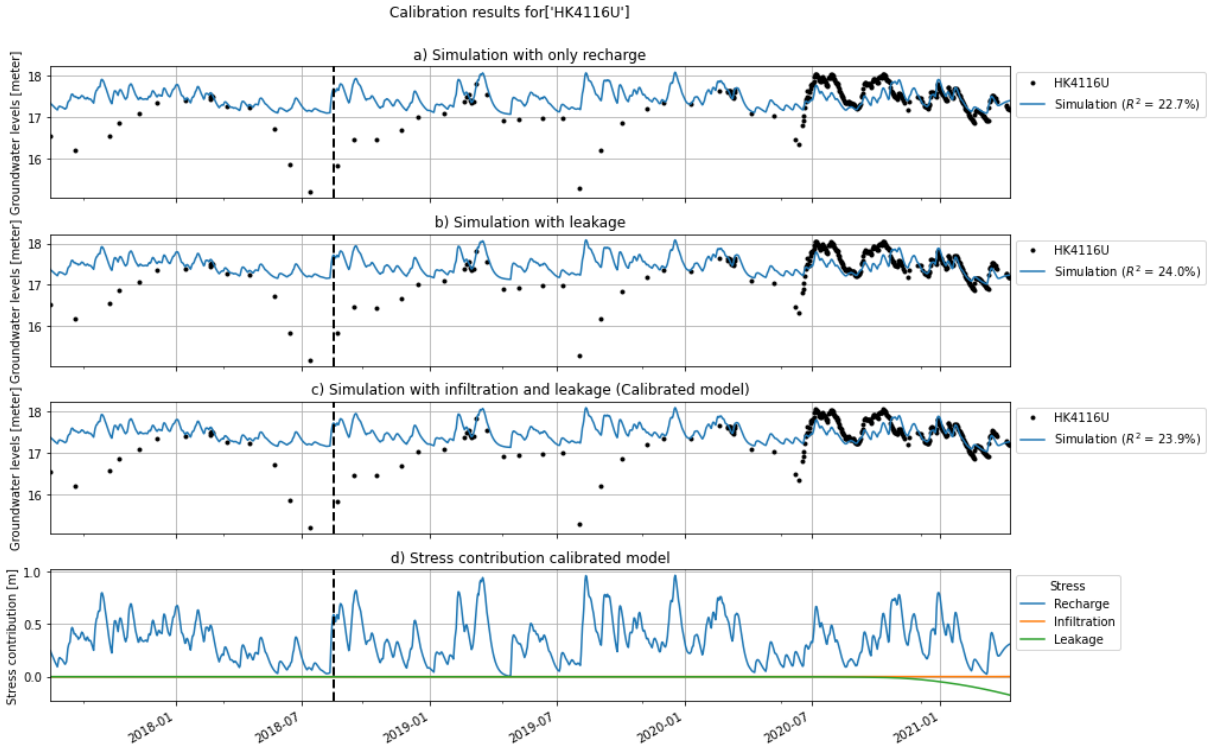

Figure 4.14: Calibration results for HK4116U. The black line visualizes the start of the construction of Haga service tunnel

4.2.3 Cluster analysis

Two cluster analysis were made, the first one was on the residuals of the simulation from the modeled scenario where only recharge contributes to the simulation which is fitted against the observed groundwater heads. The residuals therefore represent the impact the tunnel had on the groundwater level. The second cluster analysis was made on the recharge parameters of the calibrated model, which all scenarios were derived from, to evaluate if there were any spatial relations of the parametrisation.

4.2.3.1 Residuals all wells

The residual time series were clustered for the period ranging from 2017-01-01 to 2021-03-24, this period was selected to show equal parts of the residuals before the tunnel construction was started and the time during the construction while also including parts of the groundwater recovery. In some residual series a flat line is evident in the beginning or end of the series, this is due to lack of data.

It is evident in the cluster analysis, see Figure 4.15, that the wells have been divided in two main clades. The orange clades (cluster 1, 2 and 3) are the most distant in the cluster analysis and therefore not grouped together but put in individual clusters. The green clades in Figure 4.15 are represented by three clusters where one cluster (4) contains wells that were to a high extent affected by leakage but also by infiltration, one cluster (5) mainly effected by infiltration and the last cluster (6) overall less affected by the tunnel construction. Numbers within parentheses signals how many residual time series that have been clustered together, for names see a full dendrogram in appendix A.4 Figure A.1.

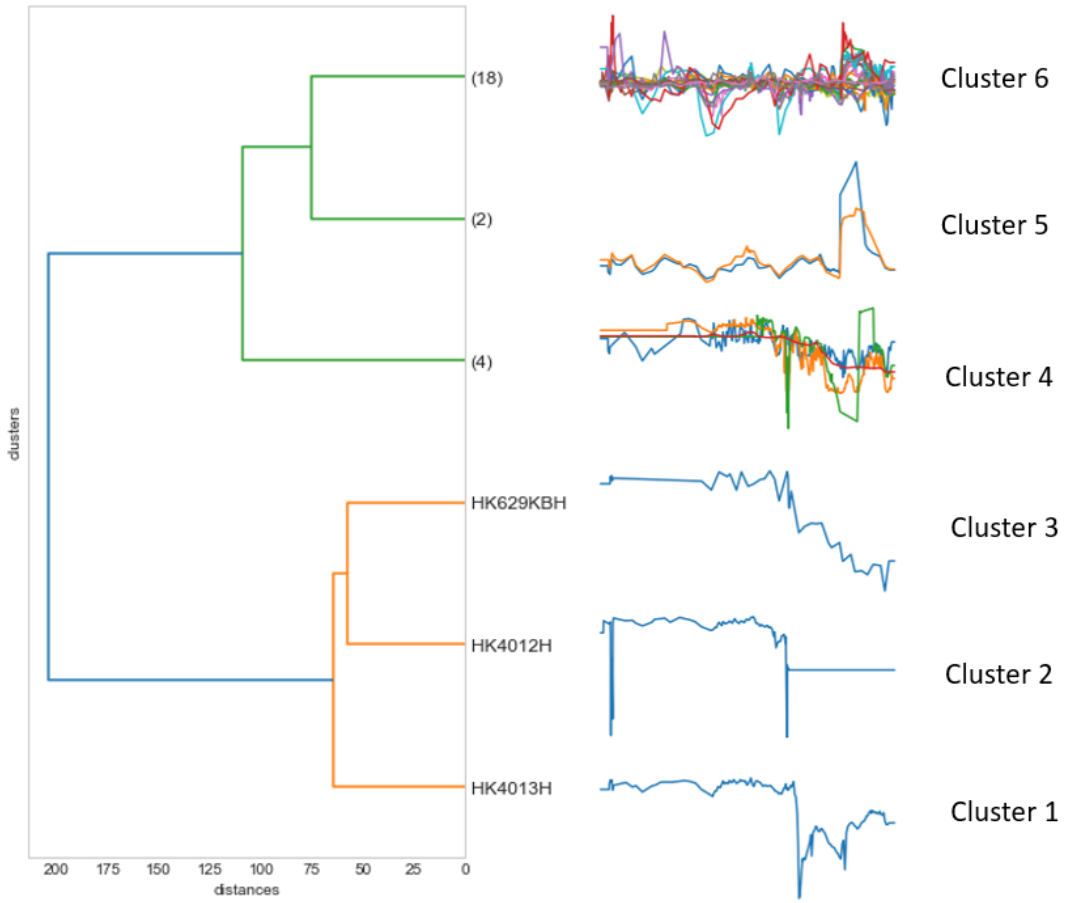

Figure 4.15: Residual time series clusters merged, six clusters.

To investigate if the wells had any spatial relations, both among wells and tied to other factors such as groundwater flow line or geological placement, the clusters created were plotted in different colors on a map, see Figure 4.16.

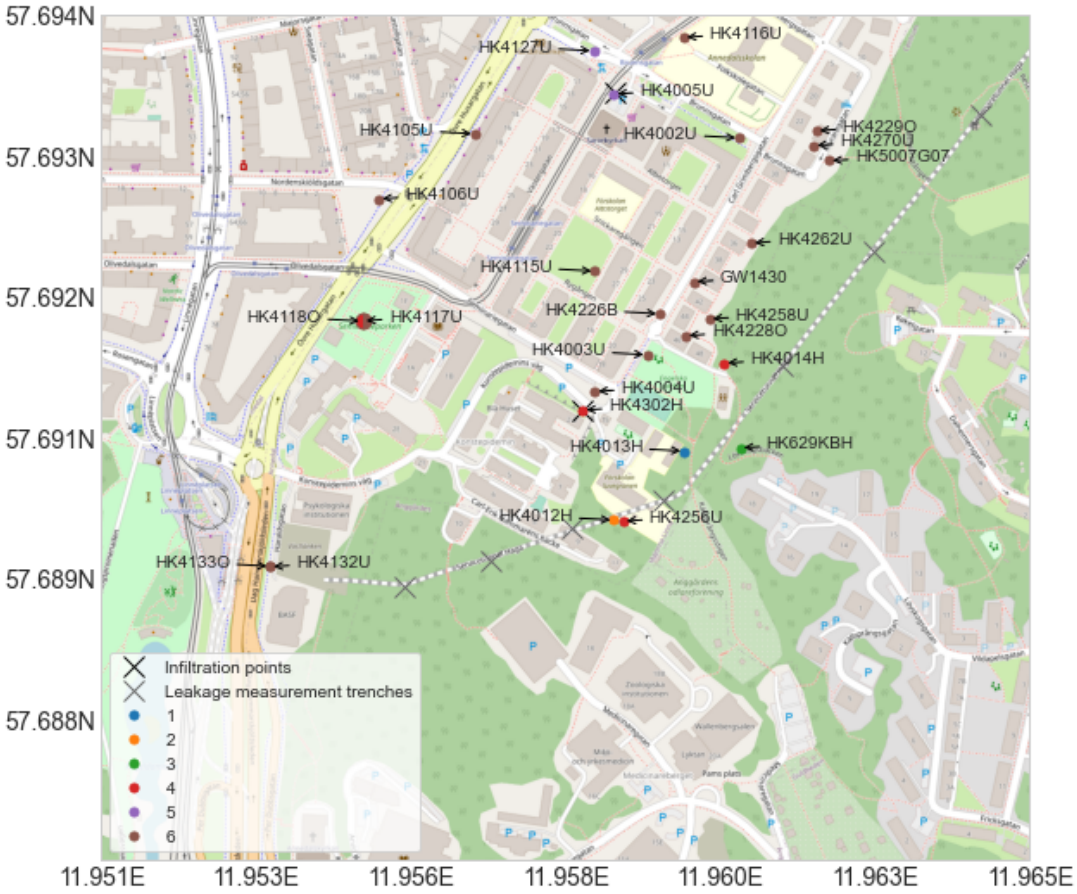

Figure 4.16: Map of all wells divided in six clusters marked by different colors.

Clusters 1, 2, 3 and 4 in Figure 4.15, were the wells most affected by leakage. Five of seven of these wells are located in rock. For the two other wells, HK4256U is located in the lower aquifer but right above the tunnel and HK4118O is located in the upper aquifer. By the wells heavily affected by leakage, all wells except HK4118O are close to the tunnel in an area were storm water from the surrounding elevations would run down to the valley. The fact that HK4118O has a strong response to the leakage, but not HK4117U which is located at the same coordinates, could be explained by the fact that HK4118O measures the groundwater level in the upper aquifer and HK4117U in the lower aquifer. HK4118O shows no significant effect caused by the infiltration, no other well in the upper aquifer is located as far from the infiltration but below the tunnel in the aspect of groundwater flow lines, which could be a possible reason for the high impact on HK4118O from the leakage but less response from the infiltration. The well HK4302H is the well used infiltration into the rock aquifer, which is visible in the residual series for the well where the heavily leakage affected groundwater levels were stabilized in the end of the series. The same upward trend although not in the same magnitude, perhaps due to elevation (8m difference), was observed in HK4256U. Since HK4256U is positioned next to HK4012H which was cast closed in September 2019 it could be presumed that both wells could have had similar responses, HK4012H is now instead clustered alone with only impact of the leakage with data after September 2019 missing. HK629KBH show no influence

by the infiltration on the groundwater levels in the residual series but do have a small contribution of infiltration in the end of period , it was installed 10 m higher in elevation than HK4012H and HK4256U whereof the infiltration might not have been such a contributing factor to the groundwater levels of that well.

From Figure 4.15, two clusters of the green clades, cluster 5 and 6, were not as affected by the leakage. HK4005U and HK4127U in cluster five, were highly affected by the infiltration and shows no larger resulting effects of the leakage on the residual series. The well HK4005U is closely located to the infiltration point where water was infiltrated in the lower parts of the soil groundwater aquifer, the response in HK4127U is probably similar as it is located in the same area for groundwater flow and height elevations which were presented in Figure 2.4. The residual series of the wells in the sixth cluster has the most related residuals, but clustering them with all other wells greatly simplifies the impact the tunnel has had on the wells. Therefore the wells of the sixth cluster were selected and clustered a second time without the highly impacted wells, to further evaluate the spatial relations of the tunnel impact.

4.2.3.2 Residuals - selection of wells for a deeper analysis

The 18 wells of the sixth cluster from Figure 4.15 were selected for a second cluster analysis. The differences and similarities in the residual series become more visible among these wells after removing the heavily impacted wells, see Figure 4.17. Numbers within parentheses signals how many residual time series that have been clustered together, for names see a full dendrogram in appendix A.4 Figure A.2. The first cluster show wells that have no apparent impacts from the infiltration or the leakage, resulting in only small residuals. In the second cluster the majority of wells show a tendency to seasonal drawdowns which the recharge does not manage to properly represent. It could be due to stresses which have not been measured, but the groundwater levels have clearly been impacted by the infiltration in the end of the residual series. The residual series of the third cluster have the same appearance as the second cluster although the residuals are of greater magnitude.

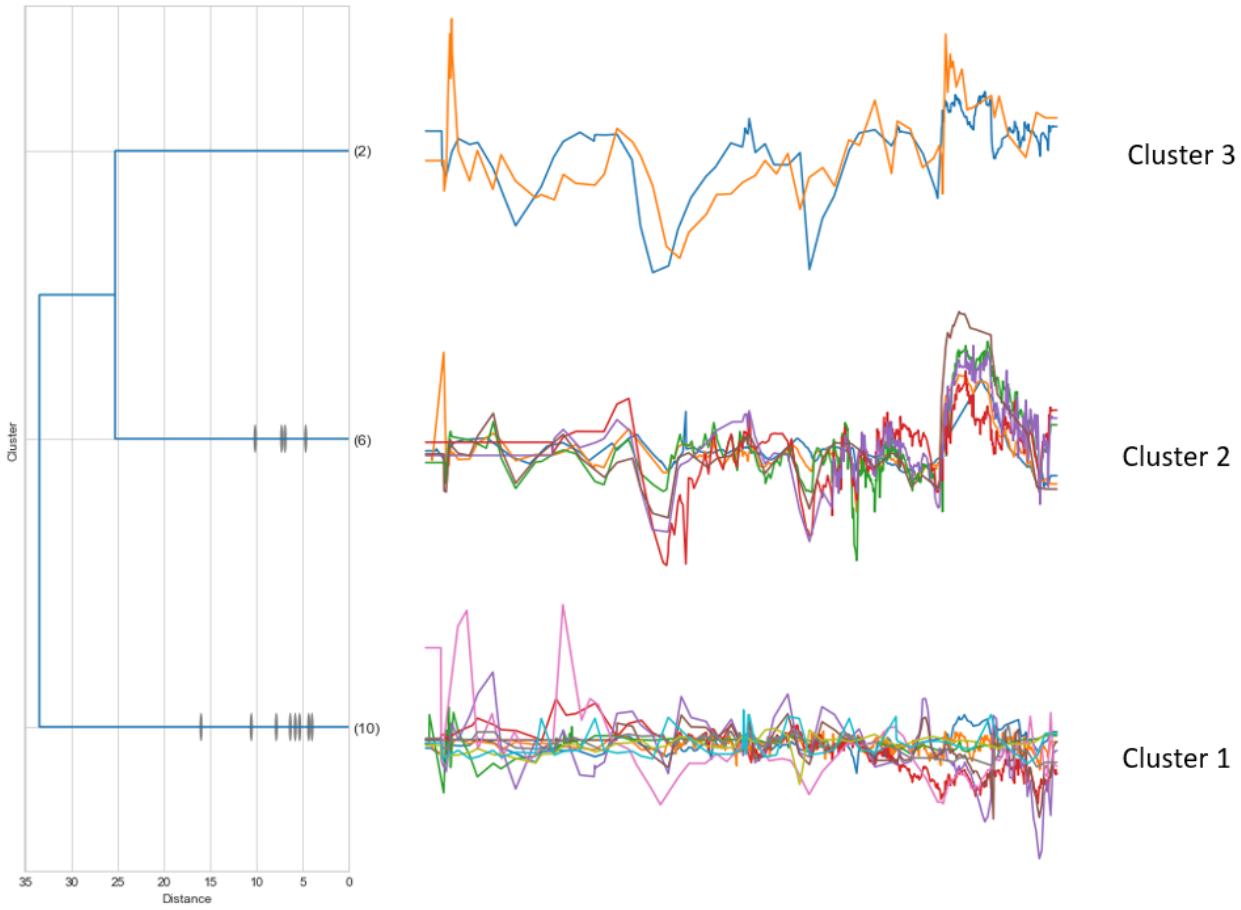

Figure 4.17: Three clusters of the lower impacted wells, that better show the difference in the residual series. Numbers within parentheses signals how many residual time series that have been clustered together, for names see figure 4.18

For analysis of spatial relations among the wells that were not as affected by the tunnel construction the three clusters were plotted in Figure 4.18. Cluster one which did not have any apparent responses that could be seen in the residual series, are spread in the area and does not seem to be on the same groundwater flow lines. Neither do they seem to share any other physical characteristics. The clustering of these wells could therefore be solely based on that these wells were not as affected by the construction as the other wells and their residuals therefore small and most related.

In the second cluster, with wells indicating drawdowns each season and later affected by the infiltration, all are in the lower aquifer located between the infiltration wells. The response from the infiltration on the residual series could therefore be expected. Close to the wells in cluster two and also to the rock infiltration well is HK4004U, HK4003U and HK4228O, although their residual series exhibits less to no effect caused by the infiltration. A well can have small to no residuals while the groundwater might have been affected by both leakage and infiltration but in the same time period and with the same contribution resulting in unchanged groundwater levels. When looking at the stress contribution for HK4004U this seems to be

the case. HK4003U have a small contribution from the infiltration but not enough to be clustered with the more affected wells. For HK4228O, this well is located in the upper aquifer and might therefore not have been affected by the infiltration as the water was infiltrated in the rock which connects mainly to the lower aquifer, this argument is supported when looking at the stress contributions for the well as it has no contribution from infiltration.

The third cluster with two wells that were clearly affected by the infiltration but also showing seasonal drawdowns which the simulation could not be fitted to, both are close to the northern soil infiltration well on the same or lower groundwater flow lines, see Figure 2.4. The larger response compared to cluster two could therefore be expected.

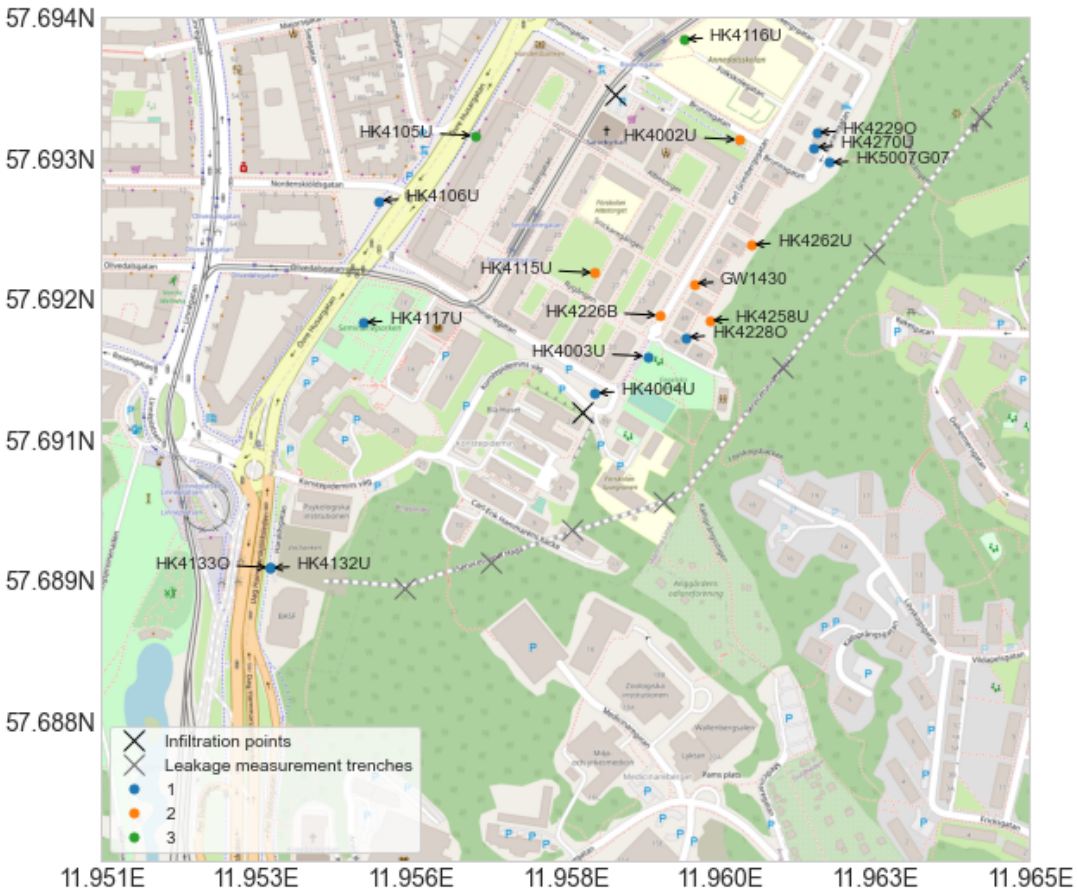

Figure 4.18: The less impacted wells spatially plotted.

The parameter values related to the recharge stress of the calibrated model were clustered in five clusters, see Figure 4.19.

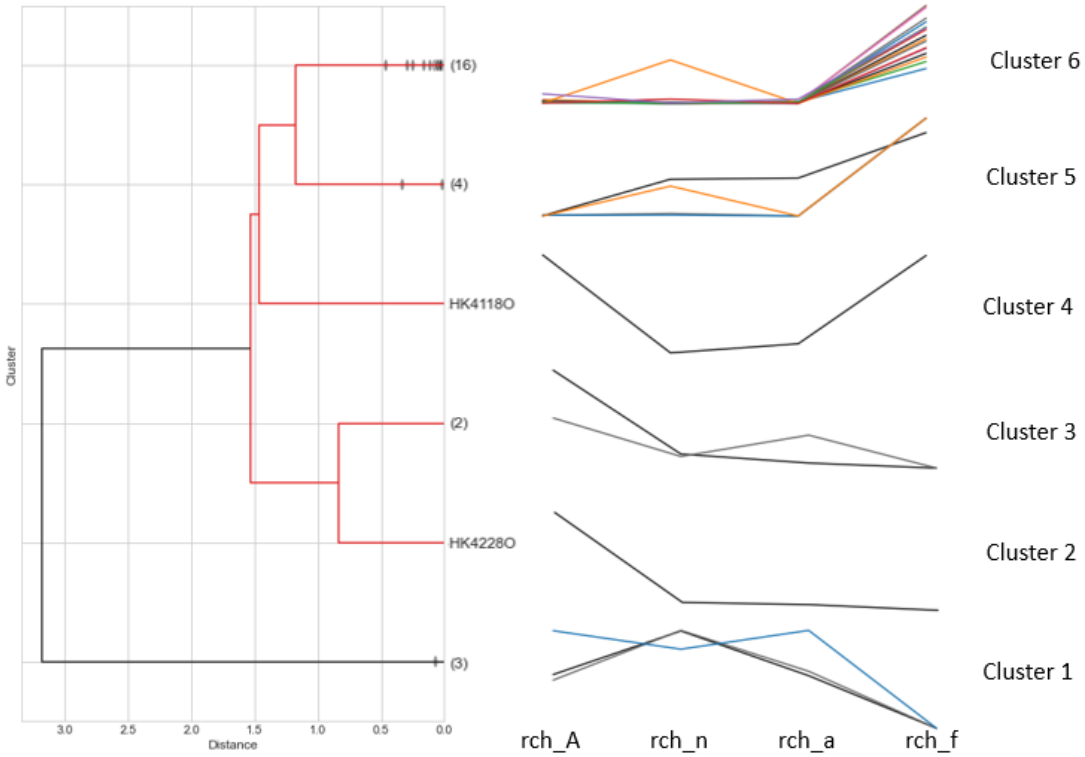

Figure 4.19: Parameter values of the calibrated model clustered for all wells, showing the series.

To analyse if the cluster analysis could be tied to any spatial factors the clusters of Figure 4.19 was plotted on a map, see Figure 4.20.

The cluster analysis indicates that the parametrisation of three wells are clear outliers (cluster 1) they are differentiated from the other clades. In cluster one wells HK4256U, HK4302U and HK4106U are grouped. The exception among these wells are HK4106U that according to previous discoveries have a different response to the construction of the tunnel but have been parametrised as two of the wells most affected, by both infiltration and leakage. Neither is it located near the other wells it has been clustered with.

In cluster two HK4188O was clustered alone. It belongs to the same clade as cluster three containing HK4005U and HK629KBH. Cluster four with HK4228O is also clustered alone, when evaluating a dendrogram with six clusters. Cluster five have four wells clustered HK4012H, HK4013H, HK4229O and HK4116U. The parametrisation of these wells can not manually be related to any spatial factors.

The cluster containing most wells (16/27) is cluster six. Most of the wells in this cluster have a high model fit, the exceptions are HK4113O and HK4258U. All wells in this cluster except HK4014H and HK4133O is located in the lower aquifer. Removing the two wells not located in the lower soil aquifer could potentially allow for studies on how to simulate the response of the wells in the lower soil aquifer where no data exists, to use for future head predictions. It is however hard to evaluate the reliability of the results as there are wells located in the lower soil aquifer which are not in this cluster, but also because of the uneven distribution of the geologic placements of the wells. The results might have been more distinct or more diverse if more wells were available that were located in rock and in the upper aquifer.

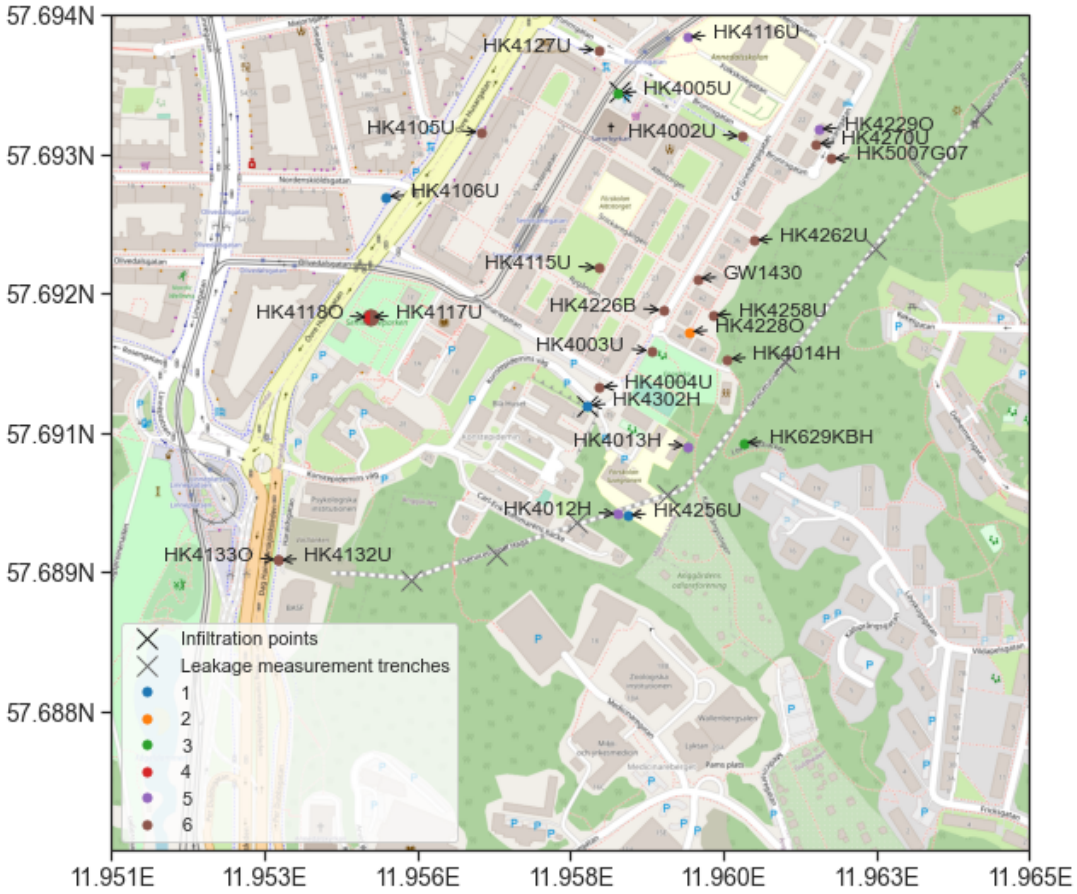

Figure 4.20: Map of clusters from figure 4.19

4.2.4 Correlation of parameters against height variables

There were several outliers in the data set of the parameters which were removed. The wells that were removed were HK4118O, HK4106U, HK4256U, HK4302H, HK4012H, HK4105U, HK4229O, HK4228O. If not removed, the outliers affected the results in an unwanted way due to the nature of the Pearson and Spearman equations.

4.2.4.1 Scatterplots of parameter values against height variables

For the parameters rch_A, rch_n, rch_a and rch_f no or only weak correlations were found, from this no reliable conclusions can be drawn. The scatterplotts for these parameters can be seen in appendix A.5.

4.2.4.2 Heatmaps and boxplots of the correlation

To further evaluate if the correlation was tied to the geological position the correlation was also plotted in heat maps and boxplots stratigrafed based of their geologic position. The heat maps when evaluating only the wells located in soil mainly showed a lower correlation for all parameters and variables. For the wells located in rock the correlation when stratified changed drastically, this was deemed to be

due to the low number of wells to correlate. No reliable conclusions could therefore be drawn from these results, further investigation into correlations between model parameters and physical height variables from the wells modeled will have to be made preferably with a larger data set that can be stratified more equally. The heatmaps are found in appendix A.6. Boxplots were also made to complemented the heat maps and picture how the correlation differs for the wells, these can be seen in appendix A.7.

5
Discussion

This chapter will discuss the results of this study and aim to answer the research questions as stated in the corresponding subsection.

5.1 Applications of a TFN model in an underground infrastructure project

As presented in this study TFN modeling in Pastas can be applied to quantify and identify the impact a specific stress, as a result of an underground infrastructure project, has had on one or several wells in an area. This is made possible by the predefined response functions which enables an identification of the stress that has caused the disturbance. The TFN model also shows great potential with the possibility to extract specific stress contributions, as presented in this study where the contribution from the infiltration wells and measuring mounds are distinguished. Further after conducting a calibration process for the TFN model and achieving an acceptable model outcome, the calibrated model can be used as a basis for stress simulation analysis. When coupled with a cluster analysis on the obtained residuals, from a simulation without the contribution from infiltration and leakage, the TFN model can be used to visualise the spatial impact in an area from an underground infrastructure project. Also it shows potential to be used as a part of a groundwater control program during construction where it can aid in making sure that the groundwater level for a well does not go below a threshold limit as well as identifying the disturbance and enabling for counteracting measures to be applied at the right time and place. In addition to this, the fact that the TFN model requires very little conceptualisation and is not particularly time demanding show high applicability as demonstrated in the evaluation of the model as a tool for groundwater modeling, made in the result section 4.1.

The obtained model fit of the calibrated model for the wells in the area, presented in section 4.2.1, where many simulations achieve a fairly high model fit, in the form of the R^2 value, further demonstrates the potential of the TFN model in evaluating the head changes in the site study area as well as being used for predictive analysis. However, for the simulations where a much lower model fit is obtained it can be argued that additional measures should be taken to improve the model fit or that these wells should be disregarded and not further evaluated in a cluster analysis. For two of the wells that displayed a lower model fit changing the calibration period improved the results. Still this was not true for all of the wells and for the purpose

of consistency the same calibration period was kept even when resulting in a lower model fit. It can also be questioned to what extent the model fit can be improved since it is obvious that for many of the wells one or several stresses are missing. Thus in order to improve the model fit more comprehensive stress measurements or estimations are required. As the TFN model relies heavily on a sufficient amount of data for both the groundwater levels and stresses acting on the well it can be said that the TFN model is less applicable in an area with insufficient or inaccurate measurements. Nonetheless, as presented in this study the TFN model can still in this case be proved useful as a compliment to a regular groundwater model in identifying missing or inaccurate measurements of both groundwater heads and stresses. For the specific site study area in this study there was however several wells with decent amount of data thus providing the option to simply remove the wells that did not perform favourably.

The in-depth analysis of five wells for the calibration process and different stress scenario simulations evaluates the applicability of the TFN model. Through evaluating wells that have been differently impacted by drainage and infiltration the potential for using the TFN model to quantify and identify which stress is causing a disturbance can be visualised. By coupling the results from the calibration process, the stress simulations and the cluster analysis to the location and hydrogeological behaviour of the well the credibility of the results can also be evaluated. Although the evaluation of the hydrogeological behaviour for the wells is not performed particularly in-depth for this study, it does indicate that for many wells the simulation results are in line with what can be expected based on their placement. However, this is not true for all wells and some questions arise which requires a deeper understanding and conceptualisation of the aquifer behaviour to answer. Thus a wider conceptualisation is recommended to better determine the credibility of the corresponding simulations.

It should be noted that before deciding on the method used to perform the different stress simulation scenarios including a scenario without the impact from the tunnel construction, different approaches were tested. These included manipulating the data for infiltration and leakage by replacing all the data with zero values or multiplying/dividing the data with a factor of 2 to account for different scenarios. It was also tested to simply delete the stress models for infiltration and leakage from the calibrated model. However, none of these methods gave a result suitable for the purpose and thus were disregarded. The method in this study, where an alteration of the stress contribution on the groundwater level simulation for the calibrated model was performed, was therefore chosen. Still the applicability of the chosen method can be questioned since it does not act as a physiological model but instead acts linearly, where if the total stress contribution is increased with a certain amount, the groundwater head simulation will increase accordingly. This could only be considered to be true to some extent, with a small increase or decrease in the stress contribution, since the real behaviour of the contribution is in fact not linear. It should also be mentioned that if the stress contribution from a stress is zero in the calibrated model, regardless how much this is multiplied the stress contribution

will be non-existent. Once again, the accuracy of these results can be questioned since in reality there is likely a tipping point where a certain amount of increase in, for example, infiltration in the area will have an impact on a currently unaffected well. Based on this, there is cause to further study other approaches for using the TFN model for different stress simulation scenarios which can better account for non-linear behaviour.

A possible extension of the usage area of TFN modeling is to ad a feature where a simulation can be interpolated forwardly based of a calibrated model. Although not completed, the TFN model that has been produced in this study show potential to be used for prediction of future impacts due to new underground constructions or future impacts by climate change. Given that the future stresses are manually estimated and that groundwater heads can be simulated using a generalised parameterisation. This is currently not possible in Pastas as the simulation requires at least one stress data set. The ability to obtain the parameters for all stresses added to the model is however a potential which can be used for this purpose. In this study the recharge parameters were evaluated with a cluster analysis to investigate if a relationship could be found between the model parameterisation and other physical factors. A majority of the wells located in the lower soil aquifer were clustered together. This can be further studied to assess if the parameterisation can be used to obtain simulations were no observed data is available, as this is a limitation of TFN models which only simulate periods where data exists. The analysis of the correlation between the parameters and the site physical characteristics could not find any clear correlation either. Further investigations are recommended preferably on a larger data set in order to evaluate the potential of cluster and correlation analysis coupled with TFN modeling.

5.2 Possible improvements to the TFN model created in this study

Some of the technical functions giving the TFN model potential could however have been explored further, which is recommended before using results obtained for inference.

Transfer function-noise models can as proven in this study obtain high model fits, largely due to the wide variety of equations for stress contribution and response functions. This is a great potential for the TFN model created in Pastas, as the package have several predefined stress models, stress model classes and response functions available. These could be used in different constellations to acquire the best fit for the data modeled. In this study the same TFN model was used for all wells, therefore the same type of stress models and response functions were used for each stress applied to the model. The selection of the stress models and response functions were mostly based on recommendations from the Pastas documentation but also on the combination that gave the overall best fit. It could therefore be argued that a higher overall model fit could be obtained if individual selections of

stress models or response functions were made. The question then would be how to compare the results of each well, and how the individual selections would affect the integrity of inferences based of the results for a larger area containing multiple wells. In an extensive project selecting individual stress models, stress model classes and response functions would also require extra time when modeling the wells. Further studies needs to be conducted to investigate which method is most correct when modeling multiple wells in the same area for a project.

In the TFN model which was used for all wells in this study a few key selections contributing to uncertainties can be additionally considered. A *RechargeModel* of linear class was used, other classes for the recharge stress model exists that might have improved the model fit for some wells due to their depth as explained in section 3.4.1. Changing the recharge model class can therefore be tested, especially on wells with a less fitted simulation, to raise the goodness of fit.

Another factor which can improved the model fit, and potentially lower uncertainties, is to use a 3D distance for the distance parameter in the *WellModel* stress model. The distance used in this study was instead the 2D distance, this might not account for the stress distribution between the measured stress and the observation wells as well, considering the different elevations they are placed at.

Although not used in this study, a great potential of a TFN model is the use of a noise model. Successful use of a noise model, where the residual series is converted to a noise series as mentioned in 3.3.2.1 increases the reliability of the model when the residuals only represent variations in the data which cannot otherwise be explained. The default noise model in Pastas, when used with the TFN model in this project, resulted in a simulation with a lower goodness of fit. It was concluded that this was due to the high frequency of the data modeled. One option to raise the goodness of fit with a noise model can be to only fit the simulation to every tenth head value observed, however several of the wells used in the modeling process had sparse data in some part of the time series. Therefore this method was not tried as it could have affected the fit in other ways. It is also suggested in the Pastas documentation to calibrate a model without the use of a noise model and then with the optimal parameters obtained, solve the model again but with a noise model applied. Using such method can potentially improve the fit when using a noise model, since the main issue is the sensitivity in the parametrisation when a noise model is applied. This was however not tested on the model due to lack of time and a late discovery of the method. When a model is solved without the use of a noise model the results should not be used for inference as residuals can exhibit strong auto correlations, it is therefore important to view the results in this study critically.

Provided that a noise model has been applied when solving the TFN model, Pastas supplies several tests for statistical analysis and diagnostic checking. Sufficient methods for analysis of the model is important to ensure reliable results, the variety of tests presented in Pastas is therefore promising even though it is still under development. When using TFN models for official projects it would be recommended

to further evaluate the use of a noise model, diagnostic checking and statistical tests or only use the TFN model as a compliment to another groundwater model.

5.3 Groundwater impact at the study site area

In the cluster analysis the groundwater head changes as a result of infiltration and drainage, for a total of 27 wells in the site study area are evaluated through the residual series obtained from the model. These are divided into six clusters with five clusters representing wells that have been heavily affected by leakage, infiltration or a combination of both and the other one representing wells that have been less affected by the tunnel construction. Nine wells are placed in the clusters classified as wells that have been heavily affected by the tunnel construction and five out of these are located in rock. It is evident that the wells located in rock are sensitive to the effects of the tunnel construction which is expected as they are located in a presumed weakness zone, see Figure 2.2. For the wells which are not located in rock reasonable spatial explanations can be provided.

The further analysis of the 18 wells in the cluster classified as wells that have been less affected by the tunnel construction divides the wells into three clusters. The first cluster contains ten wells where no significant impact by leakage or infiltration can be seen, they do not seem to have any clear spatial or other type of relation. Cluster two and three consists of six and two wells, they have seasonal variations and are impacted by infiltration toward the end of the simulation. The fact that they illustrate similar behaviour and are impacted by infiltration is expected since they are located in the lower soil aquifer mainly between the infiltration wells or below the infiltration wells in terms of groundwater flow lines.

To summarise it is clear that the service tunnel has impacted the groundwater levels for the wells in the site study area. This impact varies in the area with some wells being heavily impacted by leakage, some more or less impacted by infiltration and a few where no significant impact is seen. For most wells a spatial correlation or a correlation of physical characteristics can be established which supports the credibility of the results. Still it should be noted that the model fit for the calibrated model for a few of the evaluated wells in the cluster analysis is rather low and the results for these wells should be considered with this in mind.

6
Conclusion

This study set out to evaluate the applicability and potential for using TFN models to evaluate groundwater head changes due to drainage and infiltration and consequently evaluate the groundwater level impact due to the service tunnel in the site study area. It is argued that the created TFN model can be used to clearly identify and quantify the stress that has caused a disturbance, to simulate different stress scenarios and that coupled with a cluster analysis it can be used to evaluate spatial impact. For simulations not achieving a good model fit it is suggested to further investigate the cause before using using the simulation for any type of predictive analysis. The potential for using TFN models include the fact that the transfer function noise model with response functions generally obtain a good model fit. Limitations of the use of TFN models, in Pastas, for this study include the fact that a linear recharge model was used exclusively and that the use of a noise model was not applied. The study found that the groundwater level impact from the service tunnel varied in the area for the wells and that the impact could be spatially related. Recommendations for future studies include evaluating the use of a non-linear recharge model for simulations with a lower fit, further evaluating the use of a noise model coupled with diagnostic checking and studying different approaches for predictive analysis of different stress scenarios that better accounts for non-linear behaviour. It is also recommended to further study clustering and correlation of parameters from TFN models to assess if this can provide deeper knowledge of the conceptual hydrogeology as well as provide the ability to use TFN models were no or scarce head observations are available.

References

Allen, R. G., Pereira, L. S., Raes, D., & Smith, M. (1998). *Crop evapotranspiration - Guidelines for computing crop water requirements - FAO Irrigation and drainage paper 56* (Tech. Rep.). Rome: Food and Agriculture Organization of the United Nations. Retrieved from http://www.fao.org/3/X0490E/X0490E00.htm

Anderson, M. P., Woessner, W. W., & Hunt, R. J. (2015). *Applied Groundwater Modeling - Simulation of Flow and Advective Transport (2nd Edition).* New York, NY: Elsevier New York. Retrieved from https://app.knovel.com/hotlink/toc/id:kpAGMSFAT1/applied-groundwater-modeling/applied-groundwater-modeling

Anscombe, F. J., & Tukey, J. W. (1963). *The Examination and Analysis of Residuals* (Tech. Rep.).

Bakker, M., & Schaars, F. (2019, nov). Solving Groundwater Flow Problems with Time Series Analysis: You May Not Even Need Another Model. *Groundwater*, *57*(6), 826–833. doi: 10.1111/gwat.12927

Brownlee, J. (2020, aug). *Machine Learning Mastery : White Noise Time Series with Python.* Retrieved 2021-03-05, from https://machinelearningmastery.com/white-noise-time-series-python/

Chaitanya Reddy Patlolla. (2018). *Understanding the concept of Hierarchical clustering Technique.* Retrieved 2021-05-03, from https://towardsdatascience.com/understanding-the-concept-of-hierarchical-clustering-technique-c6e8243758ec

Chen, Z., Grasby, S. E., & Osadetz, K. G. (2002, mar). Predicting average annual groundwater levels from climatic variables: An empirical model. *Journal of Hydrology*, *260*(1-4), 102–117. doi: 10.1016/S0022-1694(01)00606-0

Collenteur, R. A., Bakker, M., Caljé, R., Klop, S. A., & Schaars, F. (2019, nov). Pastas: Open Source Software for the Analysis of Groundwater Time Series. *Groundwater*, *57*(6), 877–885. Retrieved from https://onlinelibrary.wiley.com/doi/abs/10.1111/gwat.12925 doi: 10.1111/gwat.12925

Collenteur, R. A., Bakker, M., Caljé, R., & Schaars, F. (2020). *Pastas Documentation Release 0.17.0* (Tech. Rep.). Retrieved from https://pastas.readthedocs.io/{_}/downloads/en/master/pdf/

Collenteur, R. A., Bakker, M., Klammler, G., & Birk, S. (2020). Estimating groundwater recharge from groundwater levels using non-linear transfer function noise models and comparison to lysimeter data. *Hydrology and Earth System Sciences Discussions*, *2020*, 1–30. Retrieved from https://hess.copernicus.org/preprints/hess-2020-392/ doi: 10.5194/hess-2020-392

Djeddou, M. (2016, 01). *What's the difference between noise and error in a dataset?*

Fetter, C., Jr. (2014). *Applied Hydrogeology* (4th ed.). Pearson Education Limited.

Göteborgs Stad. (2018). *Fler sprängningar för Västlänken – Stadsutveckling Göteborg – Göteborgs Stad.* Retrieved 2021-05-25, from https://stadsutveckling.goteborg.se/projekt/vastlanken/nyheter/fler-sprangningar-for-vastlanken/

Göteborgs stad. (2020). *Västlänken – Stadsutveckling Göteborg – Göteborgs Stad.* Retrieved 2021-02-01, from https://stadsutveckling.goteborg.se/vastlanken

Haaf, E., & Barthel, R. (2018, apr). An inter-comparison of similarity-based methods for organisation and classification of groundwater hydrographs. *Journal of Hydrology*, *559*, 222–237. doi: 10.1016/j.jhydrol.2018.02.035

Haaf, E., Giese, M., Heudorfer, B., Stahl, K., & Barthel, R. (2020). Physiographic and Climatic Controls on Regional Groundwater Dynamics. *Water Resources Research*, *56*(10). doi: 10.1029/2019WR026545

Hagquist, C., & Stenbeck, M. (1998). *Goodness of Fit in Regression Analysis-R 2 and G 2 Reconsidered* (Vol. 32; Tech. Rep.).

Hansson, K., Svensson, T., Möller, A., Larch, P., & Åhlen, B. (2010). Mätning av inläckande vatten till bergtunnlar. BeFo Rapport 104. Retrieved from http://www.befoonline.org/UserFiles/Archive/237/314941_BeFo_104.pdf

Hirsko, J. (2020). *Geographic Visualizations in Python with Cartopy.* Retrieved 2021-04-16, from https://makersportal.com/blog/2020/4/24/geographic-visualizations-in-python-with-cartopy

Hunter, J. D. (2007). Matplotlib: A 2d graphics environment. *Computing in Science & Engineering*, *9*(3), 90–95. doi: 10.1109/MCSE.2007.55

Hyndman, R. J., & Athanasopoulos, G. (2018). *Forecasting: Principles and Practice* (2nd ed.). Melbourne, Australia: OTexts. Retrieved from https://otexts.com/fpp2/residuals.html

Kittridge, M. (2019). *ETo Documentation Release 1.0.5* (Tech. Rep.). Retrieved from https://pypi.org/project/ETo/{#}description

Kumar, C. P. (2013). Numerical Modelling of Ground Water Flow using MODFLOW. *Indian Journal of Science*, *2*(4), 86–92. Retrieved from http://www.angelfire.com/nh/cpkbanner/publication/Modflow_Discovery.pdf

Lithén, J., & Wadsten, M. (2016). PM Hydrogeologi berg. , *1*(58), 1–58.

Met Office. (2010 - 2015). Cartopy: a cartographic python library with a matplotlib interface [Computer software manual]. Exeter, Devon. Retrieved from https://scitools.org.uk/cartopy

Mirzavand, M., & Ghazavi, R. (2015, mar). A Stochastic Modelling Technique for Groundwater Level Forecasting in an Arid Environment Using Time Series Methods. *Water Resources Management*, *29*(4), 1315–1328. Retrieved from https://link.springer.com/article/10.1007/s11269-014-0875-9 doi: 10.1007/s11269-014-0875-9

Mohanty, S., Jha, M. K., Kumar, A., & Panda, D. K. (2013, jul). Comparative evaluation of numerical model and artificial neural network for simulating groundwater flow in Kathajodi-Surua Inter-basin of Odisha, India. *Journal of Hydrology*, *495*, 38–51. Retrieved from http://dx.doi.org/10.1016/

j.jhydrol.2013.04.041 doi: 10.1016/j.jhydrol.2013.04.041

Obergfell, C., Bakker, M., & Maas, K. (2019, mar). Estimation of Average Diffuse Aquifer Recharge Using Time Series Modeling of Groundwater Heads. *Water Resources Research*, *55*(3), 2194–2210. Retrieved from https://doi.org/10.1029/2018WR024235 doi: 10.1029/2018WR024235

SMHI. (n.d.). *Ladda ner meteorologiska observationer.* Retrieved 2021-05-03, from https://www.smhi.se/data/meteorologi/ladda-ner-meteorologiska-observationer{#}param=airtemperatureInstant,stations=all

Sundkvist, U. (2016). PM Hydrogeologiska beräkningar. , *TRV 2016/3*(44), 1–44.

Sundkvist, U., & Wallroth, T. (2016). Ansökan om tillstånd enligt miljöbalken för anläggandet av Västlänken och Olskroken planskildhet Göteborgs Stad, Mölndals stad, Västra Götalands län. PM Hydrogeologi. (TRV 2016/3151). Retrieved from www.trafikverket.se

Teo, J. (2021, apr). *dendrogram-ts 0.1.2.* Retrieved 2021-05-13, from https://pypi.org/project/dendrogram-ts/

The pandas development team. (2020, February). *pandas-dev/pandas: Pandas.* Zenodo. Retrieved from https://doi.org/10.5281/zenodo.3509134 doi: 10.5281/zenodo.3509134

Trafikverket. (2018). *Om Västlänken - Trafikverket.* Retrieved 2021-02-01, from https://www.trafikverket.se/nara-dig/Vastra-gotaland/projekt-i-vastra-gotalands-lan/Vastlanken---smidigare-pendling-och-effektivare-trafik/Om-Vastlanken/

Virtanen, P., Gommers, R., Oliphant, T. E., Haberland, M., Reddy, T., Cournapeau, D., ... SciPy 1.0 Contributors (2020). SciPy 1.0: Fundamental Algorithms for Scientific Computing in Python. *Nature Methods*, *17*, 261–272. doi: 10.1038/s41592-019-0686-2

Waskom, M. L. (2021). seaborn: statistical data visualization. *Journal of Open Source Software*, *6*(60), 3021. Retrieved from https://doi.org/10.21105/joss.03021 doi: 10.21105/joss.03021

Yoo, C., Lee, Y., Kim, S.-H., & Kim, H.-T. (2012). Tunnelling-induced ground settlements in a groundwater drawdown environment - A case history. *Tunnelling and Underground Space Technology*, *29*, 69–77. Retrieved from https://www.sciencedirect.com/science/article/pii/S0886779812000211

A

Appendix 1

A.1 Evapotranspiration model

The Penman-Monteith equation from the UN-FAO 56 paper contains the following parameters:

$$ETo = \frac{0.480\Delta(R_n - G) + \gamma\left(\frac{900}{T+273}\right)u_2(e_s - e_a)}{\Delta + \gamma(1 + 0.34u_2)} \tag{A.1}$$

ETo : Reference evapotranspiration [mm/day]
R_n : Net radiation at crop surface [MJ/(m^2day)]
G : Soil heat flux density [MJ m^{-2} / day]
T : Air temperature at 2 m height [°C]
u_2 : Wind speed at 2 m height [m/s]
e_s : Saturation vapour pressure [kPa]
e_a : Actual vapour pressure [kPa]
(e_s-e_a) : Saturation pressure deficit [kPa]

For the calculations the data available for the site study evaluated in this thesis were the minimum and maximum temperature for years ranging from 1961-2020, the minimum and maximum relative humidity for dates from 1977-2020 that is used to calculate the actual vapour pressure e_a, the sun hours at years from 2008-2020, the wind speed at 2m height at dates ranging from 1961-2020 and the shortwave radiation for the years 2008-2020 used to calculate the net radiation R_n. The other parameters were estimated from this data, using the built in parameter estimation function in the ETo package. Further derivations and explanations on how the parameters of the UN-FAO 56 Penman-Monteith equation can be calculated are available in the UN-FAO 56 report (Allen et al., 1998).

The csv-files containing the data for the ETo package was read into Python, each as a pandas dataframe. The columns needed from the files were renamed, selected and placed in separate data frames where the data could be processed. The data was grouped by a 24 hour frequency to ensure that there was only one value for each date, the parameters were either summed up (sun hours, shortwave radiation), a mean was taken for each date (temperature, wind speed) or the minimum and maximum value was obtained for the day (relative humidity). The data frames were then merged on dates, into one data frame containing all five parameters. Missing values were interpolated linearly, but before a date selection was made as some data imported had longer measuring periods than others. The parameters for the

evapotranspiration was limited from 2013-2020, as the relative humidity was not measured before that.

To calculate the evapotranspiration with the ETo function the package was read into Python and initialised as in examples by Kittridge (2019).

```
from eto import ETo, datasets
import pandas as pd

et1 = ETo()
```

The built in parameter estimation function was then called to calculate the parameters missing that are essential to the UN-FAO 56 Penman-Monteith equation.

```
freq='D' #frequency where 'D' stands for day
z_msl=3.038 #height above sealevel (weather station Gteborg A)
lat=57.7156 #latitude (weather station Gteborg A)

# Parameter estimation function
et1.param_est(dataframe_climate_parameters, freq, z_msl, lat)
# view the first five rows of the estimated parameters
etlist=et1.ts_param.head()
```

For the estimation of the remaining parameters the frequecy of the data, the height above sealevel and the latitude of the weather station was needed. After the estimation the evapotranspiration could be calculated by calling the ETo function and a plot of the result could be obtained.

```
evp=et1.eto_fao()

# ploting the results
evp.plot(label='ETo', figsize=(10,4))
plt.legend(ncol=1,loc=0)
```

The evapotranpiration values could then be exported to a csv-file that was used in the groundwater modeling.

A.2 Pastas TFN model

The statistical modeling was performed using the open source Python package Pastas v.0.17.0 by (Collenteur et al., 2020).

1. **Import Packages.** Import the Python packages that will be used in the script.

```
    import pandas as pd
    import pastas as ps
    import matplotlib.pyplot as plt
```

2. **Import data.** By reading csv-files the data, time series, was imported and stored as pandas data frames. Data can be imported using different techniques but as recommended by Collenteur et al.(2019) the following method was used.

```
#Head data
WELL ID= 'name_of_column/well_in_head_csv-file'
ho = pd.read_csv(r'file_search_path\Head_Observations.csv',
    sep=';', usecols=['date␣column',WELL ID],
    parse_dates=['date'],
    index_col='date', squeeze=True).sort_index(ascending=True)
```

The csv-file with the head data was imported containing all groundwater head data for the wells of interest, seperated in different columns. The dataframe 'ho' was then altered with `usecols=['date column',WELL ID]` to only select one specified well calling `WELL ID= 'name of column/well in head csv-file'` before 'ho', to allow an easy change of the well ID in the script.

```
#Climate data
rain = pd.read_csv(r'file_search_path\rain.csv', sep=';',
    parse_dates=['date'],index_col='date', squeeze=True)}

evap = pd.read_csv(r'file_search_path\evap.csv',sep=';',
    parse_dates=['date'], index_col='date', squeeze=True)
```

The precipitation data was imported as it was retrieved. The evapotranspiration data was calculated with the Eto function, see appendix A.1.

```
#Leakage data
Leakage_n=pd.read_csv(r'file_search_path\leakage.csv',
    encoding = "ISO-8859-1", sep=';',
    usecols=['date_n','Leakage_n'],index_col=['date_n'],
    squeeze=True)
    .sort_index(ascending=True).dropna()

# add the leakage data frames to a list
L\_stresses=[Leakage_1,Leakage_2,Leakage_3,...,Leakage_n]
```

The leakage data was added separately for all leakage measurement trench IDs (7 leakage trenches were used in the modeling for this thesis) in the same way as all other data, above is a generic example, this could have been done in a for loop instead. The `usecols=['date column','leakage column]` was used again to only select the columns for that ID. The input argument `encoding =`

"ISO-8859-1" was required for this file to specify how Python is to interpret the file when read. The data frames containing the leakage data was then added to a list L_stresses.

```
#Inifiltration data
Infiltration=pd.read_csv(r'file_search_path/infiltration.csv',
    encoding = "ISO-8859-1",sep=';',
    usecols=['ID','date', 'value'],
    squeeze=True)

#create new df named Infiltration_ID
#only select rows with the ID of the infiltration well
infiltration_ID= infiltration.loc[infiltration['ID']==
    'ID_of_infiltration_well']
#Remove the now unwanted column containing the infiltration ID
# as the entire df now is named after the ID
infiltration_ID= infiltration_ID.drop(['ID'], axis=1)
    .set_index(['date'])
# convert the index to a datetime index
infiltration_ID.index = pd.to_datetime(infiltration_ID.index)
# change unit
infiltration_ID=infiltration_ID['Value']*1.44
# reindex to a daily frequency,with the function groupby.
infiltration_ID=infiltration_ID.groupby(pd.Grouper(freq='24H'))
    .mean().round(1).fillna(0).sort_index(ascending=True)

# add the infiltration data frames to a list
I_stresses=[Infiltration_1,Infiltartion_2]
```

The infiltration data was in this thesis received in an excel file where the two different types of infiltration where placed in the same column, but rows were named with the infiltration ID. The unit was also given in L/min but the input for Pastas is expected in M^3/day. Therefore this file required more manipulation before it could be processed in Pastas. The steps are described above. This was done for both infiltration IDs.

```
# Distances for leakage and infiltration

Distances_leakage_all_wells=pd.read_csv
    (r'file_search_path/distance_infiltration.csv',
    sep=';',index_col=['distance'],squeeze=True)
    .sort_index(ascending=True)
# a new dataframe with the distances
#for the currently modeled well was created
Distances\_leakage=Distances_leakage_all_wells
    .loc['Leakage_1':'Leakage_6',WELL]
# the data frame was converted to a list
```

```
Distances_leakage=Distances_leakage.squeeze()
Distances_leakage=Distances_leakage.astype(int)
Distances_leakage=Distances_leakage.tolist()

Distances_infiltration_all_wells=pd.read_csv
    (r'file_search_path/distance_infiltration.csv',
    sep=';',index_col=['distance'],squeeze=True)
    .sort_index(ascending=True)
# a new dataframe with the distances
#for the currently modeled well was created
Distances_infiltration=Distances_infiltration_all_wells
    .loc['Infiltration_ID_1':'Infiltration_ID_2',WELL]
# the data frame was converted to a list
Distances_infiltration=Distances_infiltration.squeeze()
Distances_infiltration=Distances_infiltration.astype(int)
Distances_infiltration=Distances_infiltration.tolist()
```

The distances between the leakage measurement trenches and all wells were put in one csv-file, the same was done for the distance between the infiltration points and all wells. It was therefore necessary with some file manipulation to select only the distances for the well currently modeled.

3. **Create model object** The Pastas model is created based of the groundwater head observation dataframe imported.

```
ml=ps.Model(ho)
```

4. **Create stress model.** The stress models are created and added to the model object.

```
stress_rch = ps.RechargeModel(rain, evap, rfunc=ps.Gamma,
         recharge=ps.rch.Linear, name="rch")
ml.add_stressmodel(stress_rch)

stress_leakage = ps.WellModel(L_stresses,
rfunc=ps.HantushWellModel, name="leakage",
distances=distances_leakage, settings="well")
ml.add_stressmodel(stress_leakage)

stress_infiltration=ps.WellModel(I_stresses,
rfunc=ps.HantushWellModel, name="infiltration",
distances=distances_infiltration, settings="well", up=True)
ml_Cal.add_stressmodel(stress_infiltration)
```

The selection process of the input arguments for the stress models is further explained in paragraph 3.4.1.

5. **Solve the model.** To estimate the model parameters the model object is solved using an objective function.

```
ml.solve(tmax=date_TS,report=True, solver=ps.LmfitSolve,
    noise=False)
```

6. **Plot the model results.** When the model object is solved the results can be plotted using various predefined methods for visualization.

```
# basic plot
ax=ml.plot(tmax=date_max,figsize=(10, 3))

# predefined result plot from Pastas
axes = ml.plots.results(figsize=(10,5))
```

Stress contributions and scenarios

To create different scenarios where the stress contribution affects the ground water simulation in different ways, the contributions from the calibrated model were first retrieved.

```
recharge = ml.get_contribution("rch")

infiltration=ml.get_contribution('infiltration')
infiltration_half=ml.get_contribution('infiltration')/2
infiltration_doubled=ml.get_contribution('infiltration')*2

leakage=ml.get_contribution('leakage')
leakage_half=ml.get_contribution('leakage')/2
leakage_doubled=ml.get_contribution('leakage')*2

# add original calibrated simulation
sim = ml_Cal.simulate()

# only a plot of the contributions
fig, ax = plt.subplots()
ml.get_contribution('rch').plot(ax=ax)
ml.get_contribution('infiltration').plot(ax=ax)
ml.get_contribution('leakage').plot(ax=ax)
  # plot attributes
ax.legend(["Recharge", "Infiltration","Leakage"], ncol=2, loc=3)
ax.grid()
ax.title.set_text('Contribution␣of␣recharge,␣infiltration␣and
␣␣␣␣leakage␣in␣the␣calibrated␣model')
ax.set_ylabel('Stress␣contribution␣[m]')
 # line marking the start of the tunnel construction
ax.axvline('2018-08-15',color='black',ls='--', linewidth=2)
```

The altered contributions were then added to the same plot as the calibrated model, the different scenarios were subplotted for comparison.

```
# define a figure and the individual plot axises for the subplots
fig, [ax1,ax2,ax3] = plt.subplots(3, 1, figsize=(12,9), sharex=True)
```

```
# name of entire plot
fig.suptitle('Comparison␣of␣stresses␣for␣'+ str(WELL))

# first subplot
    #calibrated simulation
sim.plot(ax=ax1, x_compat=True)
stat_1=ml_Cal.stats.summary()
    # only recharge
(recharge+ml_Cal.get_parameters("constant"))
    .plot(ax=ax1, linestyle="--")
    # w/o infiltration
(recharge+leakage+ml_Cal.get_parameters("constant"))
    .plot(ax=ax1, linestyle="--")
    # observed head values
ml.oseries.series.plot(ax=ax1, linestyle="␣", marker=".",
    zorder=-1, markersize=2, color="k", x_compat=True)
    # plot attributes
ax1.legend(["Calibrated␣model"+'␣␣(R\u00b2␣=
␣␣␣␣' +str(stat_1.at['rsq','Value'].round(2)*100)+'%)',
    'Simulation␣w/o␣leakage␣or␣infiltration' ,
    'Simulation␣w/o␣infiltration'], ncol=2, loc=3)
ax1.grid()
ax1.title.set_text('Scenarios␣without␣infiltration␣and␣leakage␣')
ax1.axvline('2018-08-15',color='black',ls='--', linewidth=2)
ax1.set_ylabel('GW␣level␣[m]')

# second subplot
sim.plot(ax=ax2, x_compat=True)
    # w/o leakage or infiltration
(recharge+ml_Cal.get_parameters("constant"))
    .plot(ax=ax2, linestyle="--")
    # double leakage
(recharge+infiltration+leakage_x2+ml_Cal.get_parameters("constant"))
    .plot(ax=ax2, linestyle="--")
    # half leakage
(recharge+leakage_half+infiltration
    +ml_Cal.get_parameters("constant")).plot(ax=ax2, linestyle="--")
    #head values
ml_Cal.oseries.series.plot(ax=ax2, linestyle="␣", marker=".",
    zorder=-1, markersize=2, color="k", x_compat=True)
    # plot attributes
ax2.legend(["Calibrated␣model"+'␣␣(R\u00b2␣=␣␣'
    +str(stat_1.at['rsq','Value'].round(2)*100)+'%)',
    'Simulation␣w/o␣leakage␣or␣infiltration',
    'Simulation␣w␣double␣leakage',
    'Simulation␣w␣half␣leakage'], ncol=2, loc=3)
```

```
ax2.grid()
ax2.title.set_text('Scenarios␣with␣different␣leakage␣rates')
ax2.axvline('2018-08-15',color='black',ls='--', linewidth=2)
ax2.set_ylabel('GW␣level␣[m]')
ax2.plot(sharey=ax1)

# Third subplot
sim.plot(ax=ax3, x_compat=True)
    # w/o infiltration
(recharge+leakage+ml_Cal.get_parameters("constant"))
    .plot(ax=ax3, linestyle="--")
    # dubble infiltration
(recharge+infiltration_dubbel+leakage
    +ml_Cal.get_parameters("constant")).plot(ax=ax3, linestyle="--")
    # half infiltration
(recharge+leakage+infiltration_half
+ml_Cal.get_parameters("constant")).plot(ax=ax3, linestyle="--")
    #head values
ml_Cal.oseries.series.plot(ax=ax3, linestyle="␣", marker=".",
    zorder=-1, markersize=2, color="k", x_compat=True)
    #plot attributes
ax3.legend(["Calibrated␣model"+'␣␣(R\u00b2␣=␣␣'
    +str(stat_1.at['rsq','Value'].round(2)*100)+'%)',
    'Simulation␣w/o␣infiltration',
    'Simulation␣w␣double␣infiltration',
    'Simulation␣w␣half␣infiltration'], ncol=2, loc=3)
ax3.grid()
ax3.title.set_text('Scenarios␣with␣different␣infiltration␣rates')
ax3.axvline('2018-08-15',color='black',ls='--', linewidth=2)
ax3.set_ylabel('GW␣level␣[m]')
```

A.3 Cluster analysis

To cluster the residuals they were first extracted for each well. The parameters were also retrieved but that was made manually after solving the models.

```
# Manual extraction of residual series, one well at a time
recharge=ml.get_contribution('rch')
    # values of the simulation with only the recharge contribution
sim_val=(recharge+ml_Cal.get_parameters("constant"))
sim_val.index.name = 'date'

    # the observed head values
head_obs=Ho.groupby(pd.Grouper(freq='24H')).mean()

    # a new data frame where the simulated values and
```

```
    # observed head values are merged
res=pd.merge(sim_val,head_obs, how='outer',on='date')
res=res.rename(columns={res.columns[0]:'simulation',
    res.columns[1]:'head'})

    #new data frame with an empty column named 'residuals'
col_name=['residuals']
df_res=pd.DataFrame(columns=col_name)

    # Concatenating the data frames and calculating the residuals
resid= pd.concat([resi,df_res])
resid['residuals']= resid['head'].subtract(resid['simulation'])

    # rename the residuals column to 'well id + res'
res_renamed=resid.rename(columns={resid.columns[2]:str(WELL)
    + '_res'})

    #put the column containing the residuals in a new df
res_df=pd.DataFrame()
res_df=res_df.append(res_renamed[str(WELL) + '_res'])
residuals=res_df.transpose().sort_index(ascending=True).squeeze()

    # reindex so that all residual series will be the same length
idxR = pd.date_range('2017-01-01', '2021-04-01')
Residuals = residuals.reindex(idxR)

    # plot residuals for visual inspection
resplot=Residuals.interpolate(method='linear').fillna(0).plot()
```

After extracting all residuals, they could be clustered. The extraction could be performed for all wells at the same time with a for loop, this however takes a long time and possibly requires a stronger computer than was used. Therefore the code is not presented here as it also required alterations to the stresses and model build up.

```
# read the residual data set
Residuals = pd.read_csv(r'file_search_path\Residuals.csv',
    sep=';', parse_dates=['date'], index_col='date',
    squeeze=True).sort_index(ascending=True)

# selection of wells included in the cluster analysis
WELLS=['Well_1','Well_2',...,'Well_n']
Residuals_data=Residuals[WELLS]

#interpolate to get a complete series (required to fill all dates)
#fill nan-values in beginning and end of series with 0
All_res_int=Residuals_data.interpolate(method='linear').fillna(0)
```

```
# centralizing the series
cent=All_res_int - All_res_int.mean()

# import package for cluster analysis
import scipy.cluster.hierarchy as hac

# define cluster analysis settings
C = hac.linkage(cent.T, method='ward', metric='euclidean')

# plot a dendrogram
plt.figure(figsize=(5, 10))
plt.title('Hierarchical␣Clustering␣Dendrogram')
plt.xlabel('distances')
plt.ylabel('clusters')
plt.grid()
    # p signals the number of clusters which will be plotted in
    # the dendrogram
hac.dendrogram(C,orientation='left',
    truncate_mode='lastp', p=18, labels=All_res_int.columns)
```

Spatial plot

```
# import packages needed for a map
import cartopy.crs as ccrs
import cartopy.io.img_tiles as cimgt
from cartopy.mpl.ticker import LongitudeFormatter, LatitudeFormatter

import io
from urllib.request import urlopen, Request
from PIL import Image

# read a file with all coordinates for the wells
coordinates_all= pd.read_csv(r'file_search_path\lat_long.csv',
    sep=';', squeeze=True,encoding = "ISO-8859-1")

# selection of wells included in the cluster analysis
array=['Well_1','Well_2',...,'Well_n']

coordinates=coordinates_all.loc[coordinates_all['WELL'].isin(array)]

# read file with infiltration and leakage coordinates
infiltration= pd.read_csv(r'file_search_path/
infiltration_leakage_lat_long.csv',
sep=';', squeeze=True,encoding = "ISO-8859-1")

# code to create a map by \cite{Hirsko2020},
```

```
#slightly altered to fit the modeling of this thesis
map_area=r'file_search_path\Area.shp'

    # this function pretends not to be a Python script
def image_spoof(self, tile):
    url = self._image_url(tile) # get the url of the street map API
    req = Request(url) # start request
    # add user agent to request
    req.add_header('User-agent','Anaconda␣3')
    fh = urlopen(req)
    # get image
    im_data = io.BytesIO(fh.read())
    fh.close() # close url
    # open image with PIL
    img = Image.open(im_data)
    # set image format
    img = img.convert(self.desired_tile_form)
    # reformat for cartopy
    return img, self.tileextent(tile), 'lower'

    # reformat web request for street map spoofing
cimgt.OSM.get_image = image_spoof
    # spoofed, downloaded street map
osm_img = cimgt.OSM()

    # open matplotlib figure
fig = plt.figure(figsize=(12,9))
    # project using coordinate reference system (CRS) of street map
ax1 = plt.axes(projection=osm_img.crs)
     # lat/lon of our place
center_pt = [57.690881,11.958454]
    # for zooming out of center point
zoom = 0.003
    # adjust to zoom
extent = [center_pt[1]-(zoom*2.0),center_pt[1]+(zoom*2.0),
    center_pt[0]-zoom,center_pt[0]+zoom]
ax1.set_extent(extent) # set extents

# empirical solve for scale based on zoom
scale = np.ceil(-np.sqrt(2)*np.log(np.divide(zoom,350.0)))
scale = (scale<20) and scale or 19 # scale cannot be larger than 19
ax1.add_image(osm_img, int(scale)) # add OSM with zoom specification
# NOTE: zoom specifications should be selected based on extent:
# -- 2     = coarse image, worldwide or continental scales
# -- 4-6   = medium coarseness,countries and larger states
# -- 6-10  = medium fineness,smaller states, regions, and cities
```

```
# -- 10-12 = fine image,city boundaries and zip codes
# -- 14+   = extremely fine image, roads, blocks, buildings
ax1.set_xticks(np.linspace(extent[0],extent[1],7),
    crs=ccrs.PlateCarree()) # set longitude indicators
ax1.set_yticks(np.linspace(extent[2],extent[3],7)[1:],
    crs=ccrs.PlateCarree()) # set latitude indicators


extent = [11.9508,11.9652,57.687,57.694] # NYC bounds
ax1.set_extent(extent) # set extents
ax1.set_xticks(np.linspace(extent[0],extent[1],7),
    crs=ccrs.PlateCarree()) # set longitude indicators
ax1.set_yticks(np.linspace(extent[2],extent[3],7)[1:],
    crs=ccrs.PlateCarree()) # set latitude indicators

    # format lons
lon_formatter = LongitudeFormatter(number_format='0.3f',
    degree_symbol='',dateline_direction_label=True)
    # format lats, numberformat decides how many decimals
lat_formatter = LatitudeFormatter(number_format='0.3f',
degree_symbol='')
    # set lons
ax1.xaxis.set_major_formatter(lon_formatter)
    # set lats
ax1.yaxis.set_major_formatter(lat_formatter)
ax1.xaxis.set_tick_params(labelsize=14)
ax1.yaxis.set_tick_params(labelsize=14)


# plotting the infiltration wells to the map
groups_i=infiltration.groupby(infiltration['cat'])
for name_i, group_i in groups_i:
    ax1.plot(group_i['lng'],group_i['lat'],zorder=1,
    markersize=12,marker='x',linestyle='',
    transform=ccrs.PlateCarree(),
    label=name_i)
    transform = ccrs.PlateCarree()._as_mpl_transform(ax1)

# plot the wells grouped by cluster
# requires a column named 'Cluster' in the coordinates data frame
groups = coordinates.groupby(coordinates['Cluster'])
for name, group in groups:
    ax1.plot(group['lng'],group['lat'], zorder=2,
    markersize=5,marker='o',linestyle='',
    transform=ccrs.PlateCarree(), label=name)
```

```
# Set text manually when text overlaps to much
#Requires a column named 'L/R' in the coordinates data frame
left=coordinates.set_index('L/R').loc[['L'],:]
right=coordinates.set_index('L/R').loc[['R'],:]

for lat_l,lon_l,name_l in zip(left['lat'],left['lng'],left['WELL']):
    ax1.annotate(name_l , xy=(lon_l, lat_l), xytext=(lon_l-0.0018,
    lat_l),transform=transform,xycoords=transform,
       arrowprops=dict(arrowstyle="->", color='k'))

for lat_r,lon_r,name_r in zip(right['lat'],right['lng'],
    right['WELL']):
    ax1.annotate(name_r , xy=(lon_r, lat_r), xytext=(lon_r+0.0004,
    lat_r),transform=transform,xycoords=transform,
       arrowprops=dict(arrowstyle="->",color='k'))
```

A.4 Dendrograms of all wells

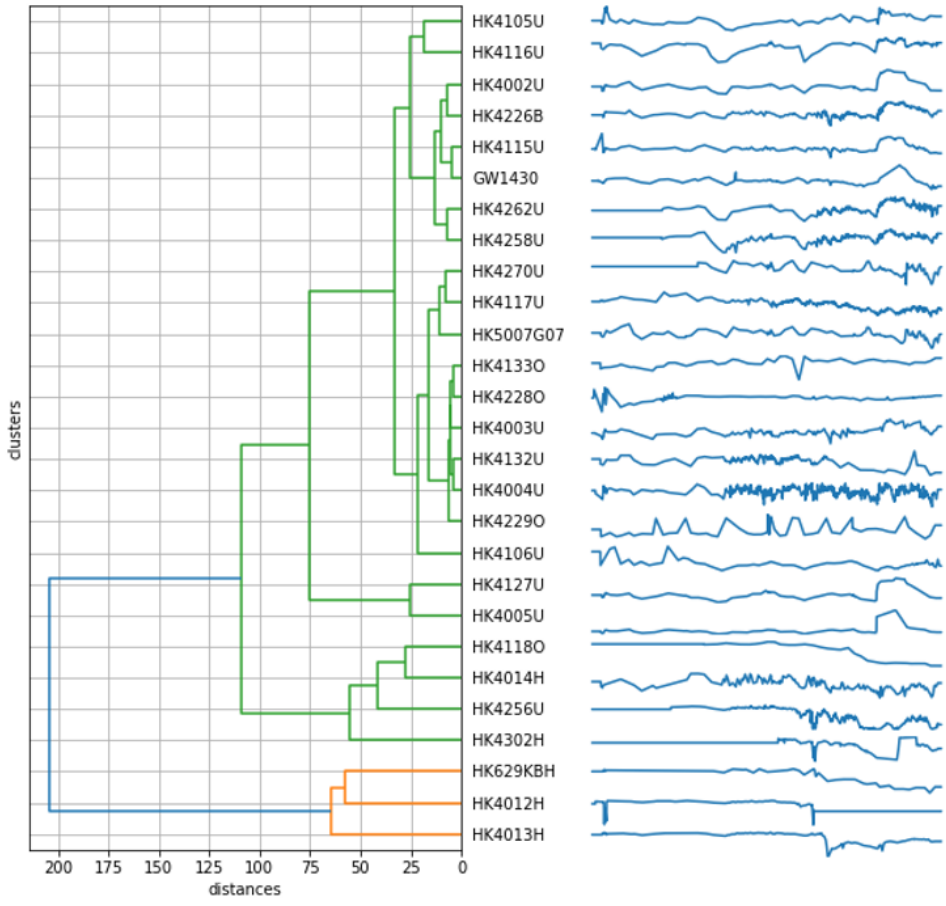

Figure A.1: Dendrogram for all wells with residual series besides.

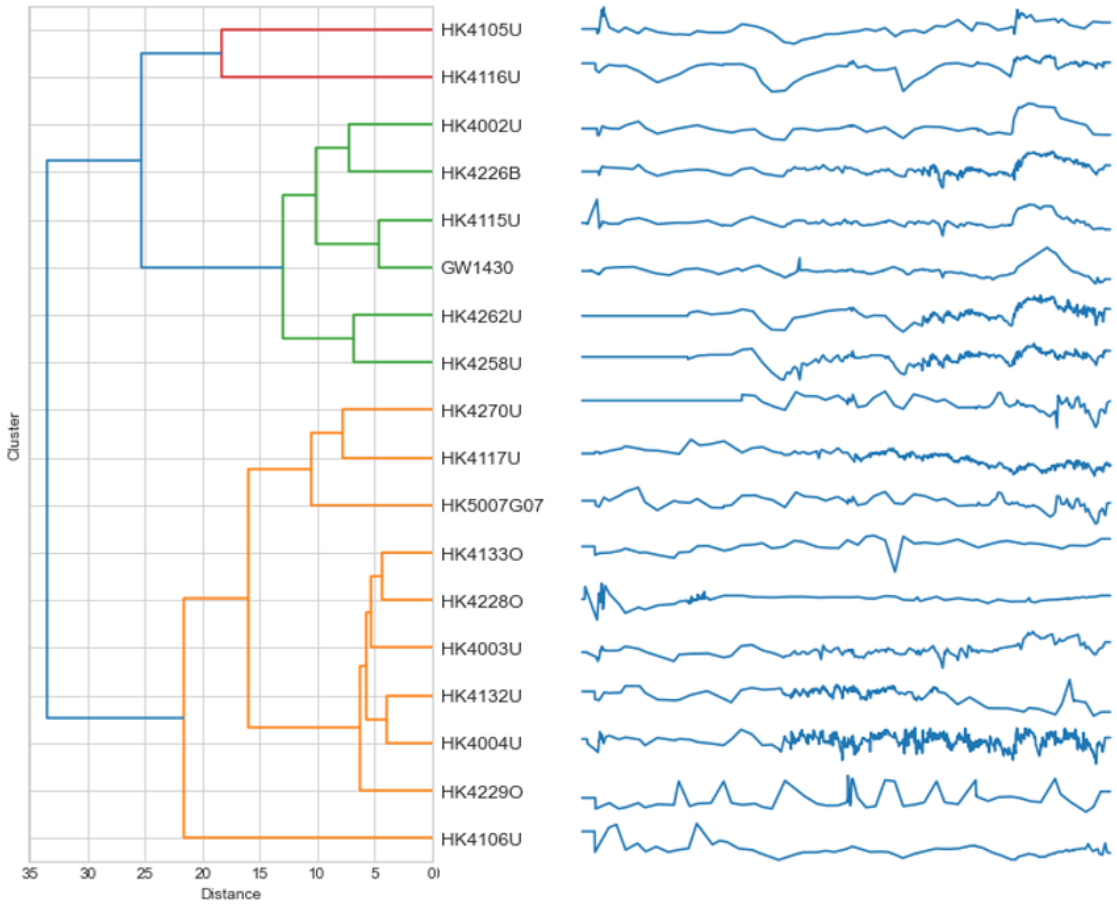

Figure A.2: Dendrogram of the residuals for the wells that are less impacted by the tunnel construction.

A.5 Correlation of parameters against height variables

In figure A.3 scatter plots of the parameter rch_A plotted against the height variables are presented. Against the $filterdepth$, rch_A shows a very weak positive Spearman correlation. For the $groundlevel$, $groundwater_{mean}$, $groundwater_{min}$ and $groundwater_{max}$ no correlation was found. HK4127U is the well which deviates and could have been considered an outlier.

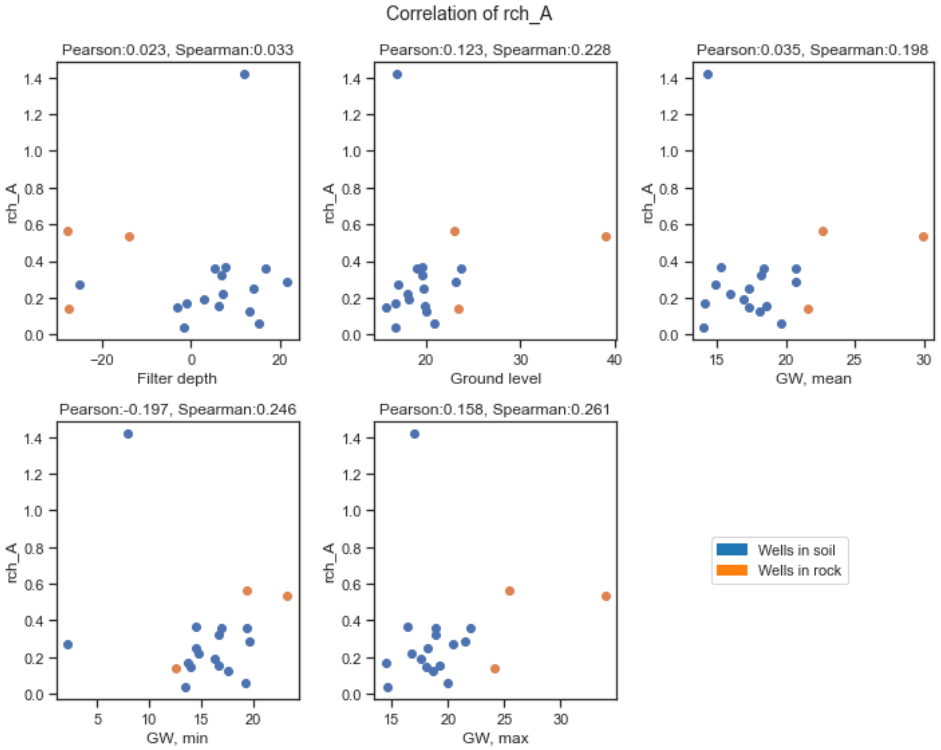

Figure A.3: Scatter plots for rch_A against height variables

In figure A.4 a weak positive Pearson and Spearman correlation is found between the parameter rch_n and the *filterdepth*. For the other height variables no correlation was shown.

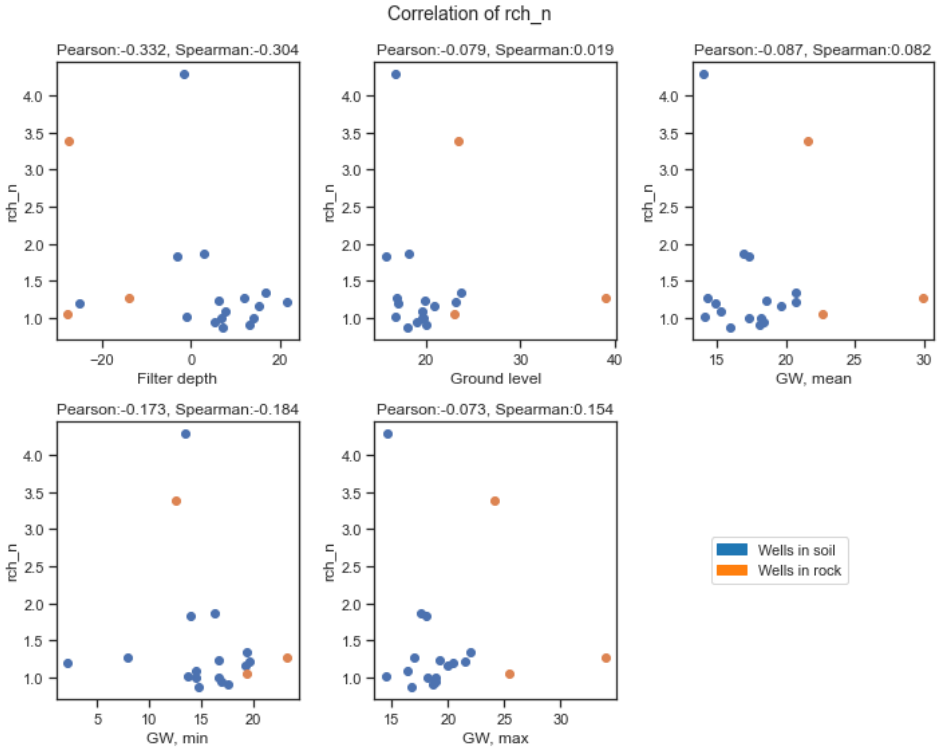

Figure A.4: Scatter plots for rch_n against height variables

In figure A.5 the shape parameter rch_a is plotted against the height variables. The $filterdepth$ shows no Pearson correlation but a weak negative Spearman correlation. The $groundlevel$ has a weak negative correlation for both the Pearson and Spearman coefficients. In the subplot presenting the $groundwater_{mean}$ against rch_a there is a weak negative Pearson and Spearman correlation. The $groundwater_{min}$ exhibits a weak negative Pearson correlation but no Spearman correlation and the $groundwater_{max}$ shows a weak negative Pearson and Spearman correlation. HK4127U is the well which deviates and could have been considered an outlier.

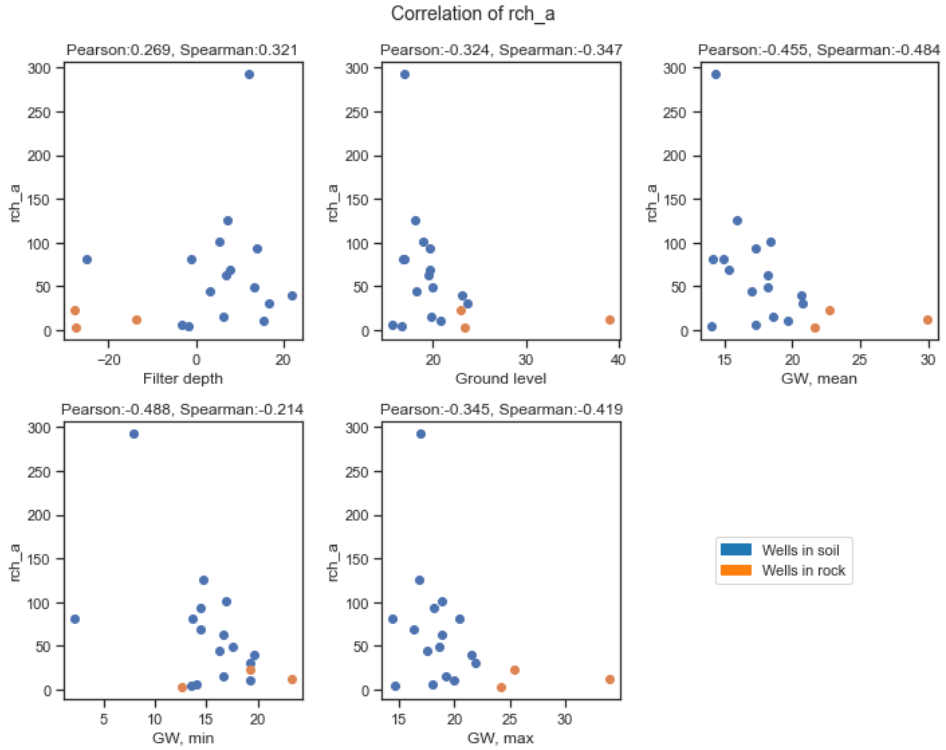

Figure A.5: Scatter plots for rch_a against height variables

In figure A.6 were the parameter rch_f is plotted against the height variables weak to no correlation was found. The filter depth show no correlation. For the ground level the Pearson coefficient show weak negative correlation while the Spearman correlation show no correlation. The groundwater mean does not correlate to the parameter, neither does the $groundwater_{min}$. The $groundwater_{max}$ however show weak negative Pearson correlation but no Spearman correlation.

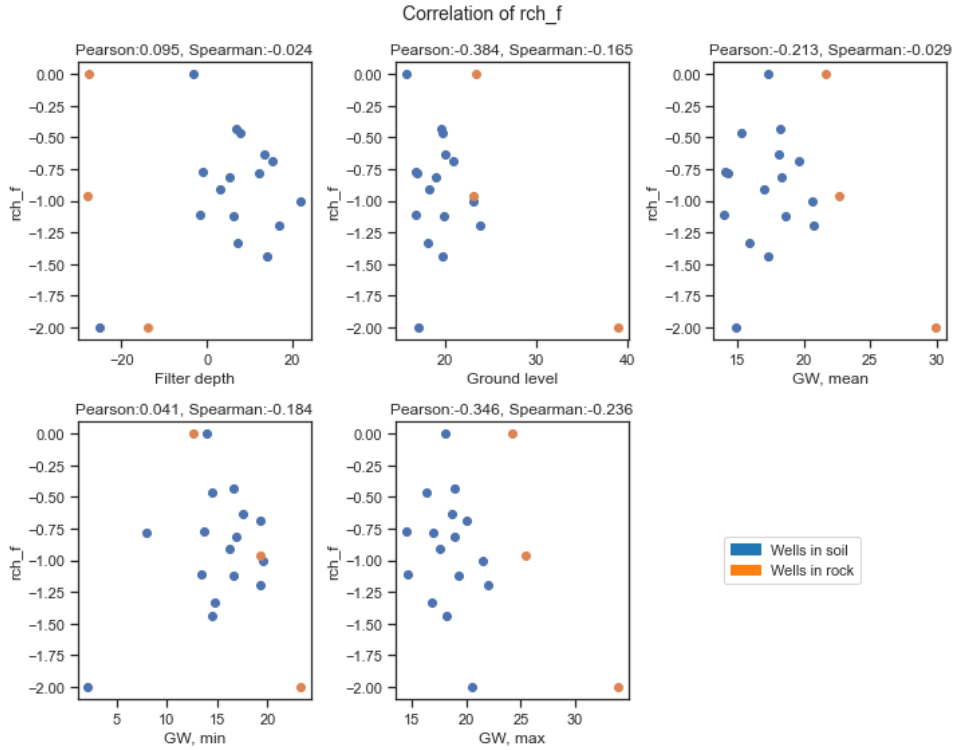

Figure A.6: Scatter plots for rch_f against height variables

A.6 Heatmaps of the correlation between model parameters and height variables

In Figure A.7 the heat map is showing the correlations between the parameters against the variables for all wells. This shows that rch_a is the parameter which correlates to the height variables the most, still only exhibiting weak correlations.

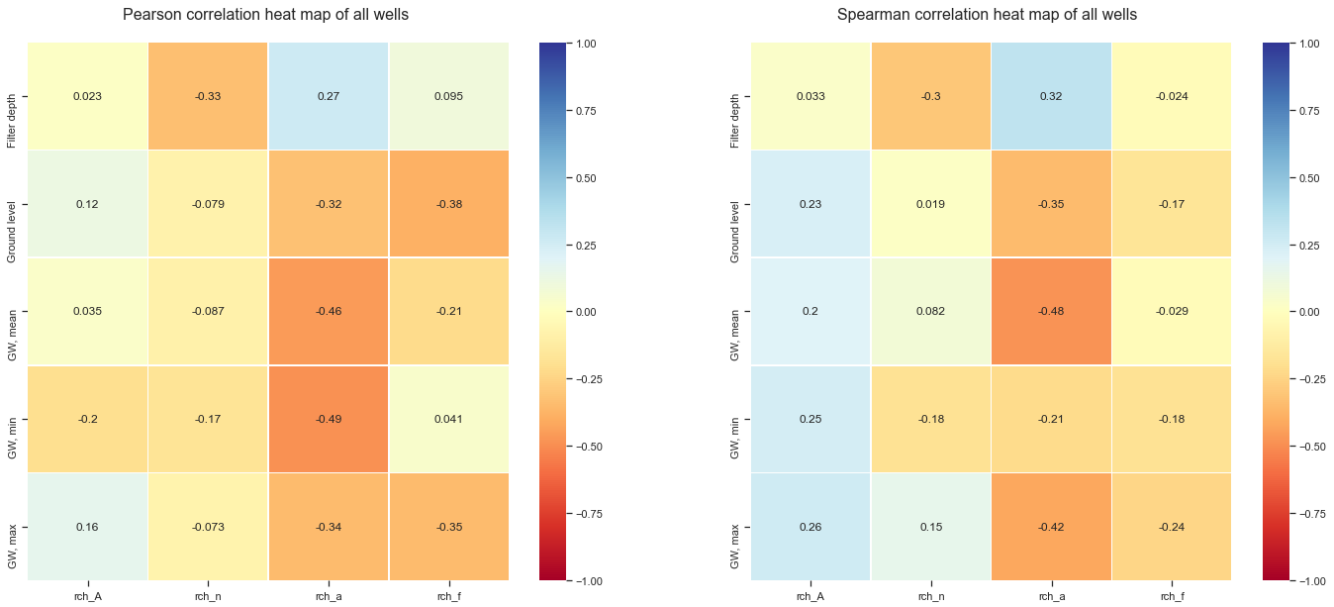

Figure A.7: Heat map of the correlations for all wells

In Figure A.8 the correlation for the wells only located in soil are presented. The changes in the Pearson coefficient are that the parameter rch_A has increased its negative Pearson correlation to a weak correlation for the variable $groundwater_{min}$. The parameter rch_n has increased the negative correlation for all variables to weak correlation except the $filterdepth$ and $groundwater_{min}$ which instead has decreased. For rch_a all variables except the $groundwater_{min}$ has decreased its correlation with the variables, the $groundwater_{mean}$ still exhibits weak negative correlation however. The Pearson coefficient for parameter rch_f has increased its correlation with the $filterdepth$ and $groundwater_{min}$ to a weak positive Pearson correlation, but decreased the before weak negative correlation for variables $groundlevel$ and $groundwater_{max}$.

For the Spearman coefficient the correlation has overall weakened. For the parameter rch_A no correlation is found against the variables. The parameter rch_n has decreased the weak correlation it showed with the $filterdepth$, and has no correlation against any variable for the wells in soil. The correlation for all variables and the parameter rch_a has also decreased, only the weak negative Spearman correlation for $groundwater_{mean}$ and $groundwater_{min}$ is left. No correlation is shown for the variables and the parameter rch_f when only looking at the wells located in soil. soil:

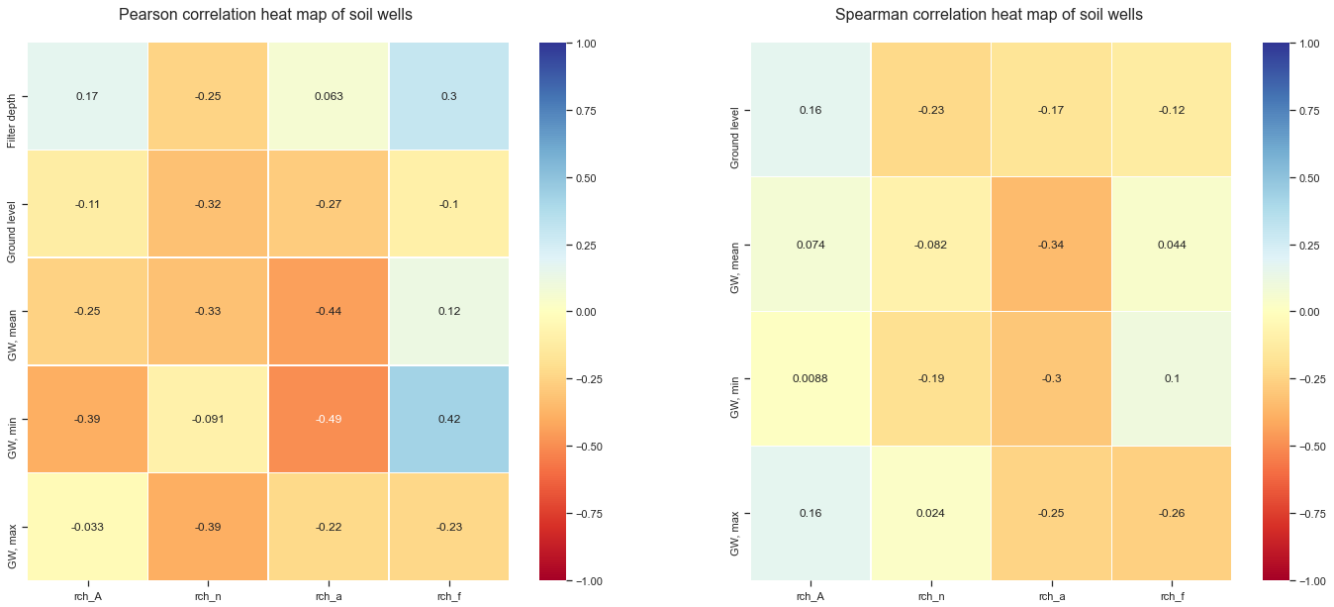

Figure A.8: Heat map of the correlations for wells in soil

The heatmap for the wells located in rock is presented in Figure A.9. All parameters and variables have increased their correlations to moderate positive or negative correlation and strong negative correlation for the parameter rch_f and the variables $groundwater_{mean}$,$groundwater_{min}$,$groundwater_{max}$. This result can be considered unreliable as there only is three wells in rock, that were not considered outliers, to correlate and should therefore not be used.

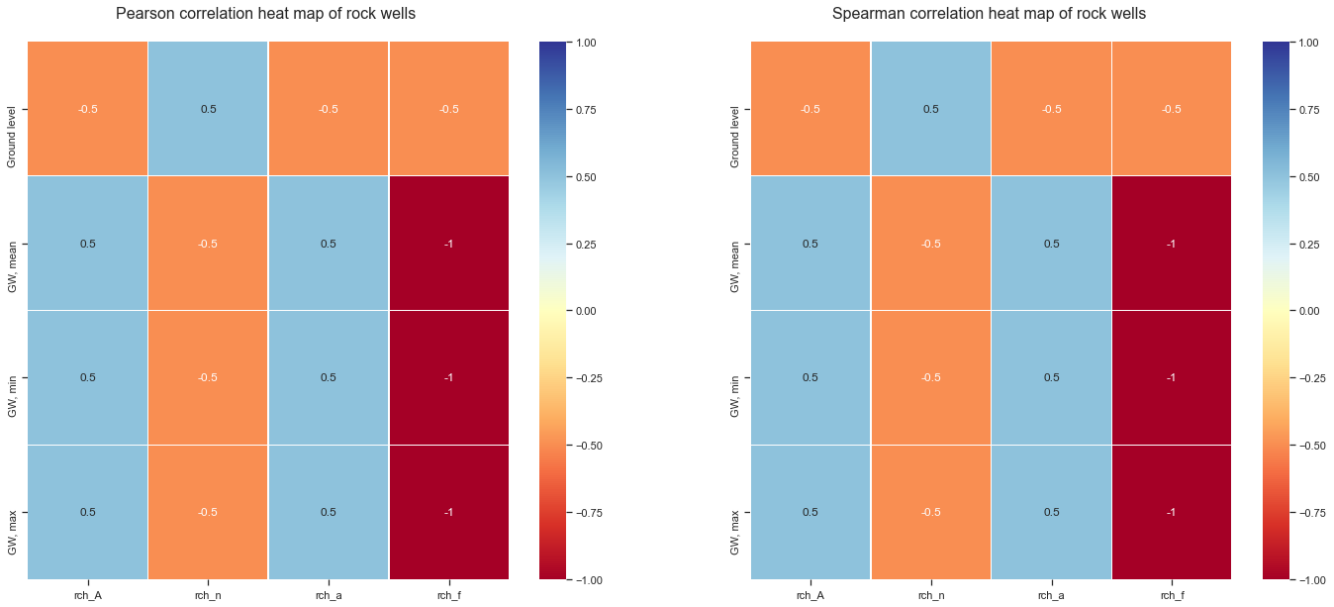

Figure A.9: Heat map of the correlations for wells in rock

A.7 Boxplot of the correlation between model parameters and the height variabes

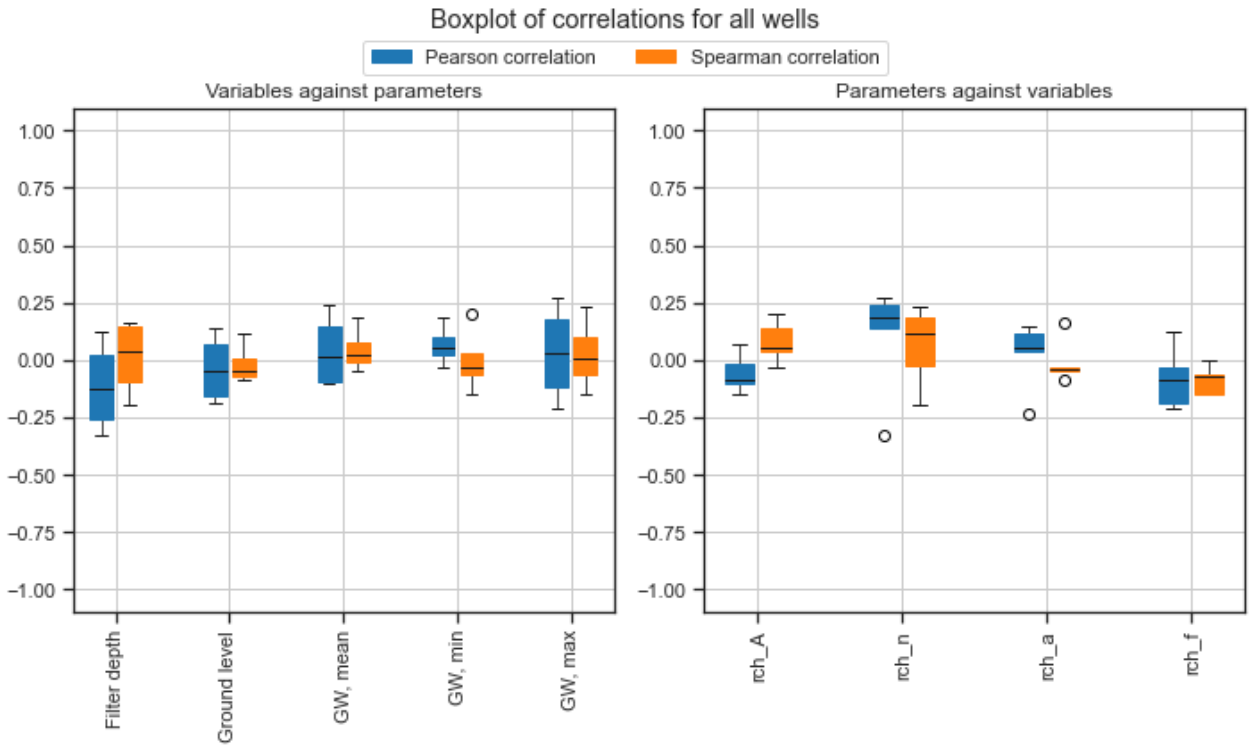

Figure A.10: Box plot of the correlation between model parameters and height variables of all wells.

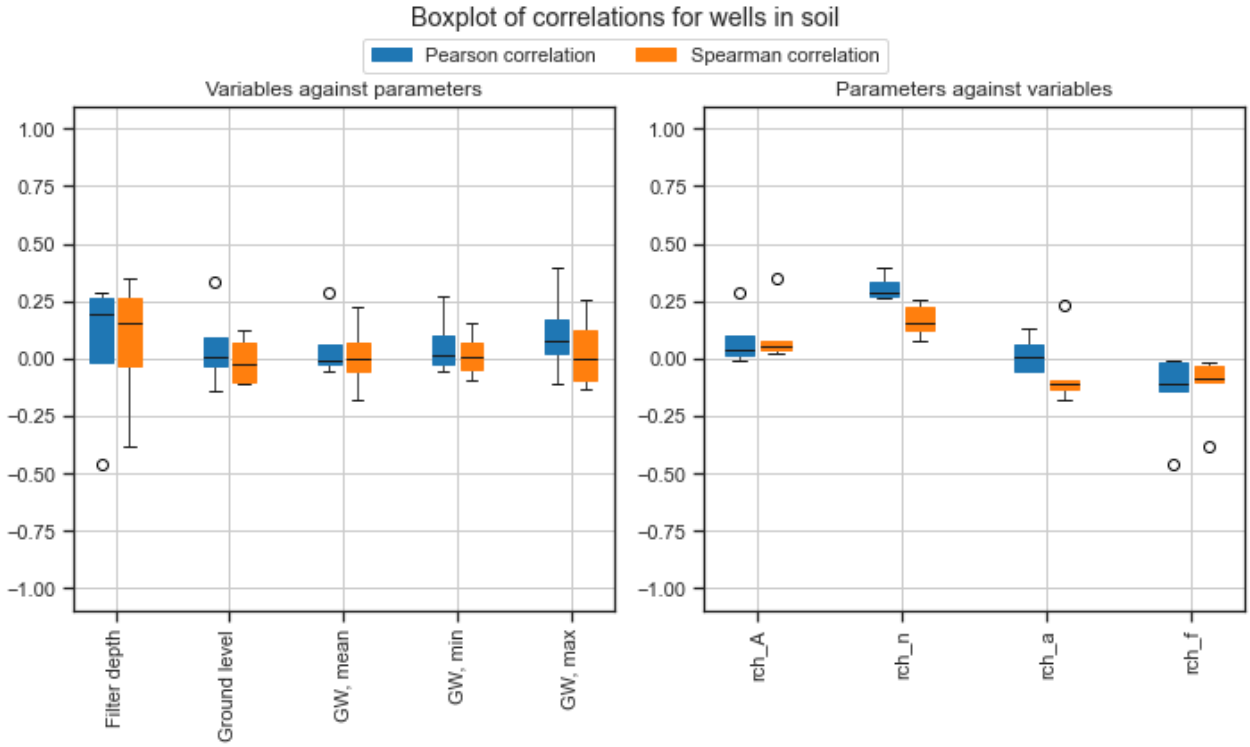

Figure A.11: Box plot of the correlation between model parameters and height variables of wells in soil.

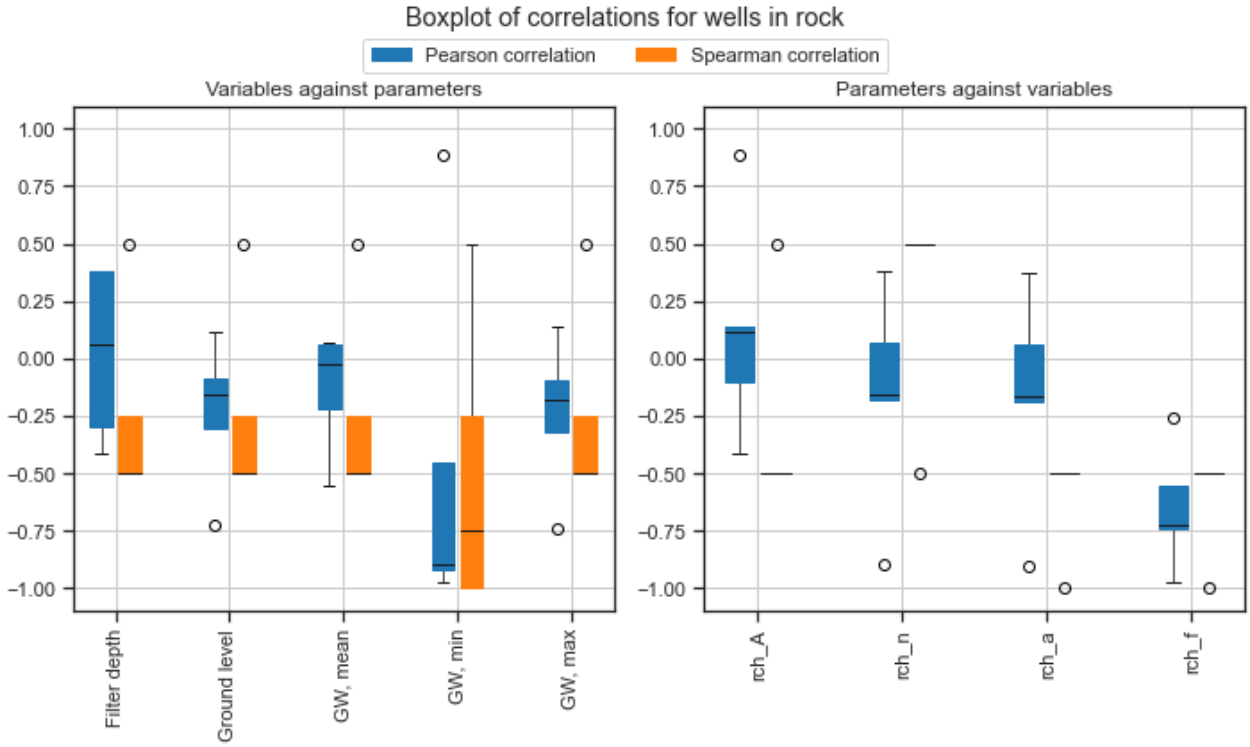

Figure A.12: Box plot of the correlation between model parameters and height variables of wells in rock.

DEPARTMENT OF SOME SUBJECT OR TECHNOLOGY
CHALMERS UNIVERSITY OF TECHNOLOGY
Gothenburg, Sweden
www.chalmers.se

CHALMERS
UNIVERSITY OF TECHNOLOGY